Effects of oxytocin receptor variants on activated signaling cascades and cellular processes

Dissertation

Zur Erlangung des Doktorgrades der
Naturwissenschaften (Dr. rer. nat.) der
Fakultät für Biologie und Vorklinische
Medizin der Universität Regensburg

Vorgelegt von

Magdalena Meyer

aus Roth

Juli 2020

Das Promotionsgesuch wurde eingereicht am 10.07.2020.

Die Arbeit wurde angeleitet von Dr. Benjamin Jurek.

Unterschrift:

Kurzfassung der Arbeit

Oxytocin ist ein Neurohormon, welches eine wichtige Rolle bei sozialen Verhaltensweisen spielt. Eine Fehlregulation des Oxytocin Systems kann daher zu tiefgreifenden Konsequenzen für die mentale Gesundheit führen. Solche Fehlregulationen können den Liganden selbst betreffen, wobei eine generell erniedrigte Konzentration bei einer Patientengruppe, die an einer Form von Autismus leidet, festzustellen ist. Des Weiteren konnte eine genetische Komponente, sogenannte Einzelnukleotidpolymorphismen (engl. single nucleotide polymorphisms, kurz SNPs), im Oxytocin Rezeptor Gen mit Autismus assoziiert werden. Aufgrund dieser Assoziationen und seiner vielversprechenden prosozialen und angstlösenden Wirkung, wird bereits seit längerem intensiv am Einsatz von Oxytocin als Therapeutikum bei psychosozialen Störungen geforscht. In den bestehenden Studien zeichnet sich jedoch ein eher kontroverses Bild ab. Während die Verabreichung einer einzelnen Dosis Oxytocin, das über ein Nasenspray appliziert wird, meist zu positiven Effekten in den Tests führte, kam es bei der wiederholten Gabe über einen längeren Zeitraum oft zu keiner Verbesserung der Symptome. Um eine langfristig sichere Therapie mit Oxytocin gewährleisten zu können, oder mögliche Alternativen zu identifizieren, müssen die molekularen Wirkmechanismen von Oxytocin und des Oxytocin Rezeptors genauer untersucht werden.

In meiner Doktorarbeit habe ich verschiedene Zelllinien verwendet, um die daran beteiligten Signalwege und zellulären Prozesse aufzuklären. So konnte ich zeigen, dass Oxytocin die Morphologie von Neuronen beeinflussen kann, indem es zu einer Änderung der Neuritenlänge führt. Ob sich dies in einer Verkürzung oder Verlängerung der neuronalen Fortsätze äußert, ist von der Expression und Aktivierung des Transkriptionsfaktors Myocyte Enhancer Factor (MEF) 2A abhängig. In diesem Zusammenhang konnte ich zwei Faktoren identifizieren, welche die Aktivität von MEF2A regulieren: den MAP Kinase Signalweg und die Phosphatase Calcineurin.

Zudem konnte ich durch einen Knock-out von MEF2A dessen zentrale Rolle bei der Funktion von Mitochondrien mit direkter Konsequenz für die Energiebereitstellung in Neuronen belegen.

Des Weiteren habe ich die Auswirkungen einer genetischen Variante des Oxytocin Rezeptors, des SNPs rs4686302, der in verschiedenen Studien mit Autismus, Empathie und sozialen Kognitionsstörungen assoziiert wurde, auf molekularer Ebene untersucht. Durch den

unmittelbaren Vergleich zweier humaner Zelllinien, wobei eine die SNP- und die andere eine Wildtyp-Variante des Rezeptors exprimierte, konnte ich Abweichungen gezielt analysieren. Durch eine Sequenzierung des Genoms fiel dabei eine Duplikation des Oxytocin Rezeptor Gens in der SNP-Zelllinie als weitere Variation auf. Auf Basis der beiden genetischen Varianten, konnte ich Unterschiede hinsichtlich der Rezeptorstabilität, des Calcium- und MAP Kinase Signalweges sowie eine umfassend differentielle Genregulation aufzeigen.

Zusammenfassend konnte ich durch meine Arbeit das Wissen über die zellulären Effekte von Oxytocin und die Auswirkungen von genetischen Variationen, die das Oxytocin Rezeptor Gen betreffen, erweitern und somit zu einem besseren Verständnis des Oxytocin Systems beitragen.

List of Publications

This cumulative dissertation is composed of the following publications or manuscripts in preparation, in which I am first author:

A. Magdalena Meyer, Ilona Berger, Julia Winter, Benjamin Jurek (2018). Oxytocin alters the morphology of hypothalamic neurons via the transcription factor myocyte enhancer factor 2A (MEF-2A). Molecular and Cellular Endocrinology 10.1016/j.mce.2018.06.013

B. Magdalena Meyer, Kerstin Kuffner, Julia Winter, Inga D. Neumann, Christian H. Wetzel and Benjamin Jurek (2020). Myocyte Enhancer Factor 2A (MEF2A) Defines Oxytocin-Induced Morphological Effects and Regulates Mitochondrial Function in Neurons. Int. J. Mol. Sci. 2020, 21, 2200; 10.3390/ijms21062200

C. Magdalena Meyer, Vladimir Milenkovic, Christian H. Wetzel, Inga D. Neumann and Benjamin Jurek (in preparation). Functional Characterization of the Oxytocin Receptor Variant A218T.

In the course of this work, I contributed to further publications, which are not part of the dissertation:

D. Benjamin Jurek and Magdalena Meyer (2020). Anxiolytic and Anxiogenic? How the Transcription Factor MEF2 Might Explain the Manifold Behavioral Effects of Oxytocin. Front. Endocrinol. 11:186; 10.3389/fendo.2020.00186

E. Julia Winter, Magdalena Meyer, Ilona Berger, Sebastian Peters, Melanie Royer, Dominik Langgartner, Stefan O. Reber, Kerstin Kuffner, Anna K. Schmidtner, Katharina Hübner, Finn Hartmann, Anna Bludau, Marta Bianchi, Simone Stang, Oliver J. Bosch, David A. Slattery, Erwin van den Burg, Inga D. Neumann, and Benjamin Jurek (in preparation). Chronic oxytocin-driven alternative splicing of CRFR2α induces anxiety.

F. Julia Winter, Magdalena Meyer, Simone Stang, Carl-Philip Meinung, Eva-Maria Rom-Jurek, Christoph Irlbeck, Katharina Limm, Peter Oefner, Gero Brockhoff, Inga D. Neumann, Benjamin Jurek (in preparation). A CRISPR-Cas-generated oxytocin receptor knock out causes morphological alterations in neuronal cells.

Personal Contributions

Publication A

The research was designed by Benjamin Jurek and myself. Ilona Berger, Julia Winter, Benjamin Jurek and myself performed and analyzed morphological experiments. Immunocytochemical stainings were performed by Ilona Berger. Cell stimulations and Western Blots were performed by myself. The work was supervised by Benjamin Jurek. The publication was written by Benjamin Jurek and myself.

Publication B

The research was designed by Christian H. Wetzel, Benjamin Jurek and myself. The CRISPR-Cas9 mediated knockout of MEF2A was done together with Julia Winter. Immunofluorescence stainings were performed by Benjamin Jurek. Mitochondrial Respiration Analysis was conducted by Kerstin Kuffner and me. The morphology experiments were analyzed by myself, Julia Winter and Benjamin Jurek. Transfections, Western Blots and cellular assays were performed by myself. The work was supervised by Benjamin Jurek and Inga D. Neumann. The publication was written by Benjamin Jurek and myself.

Publication C

The research was designed by Christian H. Wetzel, Inga D. Neumann, Benjamin Jurek and myself. Transduction and establishment of cell lines was performed by myself. Calcium Imaging was performed by Vladimir Milenkovic and myself. Assays and Western Blots were performed by myself. The work was supervised by Inga D. Neumann and Benjamin Jurek. The publication was written by Benjamin Jurek and myself.

Publication D

The publication, a mini-review, was written by Benjamin Jurek and myself.

Publication E

The research was designed by Inga D. Neumann, Benjamin Jurek and Julia Winter. The experimental work was performed by all authors including myself. In detail, I helped with animal experiments, membrane fractioning and data analysis. The work was supervised by Inga D. Neumann and Benjamin Jurek. The publication was written by Julia Winter, Erwin van den Burg, Inga D. Neumann and Benjamin Jurek.

Publication F

The research was designed by Julia Winter and Benjamin Jurek, and supervised by Benjamin Jurek. Julia Winter, Simone Stang, Carl-Philip Meinung, Eva Rom-Jurek, Christoph Irlbeck, Katharina Limm, Benjamin Jurek and myself performed and analyzed experiments. The publication was written by Julia Winter, Eva Rom-Jurek, Katharina Limm, and Benjamin Jurek.

Table of Contents

1 General introduction

This section is intended to convey and expand biological principles, basics and functions relevant to my thesis. It forms the basis for the introductions in *2.2*, *3.2* and *4.2*.

1.1 Oxytocin

The neuropeptide oxytocin (OT) enjoys a good reputation, reflected by its common description as the love or cuddle hormone. Released during physiological processes that are usually positively associated like uterus contraction during birth, milk ejection during breast-feeding, and orgasms, it promotes feelings of love, trust, bonding and well-being (Jurek and Neumann, 2018). Hence, besides its important role in reproduction, it is involved in many social actions and interactions like mother-child bonding, caregiving and trusting behavior, empathy, pair bonding, sexual behavior, as well as anxiety and aggression.

In accordance with this overall beneficial picture, there seems to be a positive correlation between our states of mental health and endogenous OT levels. People within the first stages of a romantic relationship have higher levels of OT (Schneiderman *et al.*, 2012; Acevedo *et al.*, 2012). In contrast, low levels of OT have been found in patients suffering from autism spectrum disorder (ASD) or depression (Parker *et al.*, 2017; Yuen *et al.*, 2014).

Given these correlations, and because of its prosocial and anxiolytic effects, it has been suggested as a promising therapeutic agent for many psychosocial disorders, such as anxiety disorder or ASD. Delivered through a nasal spray, OT raised hopes as a non-invasive treatment option to help people who avoid social interaction and persistently experience fear and mistrust.

However, there is a general inconsistency occurring in studies testing its potential as treatment, especially when tested in long-term administration regimens. Comparing its effects on anxiety in rodents upon acute single-dose versus chronic long-term administration, the thin line between advantages and risks becomes quite apparent. An acute infusion of synthetic OT directly into the paraventricular nucleus (PVN) of male and female rats increased the time they spent in the open arms or lit compartment in the behavioral tests of the elevated plus maze or light dark box, reflecting a decreased level of anxiety (Blume *et al.*, 2008; Jurek *et al.*, 2012). A chronic treatment with 10 ng/h intracerebroventricular OT via osmotic minipumps however, induces anxiogenesis

in male mice (Peters *et al.*, 2014) and, in combination with a mild stressor, in male and female rats (Winter *et al.*, 2020).

A similarly controversial picture of OT emerges from studies examining its efficacy and safety as treatment for ASD patients. ASD is a neurodevelopmental disorder that affects communication and social behavior. People who suffer from ASD have difficulties interacting with other people and show impaired communication skills. For example, they do not to look at or listen to people or show facial expressions and movements not matching with what is being said. They often show restricted interests and repetitive behaviors, and slight changes in their daily routine can make them feel upset and extremely irritated (Freitag and Konrad, 2014). Those psychological traits hamper their abilities to function properly in school, work, and private life. Upon administration of one single dose of OT, several studies confirmed improvements in a wide range of social behaviors, as well as a reduction of repetitive behaviors (Watanabe *et al.*, 2014; Aoki *et al.*, 2014). However, as an acceptable treatment for ASD, OT must have prolonged efficacy. While some studies claim considerable improvements in key symptoms of ASD by long-term administration of OT (Parker *et al.*, 2017; Tachibana *et al.*, 2013), other studies found no improvements (Guastella *et al.*, 2015; Dadds *et al.*, 2014).

In order to understand the opposing effects provoked by the same compound, we have to develop a deeper understanding of the molecular underpinnings and functions of the OT system. OT consists of the nine amino acids: Cys-Tyr-Ile-Gln-Asn-Cys-Pro-Leu-Gly-NH_2, and is produced in the supraoptic nucleus (SON), accessory nuclei, and PVN of the hypothalamus (Jurek and Neumann, 2018). It can be released from magnocellular neurons by axonal and somatodendritic release, and into the periphery via axonal projections. Due to its similarity to the closely related nonapeptide vasopressin, OT can bind to the three vasopressin receptor subforms V1a, V1b and V2, although with reduced affinity compared to the main target of the natural ligand – the oxytocin receptor (Chini and Manning, 2007).

1.2 Oxytocin receptor

The oxytocin receptor (OTR) belongs to the family of G protein coupled receptors (GPCRs), consisting of seven transmembrane helices, three extracellular as well as three intracellular loops (Gimpl and Fahrenholz, 2001). In humans, the OTR is encoded by the *OTR* gene located on

chromosome 3 (3p25–3p26x·2) as an inverted 17-kb single-copy gene and consists of four exons and three introns. The coding sequence encompasses only the major part of Exon 3 and the first part of Exon 4 (Peter *et al.*, 1995). The OTR forms homodimers and heterodimers with other GPCRs, which consequently results in an enhanced activation of receptor-coupled signaling cascades (Busnelli *et al.*, 2016).

In the periphery, the OTR is expressed by the myoepithelial cells of the mammary gland, in both, the myometrium and endometrium of the uterus, in cardiomyocytes of the heart, dermal fibroblasts as well as osteoclasts and osteoblasts. In the mammalian brain, the OTR is expressed throughout many brain regions including the hypothalamus, prefrontal cortex, hippocampus, and amygdala (Jurek and Neumann, 2018). However, the OTR is generally expressed at low levels, rendering its detection in some regions quite challenging (Freund-Mercier *et al.*, 1994).

In addition, the OTR membrane expression depends on ligand availability, since an increased ligand availability over prolonged periods can result in receptor desensitization and internalization. The desensitization of the OTR is initiated by the G protein-coupled receptor kinase 2, which phosphorylates and primes the OTR for subsequent ß-arrestin binding. Arrestin binding to the OTR induces uncoupling from the G proteins, blocks further signaling cascades and targets the OTR for internalization. The OTR is internalized in a clathrin pit-dependent mechanism and intracellularly stored in “Ras-related in brain 4/5”-vesicles that get recycled after four hours as shown in HEK293 cells (Conti *et al.*, 2009). Interestingly, selective OTR ligands like the agonist carbetocin have been shown to induce β-arrestin-independent internalization without recycling back to the plasma membrane (Passoni *et al.*, 2016).

These processes, resulting in a reduced membrane expression, bear consequences for a therapy that would encompass repeated daily intranasal applications of OT over a longer period.

Besides the natural ligands OT and vasopressin, there are several synthetic OTR agonists and antagonists that can exclusively activate or block the OTR based on their selectivity and affinity.

The OTR itself can occur in a high- or low-affinity state, whereby the conversion between the two affinity states is reversible (Gimpl and Fahrenholz, 2001; Wiegand and Gimpl, 2012). Two components, cholesterol and magnesium, have been found to act as strong allosteric modulators, affecting the stability and binding of ligands to the OTR.

Very recently, the crystal structure of the human OTR has been solved and published in a pre-print (Waltenspühl Y. *et al.*, 2020). In this study, the authors also localized the binding sites for cholesterol and magnesium, providing a structural understanding of the stabilization-effects for the OTR, thereby constituting a giant leap for a better understanding of the OT system and for the future development of therapeutic compounds targeting the receptor.

As a GPCR, the OTR is coupled to a trimeric complex of G proteins comprising a Gα and a Gβ/γ unit, which are separated from each other upon ligand binding. Depending on the activated Gα subtype, which can differ between tissues and cell types, the outcome can be either inhibitory or excitatory and different downstream signaling cascades get activated (Figure 1).

1.3 Oxytocin receptor-coupled signaling

Upon OTR activation there is an increase in intracellular Calcium (Ca^{2+}) caused by a Ca^{2+} influx from the extracellular space via several Ca^{2+} channels like transient receptor potential (TRP) cation channels including the canonical forms TRPC1 and TrpC3-TRPC6 as well as the vanilloid forms TRPV2 and TRPV4, but also voltage-gated Ca^{2+} channels (van den Burg *et al.*, 2015; Murtazina *et al.*, 2011; Shlykov *et al.*, 2003; Ulloa *et al.*, 2009; Ying *et al.*, 2015). In addition, OTR activation provokes a release of Ca^{2+} from intracellular stores (Sanborn *et al.*, 1998; Tobin *et al.*, 2011). Upon G protein activation, phospholipase C (PLC) gets activated cleaving phospholipid phosphatidylinositol 4,5-bisphosphate (PIP2) into diacyl glycerol (DAG) and inositol 1,4,5-trisphosphate (IP_3). Those two products are important second messenger molecules that control several cellular processes and serve as substrates for other signaling molecules. IP_3 is a soluble signaling molecule that diffuses through the cytoplasm to the endoplasmic reticulum, where it binds to its receptor, a Ca^{2+} channel, inducing the release of Ca^{2+} from the endoplasmic reticulum lumen into the cytosol. DAG, the second product of PLC activation, remains in the plasma membrane and mediates the activation of protein kinase C (PKC). The resulting elevation in cytoplasmatic Ca^{2+} levels from intracellular and extracellular sources is essential for several OTR-coupled signaling pathways.

The basal intracellular Ca^{2+} concentration and evoked Ca^{2+} signals have to be tightly regulated since important aspects of cell function are dependent on this homeostasis, including gene expression, and energy metabolism (Clapham, 2007). These cell functions depend on Ca^{2+} signal

propagation to the specific organelles like the mitochondria for synchronization of the ATP generation with cell function, or the nucleus for gene regulatory events (Zhang *et al.*, 2009; Griffiths and Rutter, 2009). Dysregulations in Ca^{2+} signaling can have severe consequences including cell necrosis or apoptosis.

The set of downstream signaling cascades comprise the already mentioned PKC, several CaMK subforms, the phosphatase Calcineurin (CaN), as well as the mitogen-activated protein kinase (MAPK) pathway. However, not only intracellular Ca^{2+} leads to the activation of this pathway. At the same time, a cross-reaction of receptor tyrosine kinases like the epidermal growth factor (EGFR) has been observed eventuating in the recruitment of the membrane-associated proto-oncoprotein GTPase Rat sarcoma (Ras) (Blume *et al.*, 2008). Ras in turn functions as an initiator of the MAPK pathway with its kinases MAP kinase kinase 1 and 2 (MEK1/2) and extracellular signal regulated kinase 1/2 (ERK1/2). Besides that, the OTR has also been linked to an activation of the MAPKs p38 and ERK5 in myometrial cells, but their coupling and downstream targets in neuronal cells remain to be elucidated (Devost *et al.*, 2008; Brighton *et al.*, 2011).

All those signaling pathways converge on transcription factors regulating the transcription of their target genes. The OT-induced targets we have mostly focused on are the transcription factor CREB, which is involved in spatial memory formation and CRF gene transcription (Tomizawa *et al.*, 2003; Jurek *et al.*, 2015) and the myocyte enhancer factor (MEF) 2 (Meyer *et al.*, 2018; Meyer *et al.*, 2020). The MEF2 family of transcription factors consists of four isoforms, namely MEF2A, -2B, -2C and -2D. All subforms share a common genetic structure consisting of an N-terminal DNA binding domain, the MEF2 domain, and a COOH-terminal transcriptional regulatory domain, whose activity is orchestrated by multiple posttranslational modifications. The phosphorylation status of the MEF2 proteins regulates the gene transcription and thereby determines the function of the respective biological process. In case of MEF2A, phosphorylation of the protein at the sites serine (S) 387, threonine (Thr) 312, and Thr319 stimulates gene transcription, whereas phosphorylation at S408 has an inhibitory outcome (Potthoff and Olson, 2007).

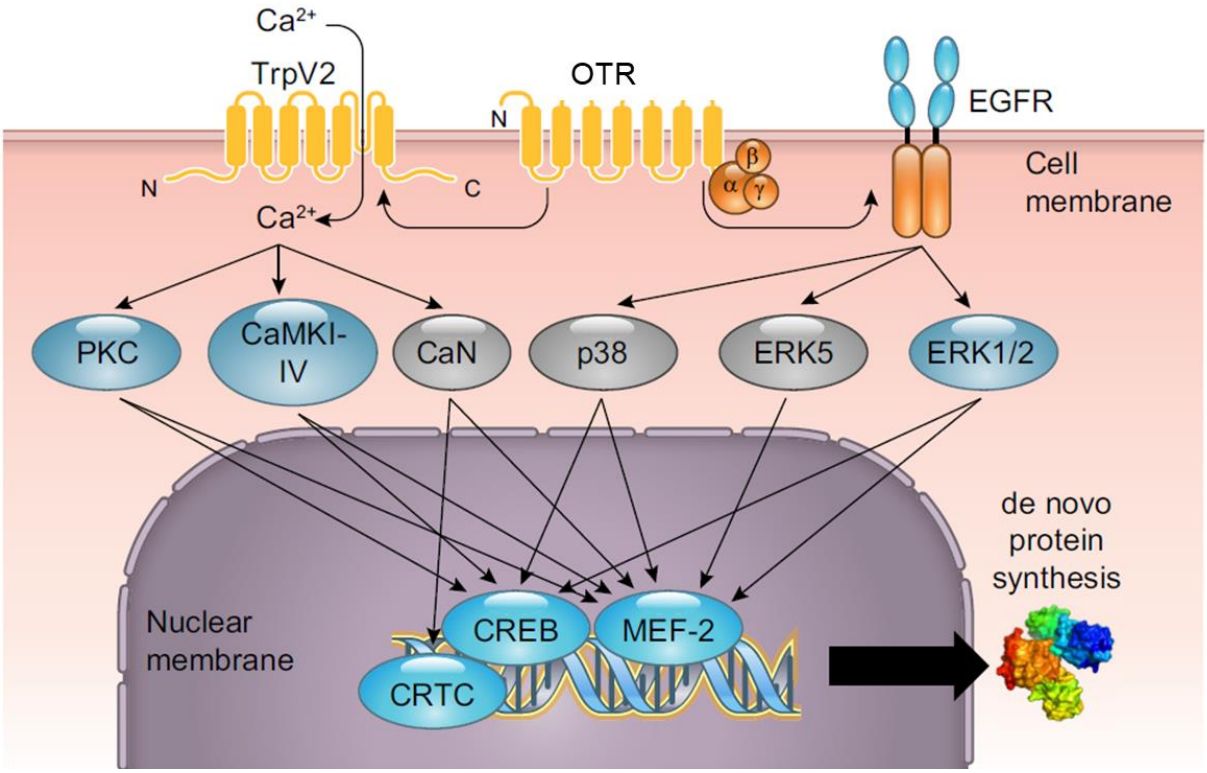

Figure 1. Overview of oxytocin receptor (OTR)-coupled signaling pathways in neurons. Binding of oxytocin to the OTR activates transient receptor potential vanilloid type 2 (TRPV2) channels and subsequent Calcium (Ca^{2+})-dependent cascades including protein kinase C (PKC), Ca^{2+}/calmodulin-dependent kinase (CaMK) I, II, IV, and calcinueurin (CaN). OTR activation also induces transactivation of the epidermal growth factor receptor (EGFR) and subsequent MAPK activation involving the extracellular signal regulated kinase (ERK) 1/2, ERK5, and p38. The signaling pathways converge on the transcription factor cyclic AMP responsive element binding protein (CREB) and cyclic-AMP-regulated transcriptional coactivators (CRTC) as well as myocyte enhancer factor 2 (MEF2), leading to the transcription of target genes. Adapted from (Jurek and Neumann, 2018).

The MEF2 proteins show distinct but overlapping sets of functions (Pon and Marra, 2016). They play an important role in muscle and cardiac cell development and affect cell differentiation, proliferation, migration, apoptosis, and metabolism (Potthoff and Olson, 2007). Furthermore, they are implicated in fundamental cellular processes in the central nervous system including neuronal morphology, survival, connectivity, plasticity, and metaplasticity (Akhtar *et al.*, 2012; Chen *et al.*, 2012; Meyer *et al.*, 2018; Meyer *et al.*, 2020). These processes are strongly intertwined since neuronal connectivity and plasticity are regulated by adaptations of the cellular morphology including neurite outgrowth, synapse formation, and cell adhesion, depending on the temporary requirements. Changes in the cellular morphology, like branching dendrites and axons or the generation of dendritic spines mediated via the cytoskeleton, serve to make wiring

among networks more efficient (Chklovskii, 2004). Therefore, the balance of these processes is essential for proper cognitive function and has to be maintained.

Dysfunctions concerning the MEF2 family have been associated with ASD, mental retardation, amyotrophic lateral sclerosis, Alzheimer's, and Parkinson's disease (Morrow *et al.*, 2008; Lipton *et al.*, 2009; Tu *et al.*, 2017).

Thus, a balanced activity of the OT system is crucial for essential behavioral responses. Genetic or epigenetic factors may influence this by contributing to individual differences in behavioral responses. Among the genetic factors that might lead to a predisposition for the development of certain psychosocial disorders like ASD are single nucleotide polymorphisms in the *OTR* gene (Bakermans-Kranenburg and van Ijzendoorn, 2014).

1.4 Single nucleotide polymorphisms in the oxytocin receptor gene

A single nucleotide polymorphism (SNP) is a variation in a single nucleotide occurring at a specific position in the genome, which is carried by more than 1 % of individuals in a population. Of the 4-5 million SNPs mapped so far in the human genome, just a few percent are within protein-coding genes, while the majority lies within regulatory or inactive regions (Freedman *et al.*, 2011; Edwards *et al.*, 2013). Depending on their location in coding or non-coding sequences within a given gene, they can affect the protein in various ways. For instance, SNPs outside the coding sequence like introns, promoters, untranslated regions, and exonal non-coding regions can regulate the gene splicing or transcription factor binding. When they are located within the coding region of an exon, they can be either synonymous or non-synonymous. Synonymous SNPs do not affect the protein sequence whereas non-synonymous SNPs result in an amino acid change in the protein. A change in the amino acid sequence affects the protein structure and its function. Thus, non-synonymous SNPs are believed to have the highest impact on the phenotype. How non-synonymous SNPs could affect the phenotype is not fully understood, however, mutations present in genes can affect transcriptional and translational output (Robert and Pelletier, 2018).

Genome-wide association studies (GWAS) that identify genetic variants linked with a specific phenotype, e.g. a disease, are a quite recent achievement, further facilitated by the declining costs and proceeding methods of high-throughput sequencing. SNP detection developed fast and

has become a major part of modern medical research. Each SNP that has been identified receives a reference ID number and can be found in online databases such as dbSNP hosted by the National Center for Biotechnology Information (NCBI) or SNPedia. The gain of knowledge by SNP studies contributes to the identification of avoidable risks or tailor-made prevention leading to personalized life-style profiles and diet recommendations provided by companies. They are promoted as a big step towards personalized medicine since SNPs cannot only determine one's susceptibility to certain diseases but also the success of a therapy.

GWAS have revealed several genetic variants of the *OTR* that have been associated with various traits and behaviors in humans, psychosocial disorders or pathological conditions (International HapMap *et al.*, 2007) (Figure 2).

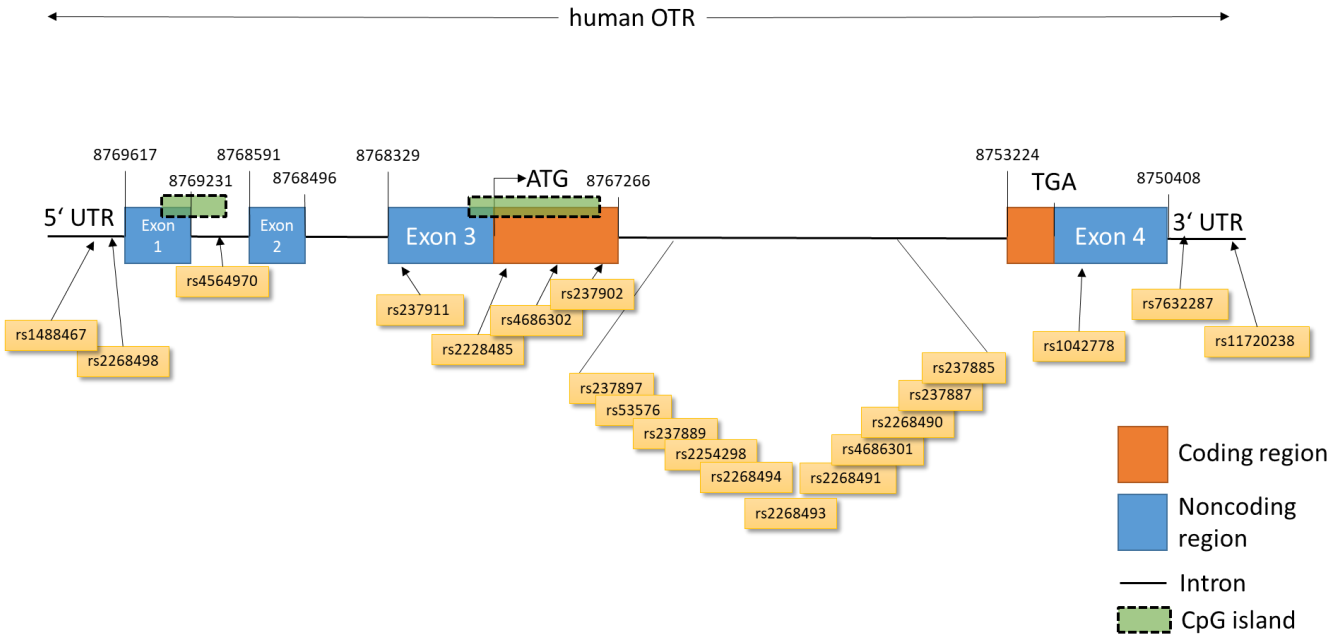

Figure 2. Overview of single nucleotide polymorphisms (SNPs) in the human oxytocin receptor (OTR) gene on chromosome 3 consisting of four exons and three introns. SNP IDs are given in orange boxes below and chromosomal positions indicated in numbers above. Only SNPs that have been associated with psychological or psychiatric traits have been included. Data extracted from ensembl data base. Adapted from (Jurek and Neumann, 2018).

The associated features comprise social behavior and communication, cognition, parental care, empathy, and symptoms that are allocated e.g. to attention deficit hyperactivity disorder, depression or schizophrenia (Walum *et al.*, 2012; Klahr *et al.*, 2015; Skuse *et al.*, 2014; Weisman *et al.*, 2015). Most of the associations in the *OTR* gene however, have been related to ASD.

Therefore, besides dysregulated plasma OT concentrations, *OTR* SNPs have been promoted as possible biomarkers for social impairments in ASD (Parker *et al.*, 2017).

However, although intensely studied, the association between ASD and SNPs in the *OTR* gene remains controversially discussed. Several studies show contradictory results about the presence of a specific SNP and its contribution to the etiology of a given disorder.

Several associations of SNPs could not be replicated and often disappeared after correction for multiple comparisons (Campbell *et al.*, 2011; Tansey *et al.*, 2010; Wermter *et al.*, 2010). An example repeatedly reported in this context is rs237887, where the association was found to be dependent on the behavioral tests performed. While few studies found the 'A' allele of rs237887 was not associated with ASD diagnosis, others confirmed an association with e.g. reduced face-recognition memory in families with an autistic child or impaired altruism in two separate behavioral tasks (Skuse *et al.*, 2014; Verhallen *et al.*, 2017).

It is not known whether disruptions in oxytocinergic signaling contribute to a risk for ASD or are associated with variability in social deficiency in ASD.

Since intranasally applied OT is considered to act through the OTR, the efficacy and inconsistent findings on symptom improvement might depend on SNPs in the *OTR* gene that might cause some loss or gain of functions. However, there are just very few studies about the functional significance of SNPs (Fueg *et al.*, 2019; Furman *et al.*, 2011). Therefore, studies regarding the molecular effects of SNPs, their role and possible combinatory effects are greatly needed to bridge the gap between genetic association and function.

1.5 Aim of the thesis

The aim of my thesis was, to study the molecular mechanisms and effects following OTR activation in order to understand the cellular changes in the context of psychosocial disorders and emotional dysfunctions. During the course of my PhD, I studied the OT system *in vitro* focusing on various intracellular aspects. After stimulating cells with OT, I identified activated signaling pathways and their consequences on cellular processes like neuronal morphology, neuronal connectivity, cell viability, mitochondrial function, and ATP production (Figure 3). Further, considering common genetic aberrations in the *OTR* gene leading to different OTR

protein variants, I assessed how this affects the receptor stability, a selection of already known coupled signaling cascades and the expression of downstream target genes.

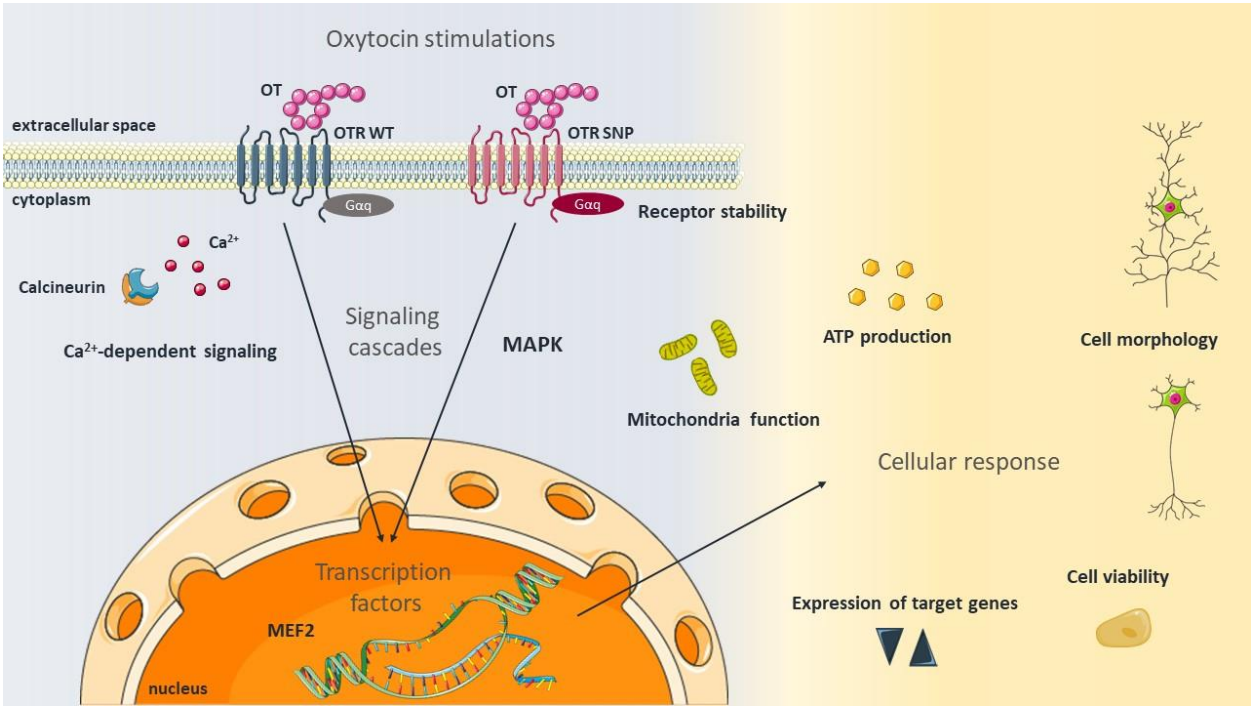

Figure 3. Aim of the thesis. This thesis aimed to assess the oxytocin (OT) -induced effects on signaling cascades including the mitogen-activated protein kinase (MAPK) pathway as well as calcium (Ca^{2+}) signaling and downstream activated transcription factors like the myocyte enhancer factor (MEF) 2. Additionally, the aim was to assess the consequences for various cellular parameters such as mitochondria function, ATP production, the expression of target genes, cellular morphology and viability as well receptor stability, also with regard to the activated oxytocin receptor (OTR) variant. The schematic art pieces used in this figure were provided by Servier Medical art (http://servier.com/Powerpoint-image-bank). Servier Medical Art by Servier is licensed under a Creative Commons Attribution 3.0 Unported License.

2 Oxytocin alters the morphology of hypothalamic neurons via the transcription factor myocyte enhancer factor 2A (MEF2A)

2.1 Abstract

OT has gained attention not only as anxiolytic drug and as potential treatment option for autistic children; it also acts as a growth and differentiation factor in neuronal cells. While behavioral effects of OT have been studied in detail, knowledge about the cellular effects of OT is relatively sparse. In this study, we present evidence for three hypotheses: 1) OT leads to neurite retraction in hypothalamic neurons via the OTR 2) The transcription factor MEF2A is a central regulator of OT-induced neurite retraction, and 3) The MAPK pathway is critical for OT-induced MEF2A activation. Incubation of rat hypothalamic H32 cells with 10 nM to 1 µM OT, vasopressin, and the specific OTR agonist TGOT, over the course of 12 h resulted in a time-dependent, significant retraction of neurites. In addition, the size of the nuclear compartment increased, whereas the overall cell size remained unchanged. OT treatment for 10 h increased the cellular viability significantly, and this effect could be blocked by a specific OTR antagonist, providing evidence for a specific and pro-active effect of OT on neurite retraction, and not as an unspecific side effect of apoptosis. The molecular mechanism that controls OT-induced neurite retraction includes a reduced phosphorylation of the transcription factor MEF2A at S408. This dephosphorylation is under the control of the OTR-coupled MAPK pathway, as blocking MEK1/2 by U0126 inhibited MEF2A activation and subsequent neurite retraction. The siRNA-mediated knockdown of MEF2A prevented the OT-induced neurite retraction, providing direct evidence for a role of MEF2A in morphological alterations induced by OT treatment. In summary, the present study reveals a previously unknown OTR-coupled MAPK-MEF2A pathway, which is responsible for OT-induced neurite retraction of hypothalamic neurons.

2.2 Introduction

The neuropeptide OT is a central modulator of complex socio-emotional behavior, such as anxiety, affective behavior, and aggression (Jurek and Neumann, 2018; Kosfeld *et al.*, 2005; Kumsta and Heinrichs, 2013; Neumann and Landgraf, 2012). The molecular underpinnings of these behavioral effects are largely unknown. The OTR is almost ubiquitously expressed in the

central nervous system (Grinevich *et al.*, 2016; Jurek and Neumann, 2018), most notably in the hypothalamus, the site of OT synthesis. The OTR is a G protein coupled receptor, whose activation by its ligand leads to promiscuous coupling to various Gα-proteins (Busnelli and Chini, 2018), Ca^{2+} release from intracellular stores (Tobin *et al.*, 2011) and subsequent influx of Ca^{2+} from the extracellular space through TrpV2 channels (van den Burg *et al.*, 2015). These G proteins in combination with the Ca^{2+} influx activate several signaling cascades, most prominently the MAP kinase pathway, with its main kinases MEK1/2 and ERK1/2 (Blume *et al.*, 2008; Jurek *et al.*, 2012). MAP kinase pathways have been associated with neurite outgrowth (Won *et al.*, 2015; Kang *et al.*, 2011; Xu *et al.*, 2015), anxiety (Blume *et al.*, 2008; Jurek *et al.*, 2012; Borges *et al.*, 2015), and memory formation (Tomizawa *et al.*, 2003). Downstream effectors of ERK1/2 are the transcription factors CREB (Tomizawa *et al.*, 2003; Jurek *et al.*, 2015) and MEF2 (Devost *et al.*, 2008). MEF2 was originally defined as a muscle-specific factor that binds an A/T-rich element in the promoter of target genes (Gossett *et al.*, 1989), and was later found to be ubiquitously expressed in all types of tissue, especially in the brain (Dietrich, 2013). One central function of MEF2 is the regulation of neuronal morphology, i.e. neurite outgrowth (Flavell *et al.*, 2006), either via gene inhibition or activation. Among the MEF2-regulated genes are immediate-early genes such as c-JUN and NUR77, as well as regulators of neuronal activity, such as ARC, SYNGAP, HOMER1A, and BDNF (Flavell *et al.*, 2006). Consequently, MEF2 represents a central factor for the regulation of neurite outgrowth, synapse formation, and, if dysregulated, was found to play a key role in the development of ASD (Potthoff and Olson, 2007). Here, the functions between OT and MEF2 may overlap, as both are implicated in ASD (Parker *et al.*, 2014; Bales *et al.*, 2013) and neurite outgrowth (Lestanova *et al.*, 2016; Lestanova *et al.*, 2017). However, the literature describes inconsistent effects of OT on cellular morphology. For instance, OT bursts during milk letdown lead to retraction of glial cells in rat dams (Langle *et al.*, 2002; Theodosis, 2002), and *in vitro* application of synthetic OT leads to neurite retraction in hippocampal neurons (Ripamonti *et al.*, 2017); however, when tested in human SH-SY5Y neuroblastoma cells and glial U-87MG cell lines, OT leads to neurite outgrowth (Lestanova *et al.*, 2016; Lestanova *et al.*, 2017). This outgrowth seems to be executed by the rearrangement of actin filaments to the apical part of neuronal cones and paralleled by changes in expression of the intermediate filament protein

nestin, which is implicated in axon growth (Bakos *et al.*, 2012). It is unknown so far, whether the differential effects of OT on neuronal and glial cells, i.e. neurite retraction (Ripamonti *et al.*, 2017) or neurite outgrowth (Lestanova *et al.*, 2016), are caused by the use of different doses of OT, by the use of different cell types (primary neurons or cell lines), different species (mouse, rat, human cells), or even the sex of the cell donor (Li *et al.*, 2016). Therefore, it is of paramount importance to choose a physiological relevant model to investigate the effects of OT on cell morphology. As OT and the OTR are expressed in the hypothalamus of the brain (Jurek *et al.*, 2015; Freund-Mercier *et al.*, 1994; Dabrowska *et al.*, 2011), rat hypothalamic neurons (H32 cells) provide a suitable *in vitro* model to provide a full characterization of the cellular response to OT. A full characterization of the cellular response is pivotal, especially since the OT molecule is known to bind the receptor of the related nonapeptide vasopressin as well at higher concentrations, with the result of mixed OTR and vasopressin receptor-mediated cellular effects. In turn, vasopressin can also bind the OTR, which could result in a similar effect of both peptides on cellular morphology. In order to circumvent any non-OTR-mediated effects we made use of specific antagonists and agonists of the OTR such as Thr^4, Gly^7-OT (TGOT), an OT agonist with a 16.000 times higher affinity for the rat OTR than for the rat vasopressin receptor (Chini *et al.*, 2008; Manning *et al.*, 2008); however, this OTR-specificity is lost in cells of human origin (Chini *et al.*, 2008). The advantage of OTR-specificity of TGOT in rat cells, in combination with the hypothalamic origin, convinced us to conduct comprehensive morphological studies regarding OT's cellular effects in H32 cells. In summary, we aim to contribute to the clarification of the effects of OT on cellular morphology and identify the intracellular signaling cascades that control the observed morphological alterations. In order to do so, we tested the hypothesis that the transcription factor MEF2 is a key regulator of neurite retraction in hypothalamic neurons, and that its activation is dependent on the OTR-coupled MEK1/2-ERK1/2 pathway.

2.3 Materials and methods

2.3.1 Cell culture

Rat hypothalamic H32 cells (passages 15–30) were cultured in 1:1 Dulbecco's Minimum Essential Medium/Ham F12 Medium (growth medium). The growth medium was supplemented with 10 % heat inactivated fetal bovine serum (Capricorn, Germany), 0.1 % nonessential amino acids, 100

U/ml gentamycin (both Invitrogen, Germany) in humidified atmosphere containing 5 % CO_2 at 37 °C. Passaging was performed at least once a week by gentle trypsination.

2.3.2 Cell viability assay

Cellular viability was tested using the PrestoBlue Cell Viability Assay (A13261, Invitrogen) according to manufacturer's protocol. Briefly, 20×10^3 cells per well were seeded the day before the test in a 96-well-plate in growth medium. The volume of the treatment and serum-free medium (DMEM/F12 + 0.1 % BSA, sterile filtered) for the stimulation was calculated to a total of 90 µl per well. 10 µl of PrestoBlue Reagent were added directly to the cells, incubated for 30 min to 2 h, before reading the fluorescence intensity with a FluoStar Plate reader (BMG). Optimal DMSO concentrations as solvent for the U0126 MAPK inhibitor (Sigma Aldrich) were determined by a separate dose response experiment.

2.3.3 Protein isolation

For the extraction of proteins from adherent H32 cells, medium was removed and cells were washed with PBS supplemented with Protease and Phosphatase inhibitors (PI, A32959, Thermo Fisher). Cells were scraped, centrifuged, and the cell pellet was resuspended in 100 µl RIPA lysis buffer (R0278, Sigma Aldrich) with HALT Inhibitor and EDTA (78444, Thermo Fisher) to extract whole cell lysate.

2.3.4 Western blot

Between 5 and 30 µg of whole cell extract and an equivalent volume of 4× loading buffer (2.4 ml TRIS, 0.8 g SDS, 4 ml 100 % Glycerol (AppliChem), 0.01 % Bromphenol Blue (Sigma Aldrich), 1 ml Mercaptoethanol and 2.8 ml H_2O) were applied to 12 % Mini and Midi PROTEAN or Criterion TGX Stain-free gels (456–8044 and 5678045, BioRad). Western blot analysis was performed using the Stain-free total protein method (BioRad) as loading control, according to the manufacturer's protocol. Stain-free gels contain trihalo compounds that covalently bind to tryptophan residues in proteins when exposed to UV light. By that, the proteins are made fluorescent directly in the gel, allowing the immediate visualization of proteins at any point during electrophoresis or blotting and permitting the user to normalize bands to total protein in each lane. This technology circumvents the problematic use of housekeeping proteins as loading controls on western

blots. In order to detect activated MEF2, a phospho-specific MEF2A S408 (CSB-PA000728, Flarebio Biotech) antibody was used at 1:5000 in 5 % BSA concentration. A MEF2A total antibody (#TA307807, OriGene, 1:5000 in 5 % BSA) was used to detect total MEF2A levels. Changes in expression levels were analyzed measuring grey density in a semi-automatic manner by Image Lab Software (Version 6.0, BioRad).

2.3.5 Cell stimulations

Cells were grown in the presence or absence of 10 nM, 100 nM, or 1 µM of OT (Bachem, Germany) for 0, 2, 4, 8, 10, and 12 h in cell culture dishes or 3-part chamber slides (BD Falcon, Germany). A separate experiment was performed using cells incubated with [Thr^4, Gly^7]-oxytocin (TGOT, 100 nM, Bachem) or vasopressin (100 nM, Bachem). When inhibitors (U0126, Sigma Aldrich) or OTR antagonist des-Gly-NH_2*d*$(CH_2)_5$[Tyr(Me)^{2}Thr^4]-OVT (kindly provided by M. Manning) were used, cells were incubated in serum free medium for 1 h, pretreated with the inhibitor or VEH (H_2O or DMSO) for 10 min, and stimulated with the according treatment. To assess the role of MEF2A, H32 cells were transfected with small interfering RNA (siRNA). 3 unique 27mer MEF2A siRNA duplexes (Origene, SR504191; for sequences see Table 1) and Lipofectamine RNAiMAX Reagent (Invitrogen), diluted in OptiMEM were added for 72 h in a concentration of 1 nM siRNA. To verify the specificity of the knockdown, additional wells were transfected with a scrambled siRNA CONTROL (siCTRL, SR30004). Effects of OT were assessed via co-stimulation with 100 nM OT for 24 h.

Table 1. MEF2A siRNA duplex sequences. All three duplexes were mixed 1:1 and added for transfection.

siRNA	Duplex sequence
SR504191A	rGrArArCrUrUrUrCrUrGrCrArArGrGrArUrArArArArUrATT
SR504191B	rGrArUrArUrUrGrArArGrArArArArUrUrArGrCrUrUrCrUGA
SR504191C	rCrUrUrArArArUrUrGrGrUrGrArArUrArArGrGrArCrArUGA

2.3.6 Morphological assessments

The cells grown in chamber slides were washed with 1 ml PBS and subsequently fixed by gently adding an equal amount of 4 % paraformaldehyde (PFA, Sigma-Aldrich, Germany), resulting in 2 % PFA on the cells. After 2 min, this solution was discarded and replaced by 4 % PFA for 15 min at room temperature. The fixed cells were washed three times with PBS and permeabilized by 500 µl PBS containing 0.1 % Triton X-100 (Sigma-Aldrich, Germany) for 5min. Unspecific binding sites were blocked by 30 min in PBS +0.1 % Triton and 10 % NGS. The actin filaments were stained by addition of 20 µl of 3.8 µM phalloidin tetramethylrhodamine B isothiocyanate (Sigma-Aldrich, Germany) directly on the cells without access to light for 20min. Phospho-MEF2A S408 specific antibody was diluted 1:500 in 5 % BSA/PBS-T and incubated on the cells overnight at 4 °C and gentle rocking. Nuclei were stained by addition of Gold anti-fade mounting medium containing 4,6-diamidino-2-phenylindole (DAPI; Life Technologies, Germany). Cells were observed using the confocal microscope Leica SP8. Images were taken from four random fields per chamber. Neurite outgrowth was determined by manually tracing the length of the longest neurite per cell (using Fiji 1.51k) for all cells in a field that had an identifiable neurite and for which the entire neurite arbor could be visualized. Length of the neurite was measured from the edge of nucleus to the apical end of the projection. Four independent members of the team evaluated neurite length in a blinded manner. Hereby the MAX intensity Z-Projection was analyzed. DAPI images were used for nucleus size measurements and as MASK for mean intensity analysis of MEF2A S408 phosphorylation exclusively in the nucleus. To assess the size of the cells, whole area measurements were performed by outlining the Phalloidin stained area. During all the measurements, grayscale images were processed. To control for staining artifacts with Phalloidin or fixation artifacts we employed a second staining approach using the ZOE Fluorescence

microscope (Bio-Rad) and live cells in cell culture dishes. For nucleus staining, Hoechst 33342 stain (Thermo Scientific, H1399) was added to the stimulation medium and incubated for 30 min at 37 °C. Hoechst staining is non-toxic and can therefore be used in living cells. After 20 min, 1× Plasmagreen membrane stain (Thermo Scientific, C37608) was added to the medium and co-incubated for at least 10 min at 37 °C to label the cell plasma. This method circumvents any potential artifacts that could arise by the use of a specific Actin staining like Phalloidin. Cells were washed two times with 1× PBS before imaging of the blue (nuclei) and green (cell plasma) channel. All Pictures were analyzed using ImageJ Fiji software.

2.3.7 Statistical analysis

Data were pooled and analyzed using SigmaPlot 13. Parametric data was analyzed by t-test or one-way analysis of variance (ANOVA), followed by Holm Sidak post hoc test. Non-parametric data was analyzed by the Kruskal-Wallis ANOVA on ranks and the Tukey post hoc test, or in case of different group sizes, Dunn's post hoc test. Statistical differences were accepted at $p < 0.05$. For morphology analysis experiments with large n-numbers, analysis of effect size was performed. As indicator of effect size, either Cohen's f^2-value where $f^2 < 0.02$ is considered as small effect size, $f^2 = 0.15$ is considered as median $f^2 > 0.35$ as strong effect or eta squared (η^2), where $\eta^2 < 0.039$ is considered as small effect, $\eta^2 < 0.06–0.110$ as intermediate, and $\eta^2 > 0.14$ as strong effect, was calculated. Data are presented as means ± or + standard error of the mean (SEM), as indicated in the figure legend.

2.4 Results

2.4.1 OTR activation mediates OT-induced changes in neurite length and nucleus size

Increasing concentrations (10 nM, 100 nM, and 1 µM) and treatment duration (0, 2, 4, 6, and 8 h) of OT were tested with rat hypothalamic H32 cells, in order to reveal dose- and time-dependent effects of OT treatment on neurite outgrowth (Figure 4A). VEH-treated cells elongate their neurites over a time course of 10 h significantly from about 37 µm up to 45 µm (# $p < 0.05$ 10 h vs 2 h). In contrast, OT treated H32 cells retracted their neurites from about 37 µm to about 27 µm over time and in a dose-dependent manner. In detail, 100 nM OT significantly reduced

neurite length (* $p < 0.05$ vs VEH, intermediate effect $f^2 = 0.123$) after 2 h, with further retraction of neurites until 10 h of treatment. 1 µM of OT induced a slower onset of neurite retraction (significant at 4 h), but with a more prominent effect size (* $p < 0.05$ vs VEH, strong effect $f^2 = 0.477$). After 8 and 10 h of cell stimulation, all treatment groups showed a reduced neurite length (* $p < 0.05$ vs VEH, median effect $f^2 = 0.267$ after 8 h, very strong effect $f^2 = 0.77$ after 10 h). As H32 cells also express the vasopressin receptor V1a, we tested whether the observed neurite retraction is mediated by the OTR, V1a, or a combination of both. Therefore, we incubated the cells with vasopressin or the specific OTR agonist TGOT. Similar to the OT-induced effect, vasopressin and TGOT (both 100 nM) significantly reduced neurite length over time (Figure 4B; * $p < 0.05$ vs VEH). However, vasopressin showed a slower onset of action compared to OT and TGOT, as after 2 h neurite length was not altered by vasopressin, but significantly reduced by OT and TGOT (100 nM; * $p < 0.05$ vs VEH, intermediate effect $f^2 = 0.123$). Despite the slow onset of vasopressin action, after 4, 8, and 10 h, neurite length was significantly reduced in all treatment groups (* $p < 0.05$ vs VEH). To further dissect the morphological changes described in Figure 4A and B, we analyzed the OT-induced neurite length, whole cell size, and nucleus size separately in presence or absence of an OTR antagonist. We found that the OT-induced neurite retraction can be blocked by the specific OTR antagonist des-Gly-NH_2*d*$(CH_2)_5$[Tyr(Me)^{2}Thr^4]-OVT (* $p < 0.05$ vs VEH, # $p < 0.05$ vs OT, Figure 4E), indicating that OT acts via the OTR on cellular morphology. There was no effect of OT or the antagonist on the whole cell size (i.e. total area covered by perikaryon, nucleus, and neurites), indicating a specific effect on cell shape, rather than growth or shrinking (Figure 4F). However, the size of the area stained by DAPI (a rough indicator of transcriptional activity) was increased by OT, and this effect was not reversed by the OTR antagonist, indicating OTR-independent transcriptional activity (* $p < 0.05$ vs VEH, Figure 4G).

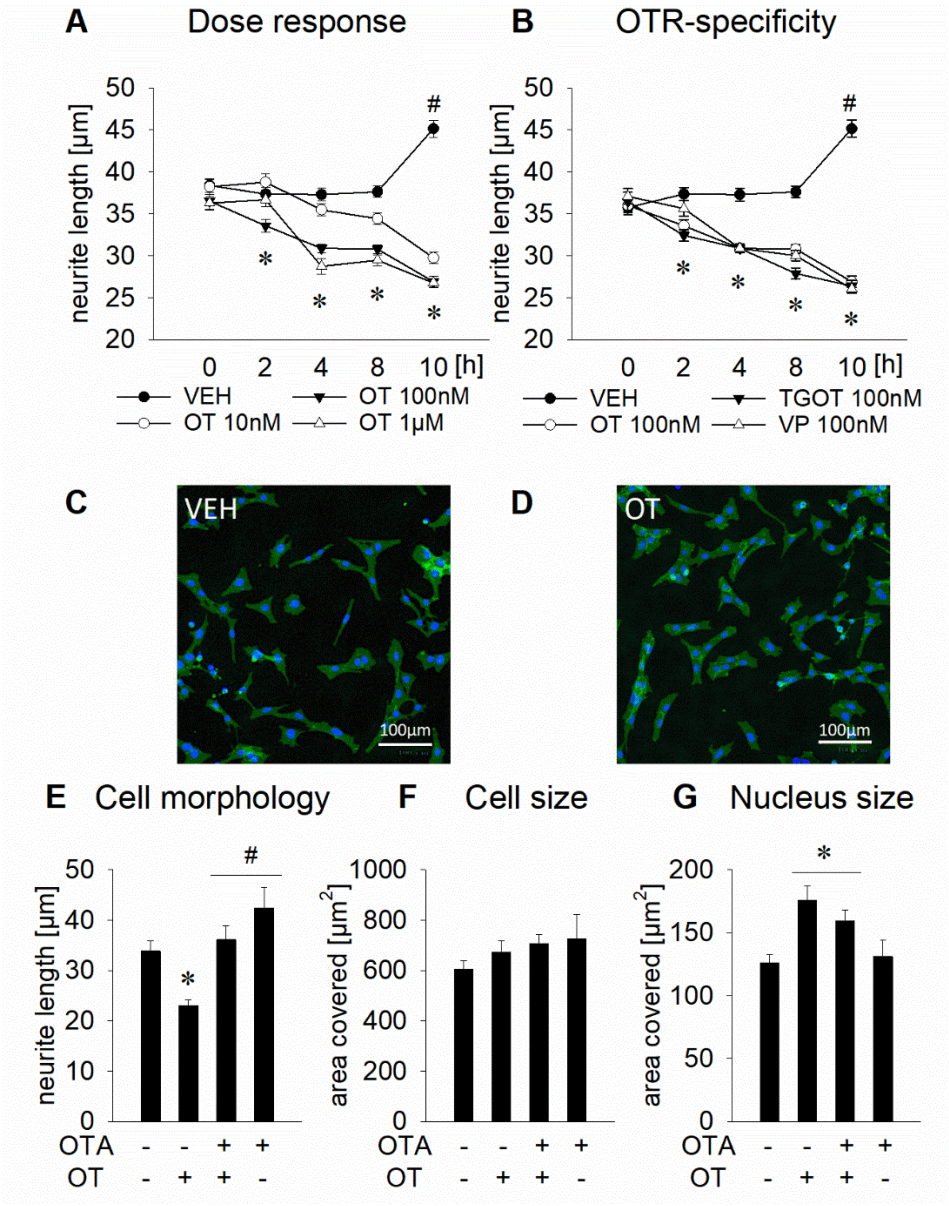

Figure 4. Effects of an OTR activation on neuronal morphology in rat hypothalamic H32 cells. (A) Mean neurite length of H32 cells determined at increasing OT concentrations from 0 h to 10 h. Neurite length decreases significantly from about 37 µm to about 27 µm over the course of 10 h of OT stimulation at 10 nM, 100 nM, or 1 µM; while VEH treated cells show increased neurite length after 10 h. * $p < 0.05$ vs VEH, #<0.05 vs previous timepoint. n = 314–628 cells. (B) Incubation of H32 cells with OT (100 nM), the OTR agonist TGOT (100 nM), or vasopressin (VP, 100 nM) over 10 h leads to neurite retraction to a similar extent as seen in Figure 4A. n = 314–801 cells. (C) and (D) Representative pictures of non-treated H32 cells (C) and 100 nM OT-treated cells (D) for 4 h; cytoplasm, including neurites stained with CellMask plasma membrane stain (green) and nuclei stained blue with Hoechst 33342. Scale bar represents 100 µm. (E) Neurite retraction of OT-treated H32 cells after 12 h of stimulation is reversed when incubated with the OT antagonist (OTA, des-Gly-$NH_2d(CH_2)_5$[Tyr(Me)^{2}Thr^4]-OVT). The OTA alone has no effect on neurite length. * $p < 0.05$ vs VEH, # < 0.05 vs OT-treated cells. (F) Whole cell size analyzed as mean of total area covered by individual cells (i.e. perikaryon, nucleus, and neurites). No effect of the treatment was determined. (G) Overnight treatment of H32 cells with 100 nM OT led to an increase of area stained by DAPI, indicative of the size of the nuclear compartment. The OTA reduced the increase of size of the nuclear compartment, without reaching basal levels. * $p < 0.05$ vs VEH. Data represents mean + SEM. n = 21–74 cells.

2.4.2 OT leads to a MAPK-dependent neurite retraction as well as increased cell viability, whereas vasopressin affects neurite length MAPK-independently

In order to exclude technical artifacts of the CellMask staining protocol in living cells used in Figure 4, we successfully reproduced our initial finding of reduced neurite outgrowth by 100 nM OT treatment with a different staining protocol (fixated cells, actin filament staining with Phalloidin, and evaluation by confocal microscopy; Figure 5A, * $p < 0.05$, intermediate effect size $\eta^2 = 0.078$). When pretreated with the MAPK inhibitor U0126 (10 µM) the effect of OT was blocked, suggesting a central role for the MAPK pathway in the OT-induced neurite retraction. Surprisingly, vasopressin also reduced neurite length, in presence or absence of U0126, indicating that neurite retraction by vasopressin is coupled to a separate, yet unknown pathway (* $p < 0.05$, intermediate effect size $\eta^2 = 0.078$). However, a partial role of the OTR cannot be excluded, as vasopressin also binds the OTR with a comparable affinity (Manning et al., 2008). Overnight stimulation with the specific agonist TGOT did not result in significantly altered neurite length. As stimulation with TGOT for only 10 h decreased neurite length from 37 to 27 µm (Figure 4A), but after prolonged (overnight) OT stimulation morphology changes were reversed to basal, we hypothesize that the exclusive OTR response is short lived (max. 10 h) and requires the additional activation of the vasopressin receptor for a prolonged response. Consequently, Figure 4B and 5A indicate that, in contrast to the fast and short-lived OTR response, vasopressin has a slow onset of action on neurite retraction (no effect after 2 h, Figure 4B), but bigger effect after prolonged incubation (overnight, mean difference of the neurite length compared to the non-treated group: −8.98 µm for VP vs. −6.47 µm for OT, Figure 5A). Morphological assessments of neuronal cells should only be conducted under optimal culturing conditions, which led us to control our experimental setup for general cell viability (i.e. ability to reduce resazurin to resafurin) and cell proliferation (cell number). Both OT and vasopressin treatment increased cellular viability, as reflected by the increased amount of resafurin, suggesting a pro-active, and not apoptosis-induced retraction of neurites. In addition, the OT-induced increase in cell viability is MAPK-dependent, as pretreatment with U0126 blocked this effect (Figure 5B). Comparable to the MAPK-independent effect of vasopressin on neurite length (Figure 5A), cell viability of vasopressin-treated cells was increased, independent of MAPK inhibition, thereby again

excluding a role for the MAPK pathway in vasopressin-mediated effects. Moreover, in support of our hypothesis of a short-lived nature of the OTR response, neurite outgrowth (Figure 5A) and cell viability (Figure 5B) returned to baseline after an overnight incubation with TGOT. This finding was further supported by the lack of effect of TGOT on cell proliferation, in contrast to the dose dependent increase of proliferation by 100 nM or 1 µM OT overnight treatment (* $p < 0.05$, Figure 5C).

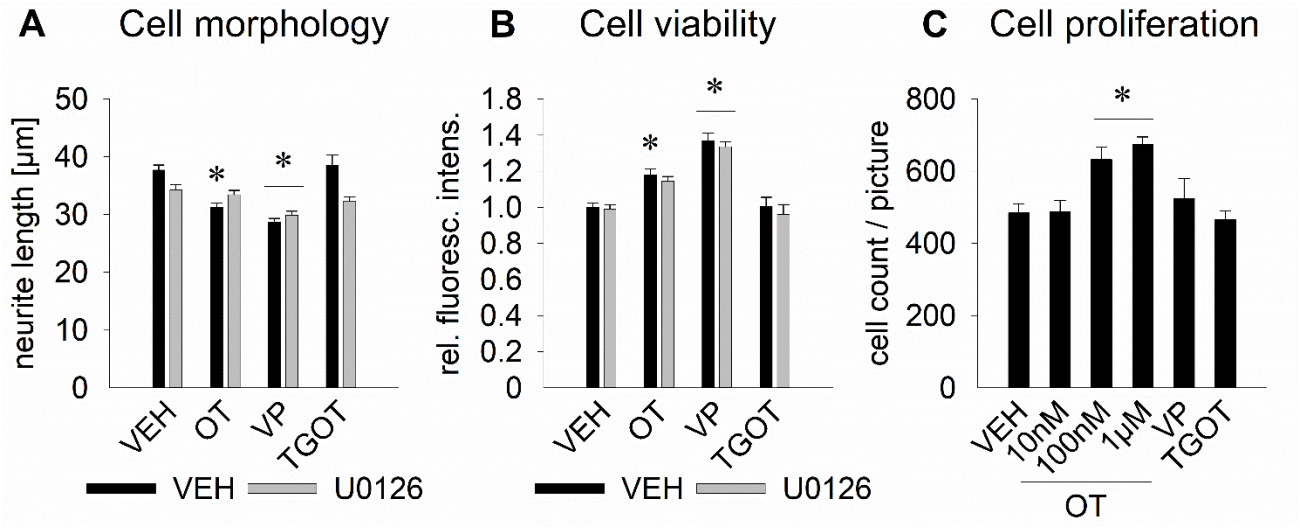

Figure 5. Effects of OTR activation on cell morphology, viability, and proliferation in rat hypothalamic H32 cells. (A) Effect of overnight incubation with 100 nM OT, vasopressin (VP), or TGOT, in presence or absence of the MEK1/2 inhibitor U0126 (10 µM) on neurite length in H32 cells. OT reduces neurite length significantly and in dependence of the MAPK pathway, whereas VP leads to neurite retraction independently of the MAPK pathway. TGOT has no significant effect. n = 65–200. (B) The effect on neurite length is accompanied by increased cell viability, which is blocked by U0126 in the OT-, but not in the vasopressin-treated cells. n = 18–48 wells. (C) Dose dependent increasing proliferation of cells treated with 10 nM (no effect), 100 nM (+~100 cells) and 1 µM OT (+~120 cells), but lack of effect with 100 nM VP and TGOT. n = 4–5 pictures. * $p < 0.05$ vs respective VEH. Data represent mean + SEM.

2.4.3 OT increases transcriptional activity of MEF2A

As increased nucleus size is a rough indicator for open chromatin, i.e. increased transcriptional activity, we tested the activation status of the transcription factor MEF2A by assessing its phosphorylation at S408. At this residue, dephosphorylation leads to transcriptional disinhibition. Western Blot analysis revealed that incubation with 100 nM OT led to a reduced level of phospho-MEF2A S408 in whole cell lysate in a MAPK-dependent manner, indicating increased transcriptional activity (Figure 6A). The observed changes were validated by

immunohistochemical stainings, which revealed reduced intensity of pMEF2A S408 staining in the nuclear compartment, while staining in the cytoplasm was virtually absent (Figure 6B and 6C), indicating a dephosphorylation event in the nucleus and not translocation of pMEF2A S408 to the cytoplasm.

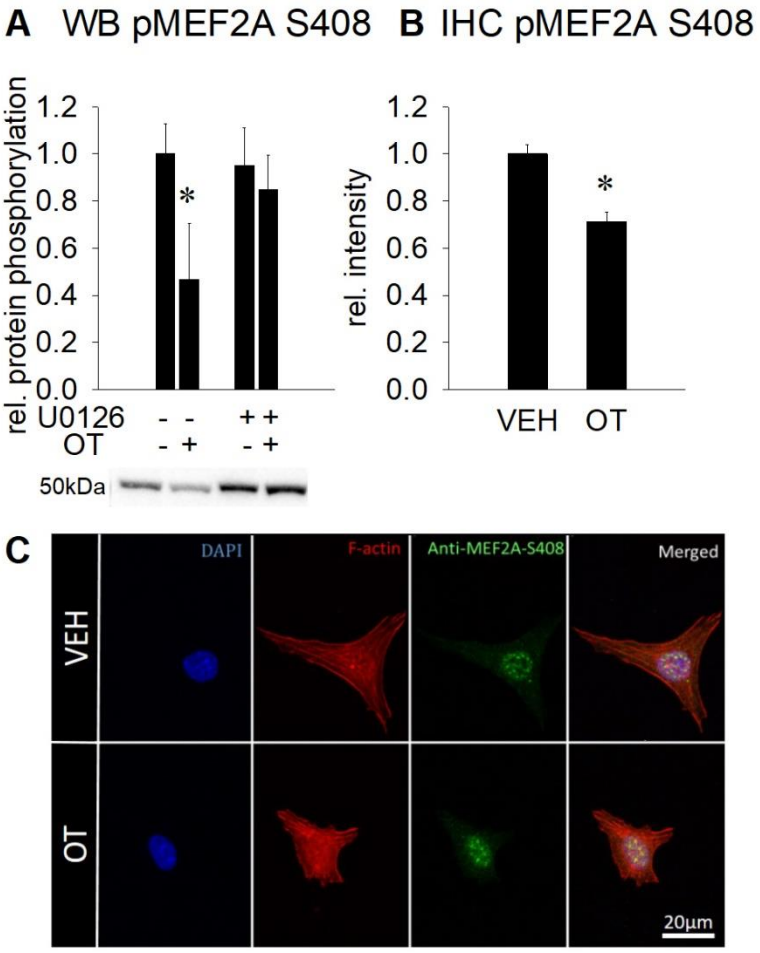

Figure 6. Effect of OT on phosphorylation of S408 and localization of MEF2A. (A) Relative MEF2A S408 phosphorylation analyzed by Western Blot in whole cell lysate after treatment with VEH, OT, in presence or absence of MAPK inhibitor U0126, with representative Blot picture below. Incubation of H32 cells with 100 nM OT over 12 h led to a ~ 50 % dephosphorylation of MEF2A at S408 compared to VEH treated. This effect is mediated via the MAPK pathway as it is reversed to basal by U0126 (10 µM). U0126 treatment without OT had no effect on MEF2A phosphorylation. n = 8. (B) Intensity of IHC stained pMEF2A S408 in the nucleus of H32 cells treated with VEH or 100 nM OT. * $p < 0.05$ vs VEH. n (VEH) = 22, n (OT) = 13. (C) Representative images of IHC staining for pMEF2A S408 in H32 cells. Images were sequentially recorded for chromatin (DAPI, blue, first column), F-actin (Phalloidin, red, second column), and anti-pMEF2A S408 (green, third column). Merged images are shown for each row in the fourth column. Labels left to the columns indicate the respective treatment for 12 h. Scale bar represents 20 µm. Data represent mean + SEM.

2.4.4 OT-induced neurite retraction is reversed by MEF2A knock down

To provide a causal link between the activation of MEF2A and the neurite retraction induced by OT, we specifically knocked down MEF2A in H32 cells by siRNA, and assessed the effects of OT on neurite length 72 h after transfection, a time point where the knock down was most effective.

MEF2A protein levels were highly effectively reduced by 85 % of the baseline level, and OT treatment did not affect this knock down (Figure 7A). Scrambled siRNA (scrRNA) served as transfection control and did not alter MEF2A protein levels significantly compared to non-transfected cells. Neurite length in cells that were transfected with scrambled or siRNA averaged around 47 µm (as compared to ~ 37 µm of non-transfected, 12 h cultured cells in Figure 4E), as a result of prolonged culturing protocol, necessitated by the preceding transfection procedure. Statistical analysis by one way ANOVA did not reveal a significant difference. However, separate statistical analysis by direct comparison of the control (-MEF2A siRNA/+OT) versus the MEF2A knock down (+MEF2A siRNA/+OT) groups confirmed the observed OT-induced reduction in neurite length whereas, in contrast, this effect was prevented by MEF2A knock down (Figure 7B). The lack of effect of OT on neurite length when MEF2A is knocked down reveals the central role of MEF2A in the regulation of cellular morphology by OT.

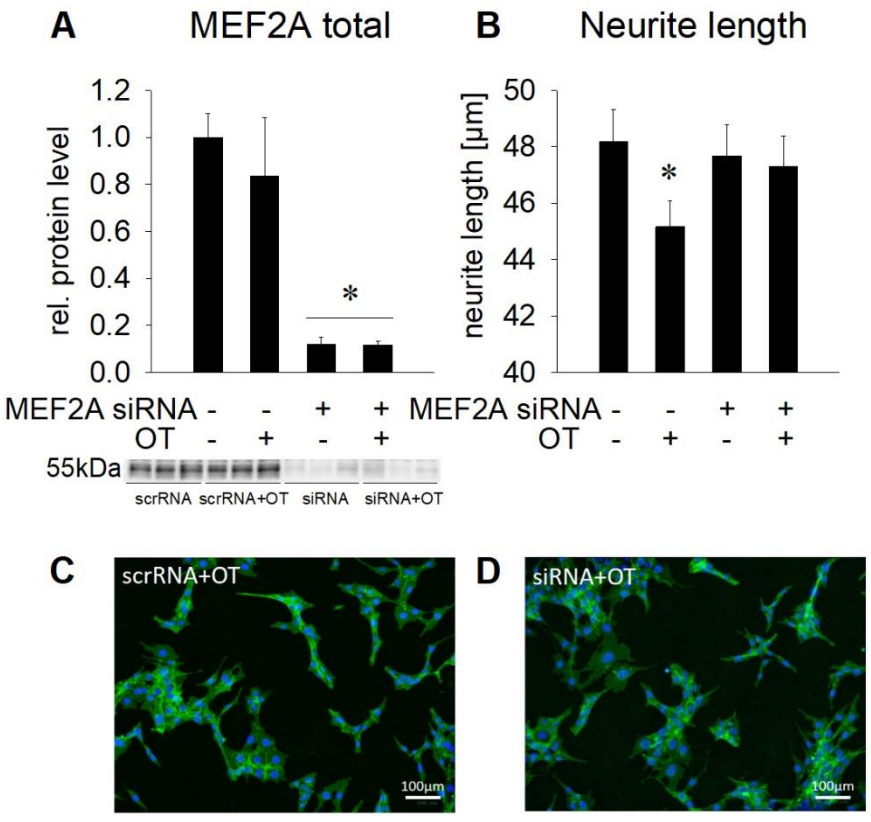

Figure 7. Effect of MEF2A knockdown on neuronal morphology. (A) Relative MEF2A protein expression in whole cell lysate after treatment with 1 nM scrRNA or 1 nM MEF2A siRNA for 72 h and overnight stimulation with 100 nM OT. Total MEF2A protein is reduced after treatment with MEF2A siRNA compared to scrRNA-treated cells, which served as control. Representative Blot below the graph. n = 6. (B) Changes in the neurite length of H32 cells treated with either scrRNA or MEF2A siRNA in presence or absence of 100 nM OT. n = 339–336 cells. * $p < 0.05$ vs scrRNA control. Data represent mean + SEM. (C) and (D) Representative pictures of H32 cells treated with scrRNA + OT (C) or siRNA + OT (D); cytoplasm, including neurites stained with CellMask plasma membrane stain (green) and nuclei stained blue with Hoechst 33342. Scale bar represents 100 µm.

2.5 Discussion

In this study, we provide evidence for the ability of OT to induce neurite retraction in hypothalamic neurons *in vitro*. Specifically, we show that OT stimulation of H32 cells reduced neurite outgrowth in a dose- and time-dependent manner, without changes in whole cell size and under conditions of optimal cell viability. TGOT-induced neurite retraction, and the blockade of the OT-effect by a specific OTR antagonist provide evidence for the central role of the OTR, while the activation of the V1a receptor contributes to this effect with a prolonged cellular response. The signaling cascade coupled to the OTR and being responsible for the neurite retraction is the MEK1/2-ERK1/2 MAPK cascade. In previous studies we could show that OT infused into the PVN activates the MEK1/2 – ERK1/2 cascade in male rats (Blume *et al.*, 2008), and similar effects of endogenous OT were found during pregnancy and in lactation in female rats (Jurek *et al.*, 2012). When OT is applied into the hypothalamic PVN, it reduces anxiety-like behavior in a MEK1/2-dependent manner (Jurek *et al.*, 2012; Blume *et al.*, 2008), indicating a behavioral relevance for this pathway. It remains to be elucidated, whether the OT-induced neurite retraction, which is also MEK1/2-dependent, underlies the decreased anxiety-like behavior in rats.

In this study, we could also identify the transcription factor that lies downstream of the MAPK pathway, MEF2A. To our knowledge, there is only one preliminary report on a link between the OTR and MEF2, and that has been described to be the big MAP kinase ERK5 (also known as bmk1) in myometrial cells (Devost *et al.*, 2008). Here, we reveal this link to be existent also in neuronal cells. In addition, the elusive functional relevance of this pathway could, at least in neurons, be pinned down to the regulation of neurite outgrowth. In the original publication, Devost and colleagues described the activation of MEF2 as ERK5-dependent using U0126 - a non-specific MEK1/2 inhibitor that also targets ERK5. Thus, the possibility of an OTR-ERK5-MEF2 pathway also exists in neurons. However, ERK5 expression in the brain decreases dramatically after the early embryonic phase (Liu *et al.*, 2003), and we could not detect ERK5 phosphorylation in H32 cells by OT stimulation (own unpublished data). Therefore, we suppose that the blockade of MEK1/2 by U0126 is causal for the inhibited effect of OT on neurite outgrowth.

Interestingly, OT had no effect on the overall cell size (consisting of the area covered by perikaryon, nucleus, and neurite processes). This indicates that neurite retraction is a consequence of rearrangement of actin filaments rather than of cell shrinking or growing. As Phalloidin staining does not differentiate between axons and dendrites in our cell culture experiments but stains actin filaments, it remains to be addressed, whether dendrites or axons of OTR-expressing neurons in the brain are affected by the OT treatment. Specific staining techniques, such as immunostaining using MAP2 antibodies for dendrites, and Tau for axons are feasible methods to settle those open questions *in vitro*. However, assessing cellular morphology *in vivo*, especially in the PVN, is difficult to achieve since axons and dendrites are extremely intermingled and difficult to map in this region (own observation). In addition to changes in the cytoplasmic actin filaments, the area covered by nucleus staining was increased in OT treated cells. However, we used DAPI, a specific stain for chromatin only, but not the total area covered by the nuclear compartment, nor the nuclear membrane. As an increased area covered by chromatin is indicative of increased gene transcription activity, future studies need to reveal the nature of the target genes of MEF2. In this context it is worth-mentioning that there exist genome-wide data on MEF2 target genes in hippocampal neurons. This potential transcriptional program is also very likely to be activated by MEF2A in hypothalamic neurons (Flavell *et al.*, 2008). Most of the target genes regulated by MEF2 are related to activity-dependent synapse development, and, if dysregulated, can contribute to the etiology of epilepsy or ASD (Flavell *et al.*, 2008). This regulatory role of MEF2 in synapse development supports our findings of OT-induced morphological changes, as those are the prerequisite to synapse formation and pruning. Disturbances in neuronal dendrite organization were associated with various neurodevelopmental disorders such as ASD (Kulkarni and Firestein, 2012). The robust effect of OT treatment on neurite retraction of H32 cells was supported by the finding that the specific OTR agonist TGOT also led to neurite retraction to a similar extent, indicating a specific OTR-mediated effect. In line with that data, the OTR antagonist blocked the OT-induced neurite retraction. It is therefore rather surprising that vasopressin treatment of H32 cells also led to neurite retraction. Consequently, there are two possibilities: both receptor types work in conjunction to induce neurite retraction, or the effect of vasopressin was caused by vasopressin

binding to the OTR. H32 cells express only one type of vasopressin receptor, the V1a (own unpublished data). As there is no selective rat V1a agonist (that does not bind the OTR) available (Marir *et al.*, 2013), we have to leave this research question to be answered by future studies, where knock out cell lines could be used to determine the exact roles of both receptors in neurite retraction. To exclude any morphological changes evoked by a reduced cellular viability, we conducted cell viability assays. We found that both OT and vasopressin rather increase the cellular viability to a similar extent, in line with the existing literature (Bakos *et al.*, 2012; Jafarzadeh *et al.*, 2014; Lestanova *et al.*, 2017), which excludes neurite retraction due to the onset of apoptosis. However, the processes of increased cell viability and therefore increased proliferation might be causally linked to the retraction of neurites. Therefore, two different scenarios are possible: either increased cell proliferation causes neurite retraction, or proliferation and neurite retraction are two independent processes, as it has been described recently (Latchney *et al.*, 2015). As both processes depend on MEF2A activity (Pon and Marra, 2016), the functional differentiation still remains to be addressed. Interestingly, there is conflicting data described in literature on OT's effects on cellular morphology. Recently, one study showed that transient OT exposure *in vitro* leads to a reduced dendrite complexity and synapse density in hippocampal glutamatergic neurons (Ripamonti *et al.*, 2017). Another study described OT as being effective in increasing gene and protein expression in human SH-SY5Y cells (Lestanova *et al.*, 2016), and this increase is associated with increased cell proliferation and increased neurite outgrowth. Own expression analyses revealed that SH-SY5Y cells lack MEF2A expression and, therefore, might show a differential response to OT than our H32 cells, which do express MEF2A. Supporting this assumption of cell-specific MEF2A expression and functioning, a central role for MEF2 in neuronal remodeling has also been detected in hippocampal neurons, cerebellar granule neurons, and medium spiny neurons of the nucleus accumbens both *in vitro* and *in vivo* (Flavell *et al.*, 2006; Barbosa *et al.*, 2008; Pulipparacharuvil *et al.*, 2008; Shalizi *et al.*, 2006).

2.6 Conclusion

In summary, this study elucidates the signaling cascade underlying the OT-mediated neurite retraction in hypothalamic neurons. We could show that this effect is mediated mainly via the OTR, with potential contributions of the V1a receptor. Stimulation of the OTR leads to an activation of the MEK1/2-ERK1/2 MAPK pathway and transcription factor MEF2A. Blocking the MAPK pathway by the MEK1/2 inhibitor U0126, as well as siRNA-mediated knock down of MEF2A, inhibited the OT-induced neurite retraction. Taken together, these results indicate a central role of the OTR-MAPK-MEF2A-pathway in morphological alterations of hypothalamic neurons.

3 Myocyte enhancer factor 2A (MEF2A) defines oxytocin-induced morphological effects and regulates mitochondrial function in neurons

3.1 Abstract

The neuropeptide OT is a well-described modulator of socio-emotional traits, such as anxiety, stress, social behavior, and pair bonding. However, when dysregulated, it is associated with adverse psychiatric traits, such as various aspects of ASD. In this study, we identify the transcription factor MEF2A as the common link between OT and cellular changes symptomatic for ASD, encompassing neuronal morphology, connectivity, and mitochondrial function. We provide evidence for MEF2A as the decisive factor defining the cellular response to OT: while OT induces neurite retraction in MEF2A expressing neurons, OT causes neurite outgrowth in absence of MEF2A. A CRISPR-Cas-mediated knockout of MEF2A and retransfection of an active version or permanently inactive mutant, respectively, validated our findings. We also identified the phosphatase CaN as the main upstream regulator of OT-induced MEF2A signaling. Further, MEF2A signaling dampens mitochondrial functioning in neurons, as MEF2A knockout cells show increased maximal cellular respiration, spare respiratory capacity, and total cellular ATP. In summary, we reveal a central role for OT-induced MEF2A activity as major regulator of cellular morphology as well as neuronal connectivity and mitochondrial functioning, with broad implications for a potential treatment of disorders based on morphological alterations or mitochondrial dysfunction.

3.2 Introduction

OT is a neuropeptide profoundly implicated in the regulation of various socio-emotional behaviors and physiological responses (Jurek and Neumann, 2018; Gimpl and Fahrenholz, 2001). Dysregulated plasma or salivary levels of OT have been associated with symptoms of ASD (Alaerts *et al.*, 2019; Parker *et al.*, 2014), depression (Yuen *et al.*, 2014), and anxiety (Carson *et al.*, 2015), and its intranasal application has been described to relieve some of those symptoms (Meyer-Lindenberg *et al.*, 2011). In particular, the pro-social effects of OT, as described by multiple groups (Lukas *et al.*, 2011; Chen *et al.*, 2011a; Chen *et al.*, 2011b; Choe *et al.*, 2015; Clipperton-Allen *et al.*, 2012), promise to relieve core deficits in social behavior in ASD patients. As a

multifactorial disorder, ASD has been associated with neuronal, morphological and mitochondrial dysfunctions (Maes *et al.*, 2019; Falougy *et al.*, 2019; Garcia-Cabezas *et al.*, 2018; Young *et al.*, 2016; Bringas *et al.*, 2013). One common factor between ASD, its underlying disturbed cellular functions and the oxytocinergic system, is the transcription factor MEF2. In this study, we provide evidence for the role of MEF2 as the central node in the regulation of those conditions. One major parameter in ASD patients is an alteration of the neuronal connectivity. Autistic patients show hyperconnectivity between amygdala and hippocampus, which is negatively correlated with peripheral OT levels, and can even be further decreased by intranasal application of OT (Alaerts *et al.*, 2019). Although neuronal cell types differ between brain regions, i.e., hypothalamus and amygdala, the underlying molecular mechanism that connects OT receptor-coupled signaling with neuronal morphology seems to be identical in various cell types ((Jurek and Neumann, 2018) and references therein). In particular, transcriptomic responses to OT are similar in hypothalamic as well as amygdalar neurons (Jurek *et al.*, 2015). Furthermore, neurons generated from iPSCs of ASD patients have more complex and longer neurites, causing increased synapse number and a state of hyperconnectivity (Zaslavsky *et al.*, 2019; Tang *et al.*, 2014). MEF2 is one factor that is responsible for the regulation of excitatory synapse number (Flavell *et al.*, 2006; Shalizi *et al.*, 2006; Morrow *et al.*, 2008), and we have recently provided evidence for its activation by OT receptor-coupled signaling pathways (Meyer *et al.*, 2018). The activation of Gq protein-coupled OT receptors leads to an increase in intracellular Ca^{2+} from either intracellular stores (Sanborn, 2007), through cation channels such as TrpV2/4 (van den Burg *et al.*, 2015; Ying *et al.*, 2015) or L-type voltage-gated Ca^{2+} channels (Zatkova *et al.*, 2018). Upon OT-induced Ca^{2+} influx, the phosphatase CaN (or protein phosphatase 2B; PP2B) is activated by binding calmodulin (Pont *et al.*, 2012). On the one hand, active CaN acts as a direct phosphatase of cytoskeletal proteins and influences the stability and interaction of microtubule and actin filaments (Descazeaud *et al.*, 2012; Xiong *et al.*, 2018; Lautermilch and Spitzer, 2000). On the other hand, it dephosphorylates MEF2A at position S408 (Flavell *et al.*, 2006; Shalizi *et al.*, 2006), leading to a genomic response that consequentially impacts cellular morphology indirectly via transcriptional control of regulators of the cytoskeleton. Such regulators have recently been identified and linked to OT signaling by Bakos and colleagues, who found increased expression of the actin-binding proteins

drebrin, the intermediate filament vimentin, or the scaffolding protein SHANK3, under the influence of OT. This caused neurite outgrowth in human SH-SY5Y neuroblastoma or U-87MG glioblastoma cells (Zatkova *et al.*, 2018; Lestanova *et al.*, 2016; Bakos *et al.*, 2018). As a consequence of neurite outgrowth, altered connectivity is observable due to increased synapse formation, which is under the OT-induced control of synaptic adhesion molecules such as neuroligin 3 or neurexin 2 (Zatkova *et al.*, 2019). Since OT is produced in the hypothalamus and we have found profound anxiolytic and anti-stress effects of OT infused into the hypothalamic paraventricular nucleus (Jurek *et al.*, 2015; Blume *et al.*, 2008; Jurek *et al.*, 2012; Martinetz *et al.*, 2019), we aimed to determine the intracellular effects of OT in a hypothalamic cell line, as opposed to neuroblastoma or glioblastoma cell types. As a cellular model of oxytocinergic effects, we have characterized the rat hypothalamic neuronal cell line H32, which expresses MEF2A endogenously, and retract their neurites upon OT stimulation, caused by MEF2A activation (Meyer *et al.*, 2018). Neurite retraction was blocked by siRNA-mediated knockdown of MEF2A, or pharmacological blockade of the OT receptor-induced activation of the MAPK pathway by U0126. The observed neurite retraction was seemingly in contrast to the above-mentioned studies showing OT-induced neurite outgrowth in SH-SY5Y or U-87MG cells, but these are not hypothalamic neurons and might therefore react differently. In support of this hypothesis, we characterized the transcriptome of SH-SY5Y cells and found absent MEF2A expression. This phenotypical contrast led us to create a MEF2A knockout cell line, derived from our MEF2A-positive H32 cells (H32ΔMEF2A), using CRISPR-Cas9. In addition, we characterized another hypothalamic cell line (mHypoE-N11), which does not express endogenous MEF2A, and used those cells to overexpress MEF2A by plasmid transfection. By site-directed mutagenesis, we substituted the serine at position 408 to aspartate, creating a permanent phospho-mimetic MEF2A mutant. This mutant, transfected into H32ΔMEF2A cells, served as control for phospho-site-specific effects of MEF2A, since MEF2A can be phosphorylated at three different residues, namely S408, Thr312, and Thr319, with opposing outcomes for gene transcription (Potthoff and Olson, 2007). Those three hypothalamic cell lines serve as internal controls in our experimental setup and aid in determining the morphological outcome of OT stimulation in hypothalamic cells in the presence or absence of MEF2A. Cytoskeletal rearrangements are energy-consuming

events, requiring proper functioning of mitochondria. The organelles produce adenosine triphosphate (ATP) and provide energy for several cellular processes in neurons including action potential generation, but also morphological changes such as neurite growth. Many neurodegenerative diseases with a loss of neuronal function and morphology show accompanying mitochondrial malfunctions (Mattson *et al.*, 2008). Intriguingly, MEF2 regulates transcription of the mitochondrial NADH dehydrogenase 6 gene, which is essential for the function of the oxidative phosphorylation system (Naya *et al.*, 2002; She *et al.*, 2011), which ultimately regulates the production of ATP. In line with that, a significant proportion of ASD patients suffer from abnormal ATP production (Rossignol and Frye, 2014; Siddiqui *et al.*, 2016), suggesting a central role for the OT-regulated transcription factor MEF2 in energy balance, structural plasticity, and ASD (also see (Shalizi *et al.*, 2006; Meyer *et al.*, 2018; Fiore *et al.*, 2009; Pfeiffer *et al.*, 2010; Brusco and Haas, 2015)). To test this hypothesis, we manipulated MEF2A activity in hypothalamic neurons and monitored morphological alterations and mitochondrial functionality.

3.3 Material and methods

3.3.1 Cell culture

Rat hypothalamic H32 cells ([48] kindly provided by Prof. Greti Aguilera (NICHD, Bethesda, MD)) and mouse hypothalamic mHypoE-N11 cells (kindly provided by Prof. Eugen Kerkhoff, University of Regensburg) were cultured in DMEM (#D8437, Sigma Aldrich, Darmstadt, Germany), supplemented with 10 % heat-inactivated Gold fetal bovine serum (#FBS-HI-11A, Capricorn, Germany), and Penicillin/Streptomycin (#P4333, Sigma Aldrich, Darmstadt, Germany) at 37 °C and 5 % CO_2 until 80 % confluency. Passaging was performed at least once a week by gentle trypsinization. Cells were counted and seeded at 3×10^6 cells/75 cm^2 density. Cell counts were recorded and compared between wildtype and knockout cell lines to extrapolate proliferation rates.

3.3.2 CRISPR-Cas9 mediated knockout of MEF2A

The rat hypothalamic neuronal cell line H32 served as host to create an MEF2A knockout cell line (H32ΔMEF2A), using the Alt-R® CRISPR-Cas9 system (IDT, Coralville, USA). RNP complexes

were composed of the functional gRNA duplex, containing the sequence-specific crRNA (sequence ID: Rn.Cas9.MEF2A.1.AC; 50-A*C*A*G*A*C*C*T*C*A*C*G*G*T*A*C*C*A*A*A-30) and the ATTO 550-labeled tracrRNA in nuclease-free duplex buffer, and the S. p. Cas9 Nuclease 3NLS. The complexes were transfected by cationic lipid delivery using Lipofectamine^{TM} RNAiMAX Transfection Reagent (Invitrogen, Carlsbad, CA, USA) and Opti-MEM (Gibco, Waltham, MA). Transfected single-cells were obtained 2 h after transfection by cell sorting and recultured for several weeks. The genotype was assessed by means of Western blotting.

3.3.3 Transfection of H32 and mHypoE-N11 Cells with MEF2A overexpression plasmids

For morphological analyses, cells were transfected with plasmids (VectorBuilder, Neu-Isenburg, Germany) by electroporation using the manufacturer's nucleofector (Thermo Scientific, Waltham, MA) protocol. In total, 1 million cells were transfected with 0.5 µg of rat/mouse MEF2A plasmids. After a 48 h incubation, cells were further processed. The mouse hypothalamic cell line mHypoE-N11 was transfected with wildtype mouse MEF2A, resulting in mHypoE-N11MEF2A cells. H32ΔMEF2A cells were transfected with either the wildtype variant of MEF2A(H32ΔMEF2A^{MEF2A}) or a phospho-mimetic MEF2A mutant (H32ΔMEF2A$^{MEF2A[S408D]}$).

3.3.4 Cell stimulations

Cells were stimulated overnight with 10, 100 or 250 nM of OT (Bachem, Bubendorf, Switzerland) in cell culture dishes or chamber slides (BD Falcon, Germany). For the inhibition of CaN, CaN autoinhibitory peptide (#1891, Tocris, Wiesbaden, Germany) was used at a concentration of 10 µM (Perrino *et al.*, 1995). Cells were pretreated with the inhibitor for 30 min and stimulated with the corresponding treatment. Non-treated cells are indicated as vehicle (VEH).

3.3.5 Protein isolation

For the extraction of proteins from OT- or vehicle (H_2O)-stimulated 80 % confluent H32 cells, the stimulation medium was removed, and cells were washed with 5 mL ice-cold PBS (#D8537, Sigma Aldrich). Cells were scraped in 1 mL ice-cold PBS using a cell scraper (#83.1830, Sarstedt, Nümbrecht, Germany), collected in 15 mL tubes in PBS, centrifuged at 300 g and 4 °C for 5 min, and then the resulting cell pellet was resuspended in 30–100 µL RIPA lysis buffer (R0278, Sigma

Aldrich, Darmstadt, Germany) supplemented with HALT inhibitor and EDTA (78444, Thermo Fisher, Waltham, MA) to obtain whole cell lysates.

3.3.6 Western blotting

Western blotting was conducted as previously described in (Meyer *et al.*, 2018). Briefly, 15 or 20 µg of whole cell extract were loaded and separated in a 12 % Mini PROTEAN or Criterion TGX Stainfree gel (Bio-Rad, Feldkirchen, Germany), respectively. Semi-dry blotting of separated proteins to nitrocellulose membranes was conducted using the FAST Blotter by Bio-Rad. Uniform total protein loading was controlled for by the Stainfree total protein method by Bio-Rad. Specific antibodies for MEF2A, pMEFA S408, pMEK 1/2 and integrin ß1 (Table 2) indicated activity and expression levels of the protein of interest.

Table 2. Summary of antibodies used in this study with corresponding dilution and host.

Antibody	Company and CAT Number	Dilution and Diluent	Secondary Antibody
MEF2A total	Acris AP06372PU-N	1:2000 in 5 % MP	HRP-coupled anti-rabbit
pMEF2A S408	CusAb PA000728	1:5000 in 5 % BSA	HRP-coupled anti-rabbit
pMEK1/2 4199	Cell Signaling 9154	1:5000 in 5 % BSA	HRP-coupled anti-rabbit
Integrin ß1 (N-20)	Santa Cruz sc-6622	1:1000 in 5 % BSA	HRP-coupled anti-goat

3.3.7 Immunofluorescence

mHypoE-N11 cells and mHypoE-N11^{MEF2A}, as well as H32ΔMEF2A and H32ΔMEF2A^{MEF2A} cell lines, were seeded on chamber slides (BD-Falcon, #08-774-25) at 6×10^4 cells per chamber and cultured overnight in growth medium at 37 °C/5 % CO_2. Next, the growth medium was removed, and cells were briefly rinsed with warm PBS. The PBS was removed and replaced with 500 µL ice-cold 3 % glyoxal solution (+20 % EtOH, Acetic acid, pH = 4–5) for 20 min. After washing the cells twice with PBS-T (0.5 % tween), unspecific binding sites were blocked (PBS+0.5 % TritonX, 1 % glycine, 10 % BSA, 1 % normal goat serum) for 30 min, and antibody incubated overnight at the corresponding dilution. After intense washing with PBS-T, secondary antibody (CF488A highly cross-adsorbed #20123 BioTrend, Köln, Germany) was incubated at 1:500 in PBS for 30 min. After washing, cells

were incubated with Phalloidin-iFluor 594 Reagent (abcam ab176757), mounted with ProLong Glass-Antifade mounting medium with DAPI (Thermo Scientific, #P36982) and covered by cover slips (Thor Labs, refraction index 1,5; #CG15KH). Images were taken on a Zeiss AiryDisc Confocal microscope with a 63 × objective with identical laser and gain intensities to guarantee comparability between images.

3.3.8 Morphological characterization

For nucleus staining, Hoechst 33342 stain (H1399, Thermo Scientific, Waltham, MA) was added to the stimulation medium in the 6-well plates where cells were stimulated, and incubated for 30 min at 37 °C. The cells grown in cell culture dishes were washed with 1 mL PBS and subsequently fixed by gently adding 3 % glyoxal solution for 20 min (3 % glyoxal in H_2O, #128465, (Sigma Aldrich, Darmstadt, Germany), supplemented with 20 % EtOH and acetic acid to acquire pH = 5). All pictures were taken using the ZOE Fluorescence microscope (Bio-Rad, Feldkirchen, Germany). Neurite outgrowth was determined by manually tracing the length of the longest neurite per cell (using ImageJ Fiji version 1,52r software, NIH, USA) for all cells in a field that had an identifiable neurite and for which the entire neurite arbor could be visualized. Length of the neurite was measured from the edge of nucleus to the apical end of the projection. Only neurites that did not contact other cells were evaluated. At least two members of the team independently evaluated neurite length in a blinded manner.

3.3.9 Cell viability assay

Cellular viability was tested using the PrestoBlue Cell Viability Assay (A13261, Invitrogen, Carlsbad, CA) according to the manufacturer's protocol and as described in (Meyer *et al.*, 2018). Briefly, 10×10^3 cells per well were seeded the day before the test in a 96-well plate in growth medium. The volume of the treatment and medium for the stimulation was calculated to a total of 90 µL per well. In total, 10 µL of PrestoBlue Reagent was added directly to the cells and incubated for 30 min before reading the fluorescence intensity with a FluoStar Plate reader (BMG Labtech, Ortenberg, Germany).

3.3.10 Mitochondrial respiration analysis

The oxygen consumption rate (OCR) of intact H32 and H32ΔMEF2A cells was measured with the Agilent Seahorse XF Cell Mito Stress Test Kit (Agilent Technologies, Waldbronn, Germany) according to the manufacturer's protocol. The live cell assay monitors OCR in real time and assesses the key parameters of mitochondrial function. Mitochondrial stress compounds used for this assay are oligomycin (1 µM), carbonyl cyanide-4 (trifluoromethoxy) phenylhydrazone (FCCP; 2 µM), and rotenone/antimycin A (1 µM). On the day before the measurement, 20×10^3 cells were seeded in matrigel-coated XFp 8-well miniplates (Agilent Technologies, Waldbronn, Germany) at 37 °C, humidified air and 5 % CO_2. Cartridges were prepared according to the provided protocol. The obtained values were normalized to the cell number present in the region of interest, reflecting the field of measurement by ImageJ. Data was analyzed using the WAVE software (Agilent Technologies, CA, USA) according to the manufacturer's protocol.

3.3.11 CellTiter-Glo 2.0 assay

The CellTiter-Glo 2.0 assay (Promega) was conducted to measure cellular ATP content under basal/non-stimulated conditions in H32 and H32DMEF2A cells, according to the manufacturer's protocol. Briefly, 10×10^3 cells per well were seeded the day before in a Nunclon Delta Surface 96-well plate (Thermo Scientific, #136101). On the next day, an ATP standard curve was generated, and an equal volume of Cell Titer Reagent 2.0 was added to the culture medium present in each well. After a 12 min incubation, luminescence intensity was recorded with the GloMax Luminometer (Promega, Waldorf, Germany). The assay was repeated three times.

3.3.12 Statistical analysis

Statistical analyses were performed using Sigma Plot (version 13.0, Systat Software, Erkrath, Germany). Parametric data was analyzed by t-test or one-way ANOVA followed by the Holm–Sidak post hoc test. Non-parametric data was analyzed by the Mann–Whitney Rank Sum test or Kruskal–Wallis ANOVA on ranks and the Tukey post hoc test. Statistical significance was accepted at $p < 0.05$. In morphological experiments, n represents the number of cells. In Western blotting, n represents the number of cell lysates. In the ATP and cell viability assays, n is number of wells. Parametric data is presented as the mean + standard deviation (SD). Non-parametric data is

represented in box plots as the minimum, first quartile, median, third quartile, and maximum. Details on statistics have been summarized in the Supplementary Materials.

3.4 Results

In order to study the impact of MEF2A in OT-induced effects on cellular morphology, we used cell lines that lacked, endogenously expressed, or were transfected with MEF2A. The mother cell line as well as all genetically altered daughter lines express the OT receptor, as validated by RT-qPCR. The hypothalamic rat cell line H32 was subjected to CRISPR-Cas-mediated knockout of MEF2A (H32ΔMEF2A), and retransfected with either wildtype rat MEF2A (H32ΔMEF2A^{MEF2A}) or the mutant version H32ΔMEF2A$^{MEF2A[S408D]}$, in which site-directed mutagenesis at S408D mimicked a permanently phosphorylated, and therefore transcriptionally inactive transcription factor. The mouse hypothalamic cell line mHypoE-N11 lacked MEF2A expression with levels below the detection limit of a qPCR. Transfection of those cells with a plasmid encoding for mouse MEF2A resulted in exogenous overexpression of MEF2A, as verified with immunofluorescence. The cell lines created and their MEF2A expression profile are summarized in Table 3.

Table 3. Summary of cell lines used and created in this study. MEF2A protein levels have been assessed by means of Western blotting (Figure A3). mHypoE-N11 are derived from mouse hypothalamus neurons and lack endogenous MEF2A expression. Plasmid transfection caused MEF2A overexpression in those cells (mHypoE-N11^{MEF2A}). H32 cells are immortalized neurons derived from a rat hypothalamus (Mugele *et al.*, 1993) and show moderate endogenous expression of MEF2A (wildtype). CRISPR-Cas directed knock out of MEF2A produced H32ΔMEF2A cells, retransfection of intact MEF2A into H32ΔMEF2A cells rescued MEF2A expression (H32ΔMEF2A^{MEF2A}).

Cell line	**mHypoE-N11 (Mouse)**		**H32 (Rat)**			
Manipulation	Wild-type	mHypoE-N11^{MEF2A}	Wild-type	H32ΔMEF2A	H32ΔMEF2A^{MEF2A}	H32ΔMEF2A$^{MEF2A[S408D]}$ (inactive)
Level of MEF2A	-	++	+	-	++	++

Treatment of mouse hypothalamic MEF2A-deficient mHypoE-N11 cells (see Table 3), with increasing concentrations (10, 100 and 250 nM) of OT overnight, led to a dose-dependent increase in neurite length, which reached significance in the 100 and 250 nM treatment group, but not in the 10 nM group (Figure 8A). Statistical analyses for all figures are summarized in the Supplementary Materials, including details on p values and effect sizes. Overexpressing MEF2A in mHypoE-N11 cells by plasmid transfection with subsequent OT stimulation 48 h later revealed

a significant OT-induced retraction of neurites after 12 h in all doses tested (Figure 8B). Successful overexpression of MEF2A was controlled by immunostaining with an MEF2A-specific antibody (Figure 8C). As expected, we found mainly nuclear location of MEF2A, with partial cytosolic location, representing a normal localization of the transcription factor (Potthoff and Olson, 2007). Neither of the effects on neurite length was caused by altered cell viability. We found no decrease in cellular viability in H32 or H32ΔMEF2A cells, and no increased cell viability in mHypoE-N11 cells under the influence of OT (Figure A2). This suggests that the OT-induced morphological effects are primarily alterations of the cytoskeleton, and not mere side effects of an apoptotic or otherwise constricted cell. The OT receptor specificity of the morphological effect has been addressed by the use of a specific OT receptor antagonist (des-Gly-NH_2*d*$(CH_2)_5$[Tyr(Me)^{2}Thr^4]-OVT) and agonist (Thr^4 Gly^7-OT, TGOT) in a previous publication (Meyer *et al.*, 2018).

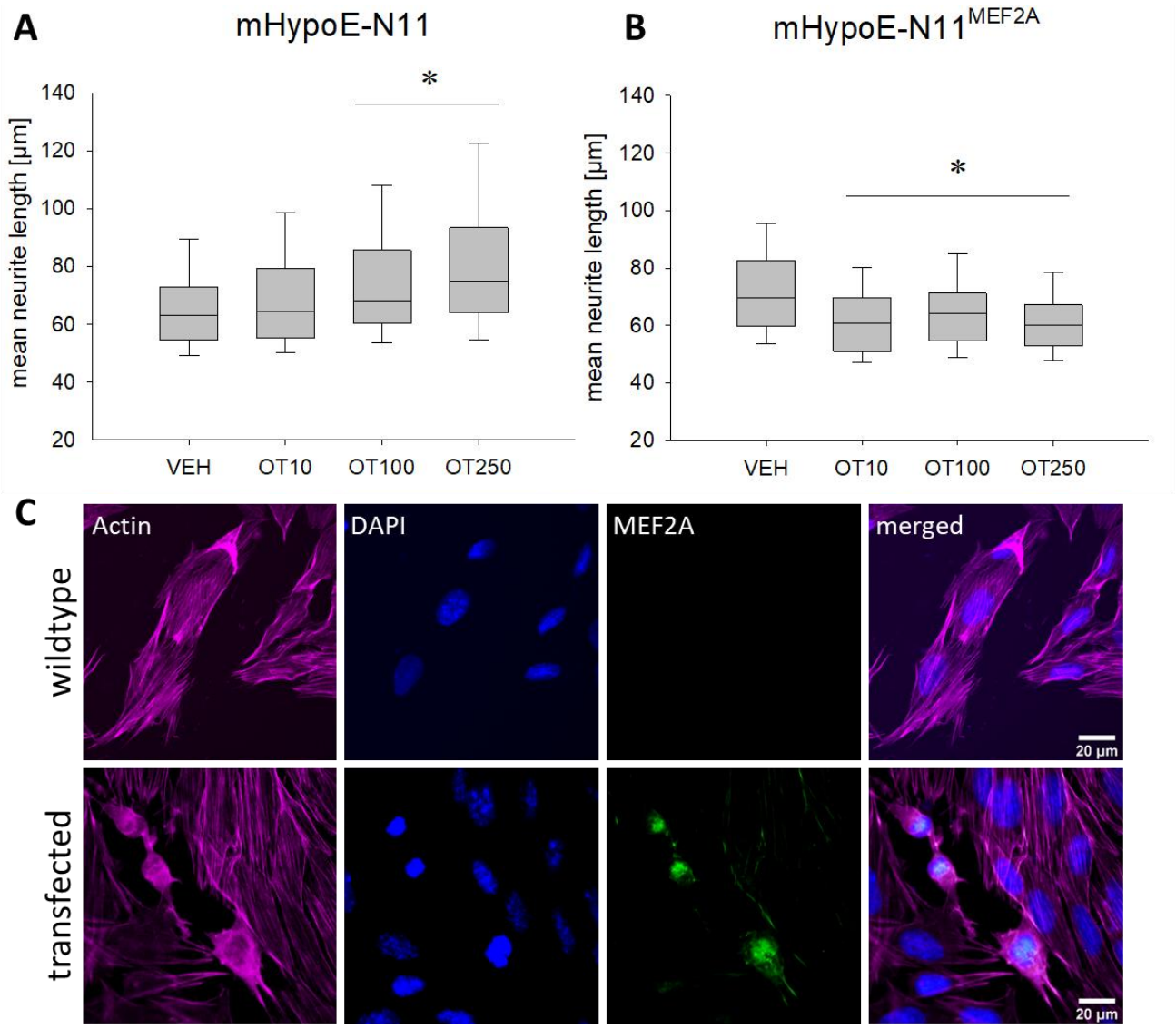

Figure 8. Effects of oxytocin (OT) on neuronal morphology in the mouse hypothalamic cell line mHypoE-N11. (A) Median neurite length increases significantly in wildtype mHypoE-N11 cells treated overnight with 100 or 250 nM OT. n = 100 cells per treatment; * $p < 0.012$ vs. VEH. (B) Treatment with 10, 100 and 250 nM of OT induces a significant neurite retraction in MEF2A overexpressing mHypoE-N11 cells. n = 100 cells per treatment; * $p < 0.003$ vs. VEH. (C) Representative images of immunofluorescence labelling for MEF2A. Images were sequentially recorded for F-actin (Phalloidin, red, first column), chromatin (DAPI, blue, second column), and MEF2A (green, third column). Merged images are shown for each row in the fourth column. Labels left to the columns indicate the respective cell type (wildtype vs. transfected).

Having established the 'gain-of-function-MEF2A' model with the mHypoE-N11 cells, we determine whether a 'loss-of-MEF2A-function' model would reverse the oxytocinergic effect on cellular morphology. To obtain a permanent knockout of MEF2A, we made use of the CRISPR-Cas9 technology to create a monoclonal knockout cell line derived from a single edited H32 clone. The efficiency of the knockout was validated by Western blotting. In contrast to OT-induced

neurite retraction in H32 wildtype cells, we found neurite elongation after stimulating H32ΔMEF2A cells overnight with 100 and 250 nM OT (Figure 9A). Retransfection of those knockout cells with an intact wildtype MEF2A reversed the effect and initiated OT-induced neurite retraction (Figure 9B, light blue columns). However, when a phospho-mimetic, permanently inactive MEF2A [S408D] mutant was retransfected, neurite elongation was observed (Figure 9B, dark blue columns). This cellular response was comparable to the H32ΔMEF2A cells (Figure 9A), revealing the S408 residue as the main phosphorylation site that orchestrates the OT effect on cellular morphology.

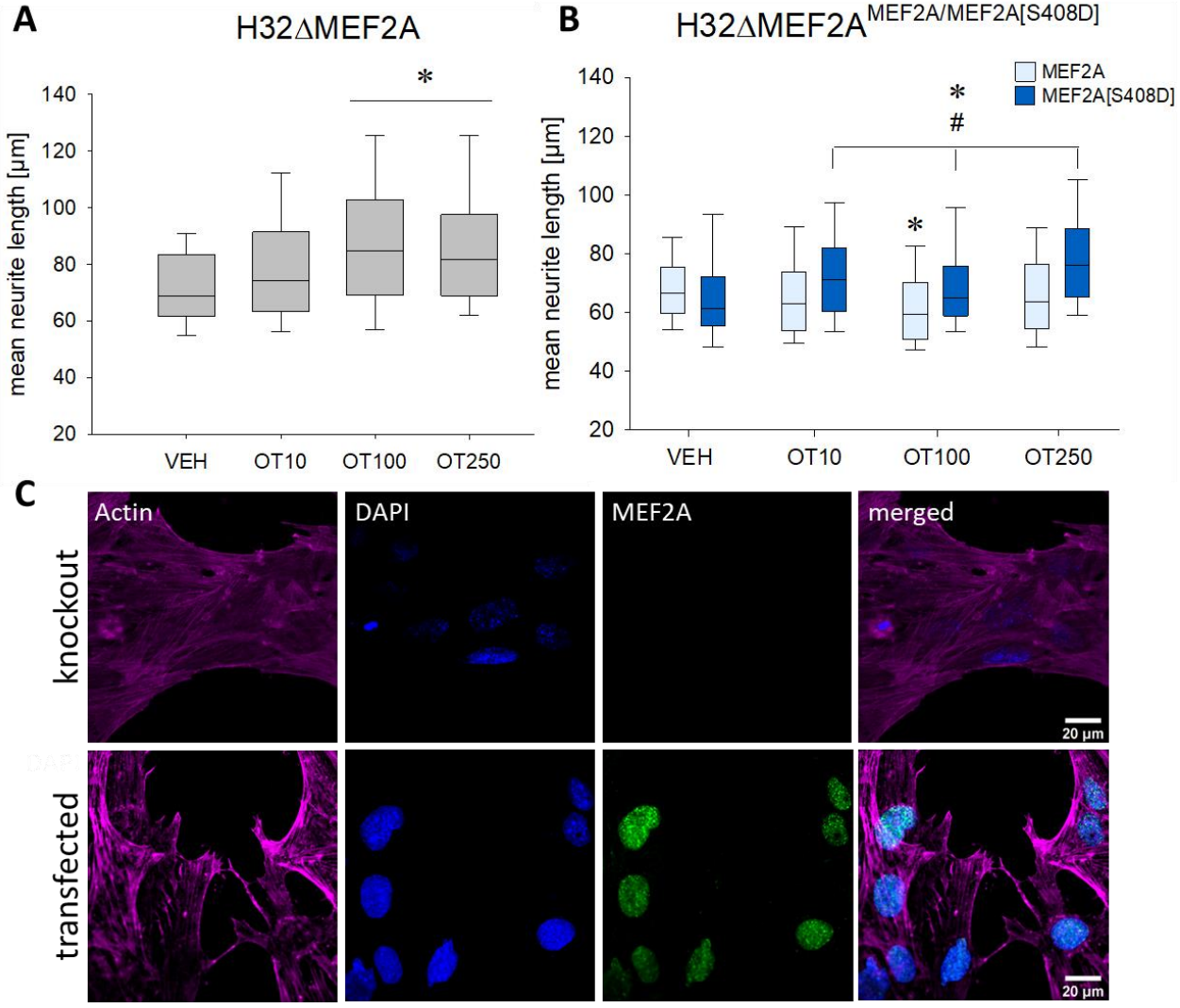

Figure 9. Effects of oxytocin (OT) on neuronal morphology in the rat hypothalamic cell line H32. (A) Incubation of H32ΔMEF2A cells with 100 or 250 nM OT leads to a significant neurite elongation. n = 100 cells per treatment; * $p < 0.001$ vs. VEH. (B) H32ΔMEF2A cells were retransfected with wild-type MEF2A and a mutant version MEF2A[S408D], which mimics a permanently phosphorylated and therefore inactive MEF2A. The wild-type MEF2A generated OT-

induced neurite retraction, whilst the mutant MEF2A lacked the ability to induce neurite retraction. Instead, the mutant response to OT resembled the MEF2A knockout cells. n = 100 cells per treatment; two-way ANOVA; * $p < 0.031$ treatments vs. VEH within the same group; # $p < 0.002$ groups (wildtype vs. mutant) within the same treatment. (C) Representative images of immunofluorescence labelling for MEF2A. Images were sequentially recorded for F-actin (Phalloidin, red, first column), chromatin (DAPI, blue, second column), and MEF2A (green, third column). Merged images are shown for each row in the fourth column. Labels left to the columns indicate the respective cell type (knockout vs. transfected).

We have shown in a previous publication (Meyer *et al.*, 2018) that incubation of H32 cells with 100 nM OT overnight led to a dephosphorylation and, therefore, activation, of MEF2A at S408, compared to VEH treated cells. This effect is indirectly mediated via the MAPK pathway, as it is reversed to basal by the MEK1/2 inhibitor U0126. This treatment does not alter the level of total MEF2A or MEK1/2 protein, as previously published by our group (Jurek *et al.*, 2015; Meyer *et al.*, 2018; van den Burg *et al.*, 2015; Jurek *et al.*, 2012; Martinetz *et al.*, 2019).

In the present study, OT stimulation led to decreased MEF2A S408 phosphorylation, whereas addition of CaN inhibitor reversed the phosphorylation back to basal (Figure 10A).

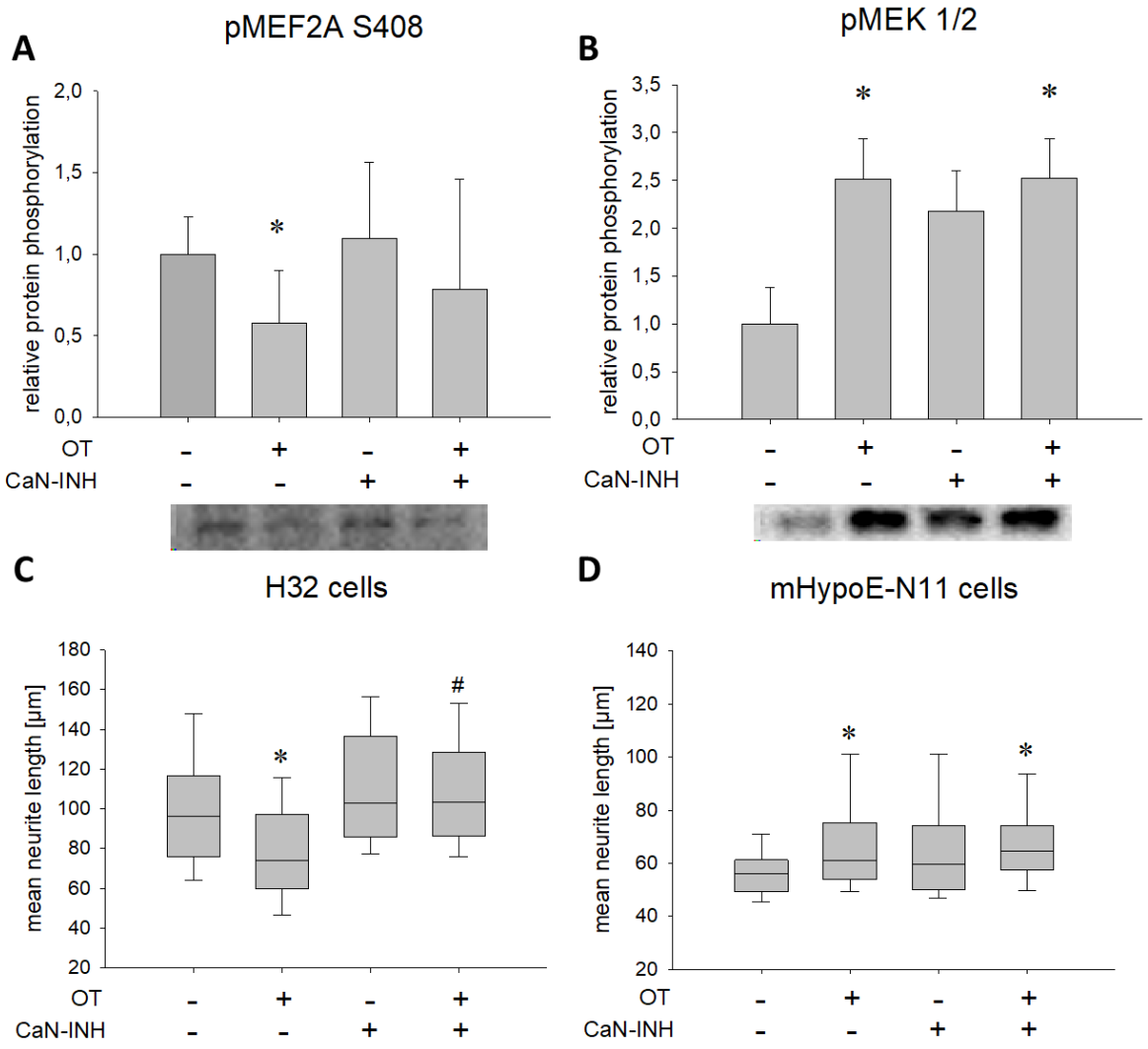

Figure 10. Effect of oxytocin (OT) stimulation and calcineurin inhibition on phosphorylation of S408 of MEF2A and MEK1/2 as well as on the median neurite length in H32 cells. (A) Relative MEF2A S408 phosphorylation analyzed by Western blotting in whole cell lysate after treatment with VEH and OT, in the presence or absence of a CaN inhibitor (CaN-INH), with representative blot below. Overnight incubation of H32 wild-type cells with 100 nM OT led to a significant dephosphorylation of MEF2A at S408 compared to VEH treated cells (one-way ANOVA, $p = 0.056$; independent t-test VEH vs. OT, $p = 0.006$). This effect is dependent on CaN activity, as it is reversed to basal by a CaN-INH. The inhibitor without OT had no effect on MEF2A phosphorylation. n = 6 per treatment. (B) Relative phosphorylation of MEK1/2 analyzed by Western blotting in whole cell lysate after treatment with VEH and OT, in the presence or absence of a CaN inhibitor, with representative blot picture below. Treatment of the cells with 100 nM OT overnight led to a significant phosphorylation of MEK1/2 compared to VEH. Statistical analysis using one-way ANOVA revealed no significant effect of the inhibitor treated cells, but a significant phosphorylation of MEK1/2 when cells were treated with OT and the CaN-INH. n = 6 per treatment; * $p < 0.05$ vs. VEH. (C) In H32 cells, 100 nM of OT led to a significant retraction compared to VEH, while inhibition of CaN resulted in elongation of neurites overnight compared to VEH and OT. Combining the OT treatment with a CaN-INH increased the neurite length significantly. n = 100 per treatment; * $p < 0.001$ vs. VEH-treated cells; # $p < 0.001$ vs. OT-treated cells. (D) Incubation of mHypoE-N11 cells with 100 nM OT overnight led to an increased neurite length. Inhibition of CaN had no effect on the neuronal morphology, in line with the absent MEF2A expression in this cell line. n = 50 per treatment; * $p < 0.05$ vs. VEH-treated cells.

To test whether the observed CaN activation is related to the MAPK pathway, we assessed MEK1/2 phosphorylation after OT/CaN inhibitor treatment. Western blotting revealed MAPK pathway activation after OT treatment irrespective of the CaN inhibitor application, indicated by persistent MEK1/2 phosphorylation in the presence or absence of the CaN inhibitor. The inhibitor alone, despite a visual increase, had no significant effect on MEK1/2 phosphorylation (Figure 10B). As expected, those effects translated into morphological changes, i.e., OT treatment (as shown in Figure 9B and (Meyer *et al.*, 2018)) reduced neurite length from approximately 100 µm to approximately 75 µm, an effect that was blocked by the CaN inhibitor (Figure 10C). In line with this data, when CaN was blocked in mHypoE-N11 cells (which do not express MEF2A), OT retained its ability to increase neurite length (Figure 10D). This is in line with our hypothesis of the central role for the CaN-MEF2A pathway in OT-induced neurite retraction, but OT induces neurite outgrowth when MEF2A is absent. For examination of mitochondrial function, we analyzed intact H32 wild type and H32ΔMEF2A cells with the Agilent Seahorse XF Cell Mito Stress Test Kit. After application of different stressors to the cells, the oxygen consumption rate was measured, which serves as an indicator for mitochondrial functioning (Figure 11A). H32ΔMEF2A cells showed a significantly higher maximal respiration (Figure 11B) as well as spare respiratory capacity (Figure 11C) compared to the MEF2A expressing H32 wildtype cells. This increased respiratory capacity in the H32ΔMEF2A cells suggests an inhibitory role for MEF2A in mitochondrial functioning. As a direct consequence of this altered mitochondrial performance, basal cellular ATP content was significantly elevated in the H32ΔMEF2A cells, when compared with the wildtype cells (Figure 11D). This additional energy supply might contribute to the cytoskeletal rearrangements that cause neurite elongation observed under OT treatment. Neurite outgrowth serves to increase cell–cell contacts, which we hypothesized to simultaneously decrease cell–matrix contacts (Bikbaev *et al.*, 2015; Chklovskii, 2004). As a representative indicator for decreased cell–matrix contacts, we assessed integrin ß1 receptor expression (Tomaselli *et al.*, 1993), and found decreased protein expression in H32ΔMEF2A cells compared to H32 wildtype cells (Figure 11E).

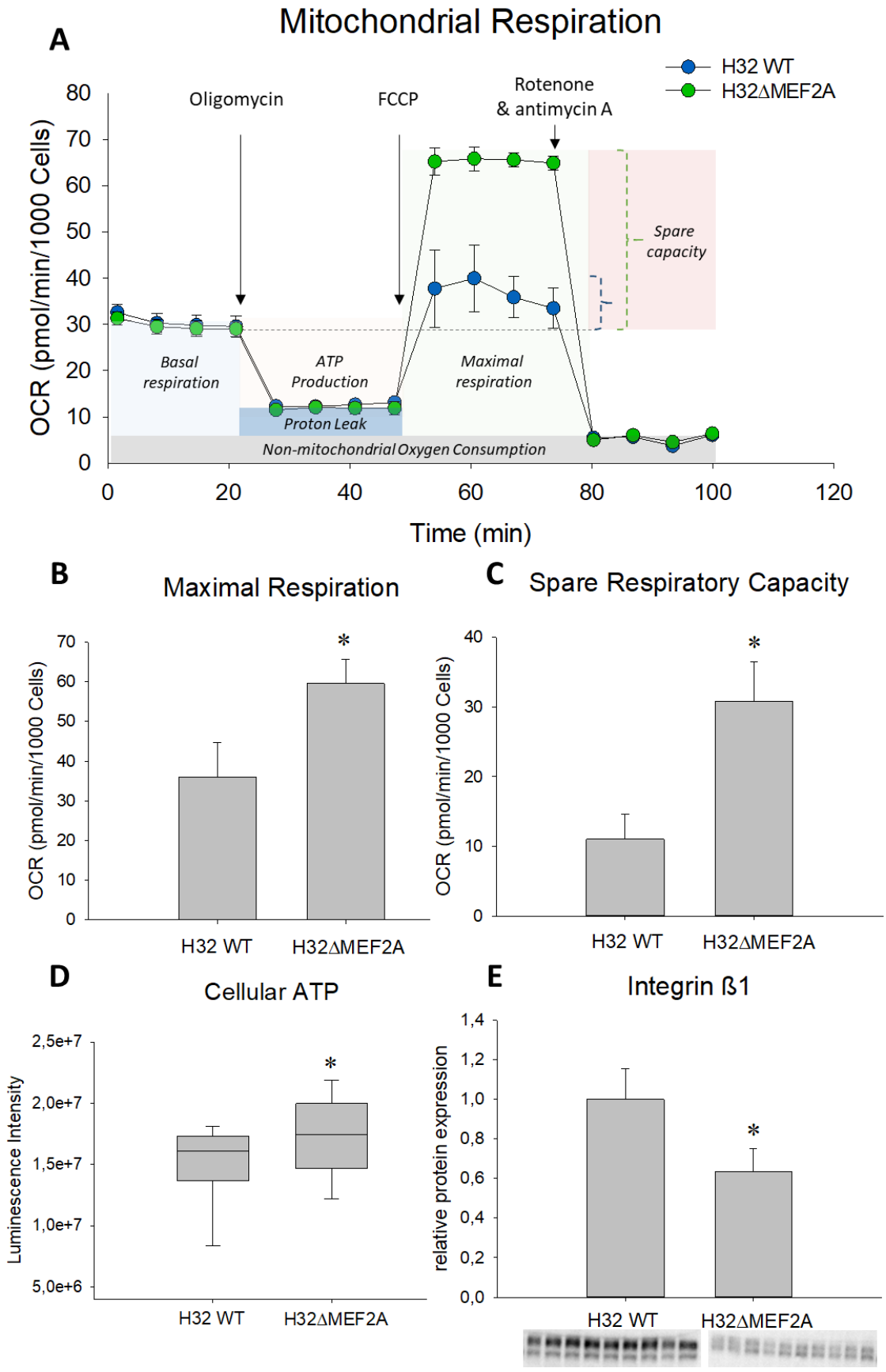
A
Mitochondrial Respiration
H32 WT
H32ΔMEF2A
Oligomycin
FCCP
Rotenone
& antimycin A
Spare capacity
Basal respiration
ATP Production
Maximal respiration
Proton Leak
Non-mitochondrial Oxygen Consumption
OCR (pmol/min/1000 Cells)
Time (min)
B
Maximal Respiration
C
Spare Respiratory Capacity
D
Cellular ATP
Luminescence Intensity
E
Integrin ß1
relative protein expression
H32 WT
H32ΔMEF2A

Figure 11. Effect of MEF2A knockout on mitochondrial function and neuronal connectivity. (A) The Agilent Seahorse XF Cell Mito Stress Test profile shows the oxygen consumption rate (OCR) in H32 wildtype (WT) and H32ΔMEF2A cells representing key parameters of mitochondrial function. (B) and (C) The OCR of both cell lines in the mitochondria stress test measured by Seahorse. H32ΔMEF2A cells show a significantly increased maximal respiration (* $p = 0.004$) and spare respiratory capacity (maximal vs. basal respiration, * $p = 0.01$) compared to H32 cells. n = 3 test repetitions with 4 measurement replicates per group. (D) Cellular ATP content under basal conditions is significantly higher in H32ΔMEF2A than H32 WT cells. n = 24 per group; * $p = 0.038$. (E) Relative protein expression of integrin ß1 is significantly downregulated in H32ΔMEF2A cells compared to H32 WT cells. n (H32 WT) = 9, n (H32ΔMEF2A) = 10; * $p < 0.001$.

3.5 Discussion

In recent publications, OT has been considered as a potential treatment for the alleviation of adverse psychiatric traits, e.g., ASD-related symptoms (Meyer-Lindenberg *et al.*, 2011; Hurlemann, 2017; Kosfeld *et al.*, 2005; Tost *et al.*, 2010). The effects range from improving social skills in autistic children (Yatawara *et al.*, 2016; Parker *et al.*, 2017) to increased reciprocal trust in adult healthy probands (Kosfeld *et al.*, 2005). However, the underlying molecular mechanism of the OT's alleviating properties on the symptoms of ASD are not fully understood. Considering the cellular changes apparent in ASD patients, we focused on the main parameters of cellular morphology, mitochondrial function and neuronal connectivity in this study, providing evidence for MEF2A as central regulator of those processes (Figure 12). We have identified the transcription factor MEF2A as the defining parameter that shifts the OT-induced neuronal response from neurite outgrowth towards neurite retraction. Knockin or knockout of MEF2A produced dichotomic effects on neuronal morphology, but only in the presence of OT. When MEF2A is expressed, OT leads to transcriptional activation by dephosphorylation of the inhibitory site S408 of MEF2A, which promotes a switch from sumoylation to acetylation at Lys403 and subsequent inhibition of dendritic morphogenesis (Shalizi *et al.*, 2007). In contrast, when we transfected MEF2A knockout cells with the transcriptionally inactive mutant (H32ΔMEF2A$^{MEF2A[S408D]}$), sumoylation at Lys403 was retained and dendritic morphogenesis occurred. Interestingly, the knockout of MEF2A and its phospho-mimetic mutation did not just inhibit neurite retraction, but actively induced neurite outgrowth under the influence of OT. This implies alternative OTR-coupled pathways, which are silenced or overruled when MEF2A is expressed and active. One potential pathway is the MAPK pathway, which is activated by the OTR, but not affected by the MEF2A knockout or inhibition of CaN. The MAPK pathway has been

associated with OT-induced anxiolysis, i.e., reduction of anxiety-like behavior in rats (Jurek *et al.*, 2015; van den Burg *et al.*, 2015; Blume *et al.*, 2008; Jurek *et al.*, 2012; Martinetz *et al.*, 2019) and targets transcription factors such as CREB and its cofactor CRTC3 (Jurek *et al.*, 2015; Martinetz *et al.*, 2019). The MAPK pathway is certainly one of the main effectors of OTR signaling (Jurek and Neumann, 2018); however, it might not be directly linked to MEF2A activation, mainly because the S408 residue requires dephosphorylation, not phosphorylation, for full transcriptional activation. Evidence from hippocampal neurons suggests that a Ca^{2+}-dependent activation of MEF2A requires the CaN-dependent dephosphorylation of MEF2A (Flavell *et al.*, 2006; Shalizi *et al.*, 2006). Based on this data, we identified CaN as the central part of a signaling cascade coupled to the OTR and thereby influencing the morphological response. Inhibiting CaN diminished the OT-induced neurite retraction in the H32 cells, strongly suggesting CaN as the upstream phosphatase responsible for OT-induced MEF2A activation. Moreover, mHypoE-N11 cells that lack MEF2A as a target of CaN should not be affected by CaN inhibition. Indeed, blocking CaN activity did not interfere with OT-induced (MEF2A-independent) neurite elongation. Since the actions of CaN and the MAPK signaling pathway have been shown to be co-dependent (Zhou *et al.*, 2001; Ichida and Finkel, 2001; Molkentin, 2004), we tested MEK1/2 activity under OT/CaN inhibition. In line with our hypothesis, OT-induced MEK1/2 phosphorylation was not affected by CaN inhibition, implying a direct activation of CaN by OTR-mediated $Ca2^{+}$ influx through either TrpV2 channels (van den Burg *et al.*, 2015), or release from intracellular stores ((Jurek and Neumann, 2018) and references therein). Furthermore, we provide evidence that a knockout of MEF2A has fundamental effects on mitochondrial functioning. While the basal respiration remains unaffected, the induced maximal respiration and spare respiratory capacity is significantly disinhibited compared to the wildtype cells. Next, we asked whether the increased respiratory capacity correlates with the ATP levels available for the cells. Interestingly, we found a significantly higher cellular ATP content under basal conditions in the H32ΔMEF2A cells. Although basal respiration does not differ between the two cell types, the increased respiratory capacity of the H32ΔMEF2A cells allows them to produce more ATP on demand, mainly due to the use of the more efficient aerobic pathway (see Energy Map, Figure A1). Whether the activity of MEF2A influences mitochondrial morphology or motility, and thereby respiratory

functionality, remains to be addressed by future studies. Whatever the effects on mitochondrial morphology and motility might be, the elevated ATP level present in the H32ΔMEF2A cells is pivotal for the OT-induced neurite outgrowth. Changes in neurite outgrowth and plasticity are strongly intertwined processes implicated in the regulation of neuronal connectivity. Recent findings indicate that a state of neuronal hyperconnectivity may play an essential role in the etiology of ASD (Zaslavsky *et al.*, 2019; Tang *et al.*, 2014; Zhang *et al.*, 2016). Many genes which have been associated with ASD and changes in neuronal connectivity belong to the integrin family (Lilja and Ivaska, 2018) and Ingenuity Pathway Analysis in myotube cells with MEF2 downregulations revealed that integrin signaling is one of the few pathways targeted by all MEF2 isoforms (Estrella *et al.*, 2015). One member of this family is integrin β1, a cell surface receptor linking the actin cytoskeleton with the extracellular matrix (ECM), mediating cell adhesion and thereby information that influences cellular morphology (Werner and Werb, 2002). We showed that this receptor is significantly downregulated in the H32ΔMEF2A cells. The effects of the MEF2A knockout on mitochondrial function and integrin signaling might not be causally connected. However, it has been suggested that alterations in mitochondrial function and integrin-mediated cell adhesion are functionally coupled processes (Werner and Werb, 2002). Crosstalk between cell adhesion and mitochondria is feasible, since it has been shown that mitochondria react to ECM composition changes, and in turn, modifications of the ECM can result as a consequence of mitochondrial functioning (de Cavanagh *et al.*, 2009). Mitochondria play a role in the mechanosensing processes of cells since mechanical forces from the ECM are transmitted to mitochondria via focal adhesions (Bartolak-Suki *et al.*, 2017). Therefore, it might be possible that the MEF2A knockout directly affects mitochondria by targeting the mitochondrial transcriptome or indirectly via mechanobiological changes transmitted by integrin receptors into the cells. Taken together, our results reveal a central role for MEF2A in the OT-induced regulation of neuronal morphology, connectivity, and mitochondrial function.

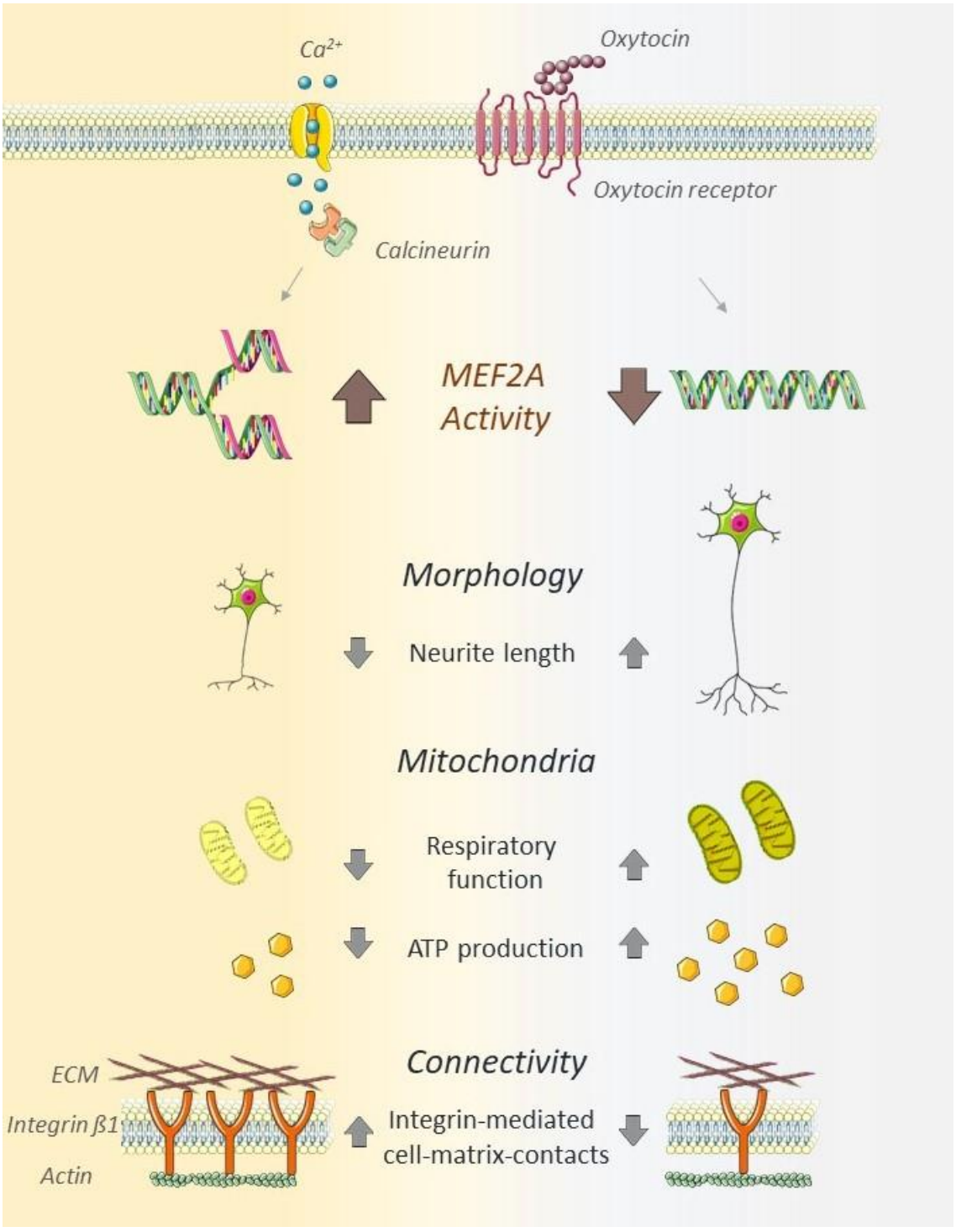

Figure 12. Schematic summary of MEF2A activity in OT-stimulated neurons. Neuronal MEF2A activity, induced by OT, reduces neurite length, decreases mitochondrial respiratory function, decreases ATP production, and increases integrin β1-mediated cell–matrix contacts. The absence or inhibition of MEF2A induces neurite outgrowth, increased respiratory function, ATP production, and decreased cell–matrix connectivity. The schematic art pieces used in this figure were provided by Servier Medical art (http://servier.com/Powerpoint-image-bank). Servier Medical Art by Servier is licensed under a Creative Commons Attribution 3.0 Unported License.

3.6 Appendix

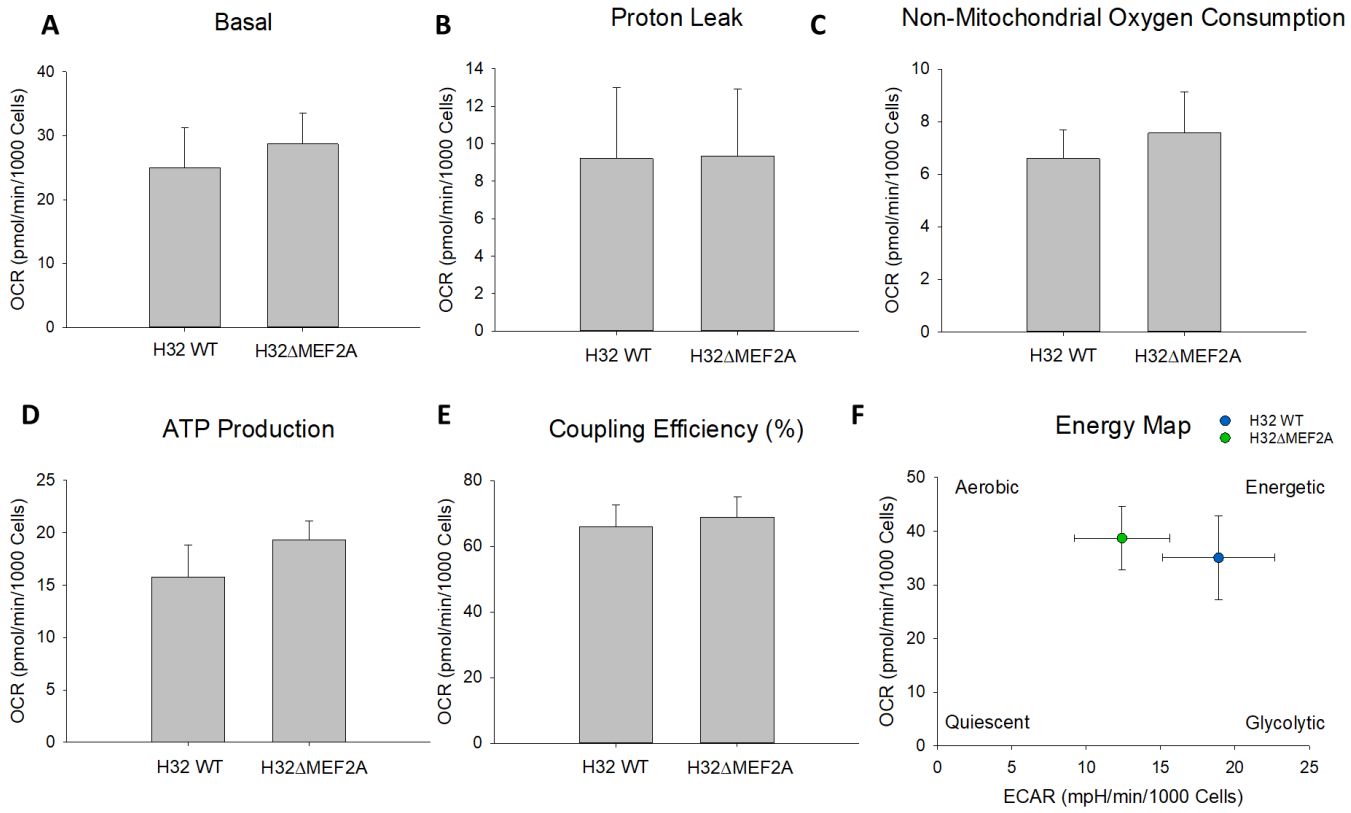

Figure A1. Mitochondrial function in H32 wildtype and H32ΔMEF2A cells. n = 3 per group.

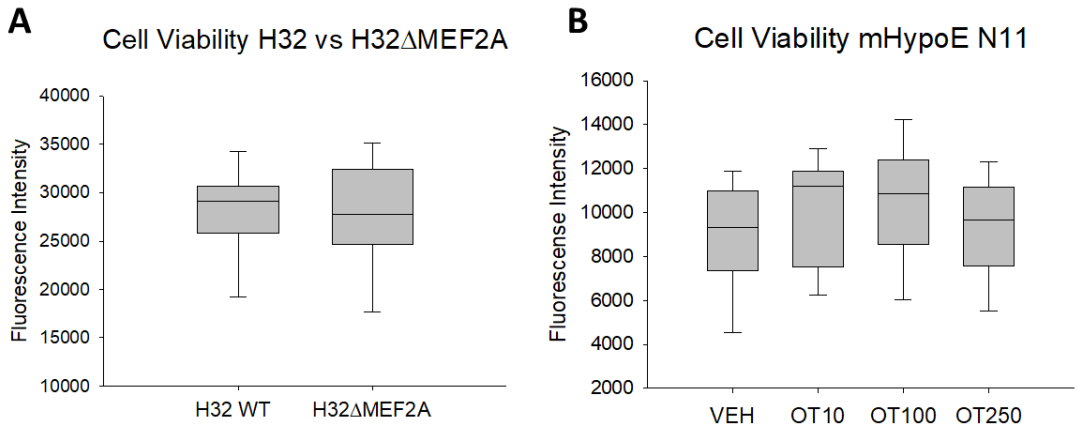

Figure A2. (A) Cell viability in H32 vs. H32ΔMEF2A. n = 24 per group. (B) Cell viability in OT-treated mHypoE-N11 cells. n = 22–24 per group.

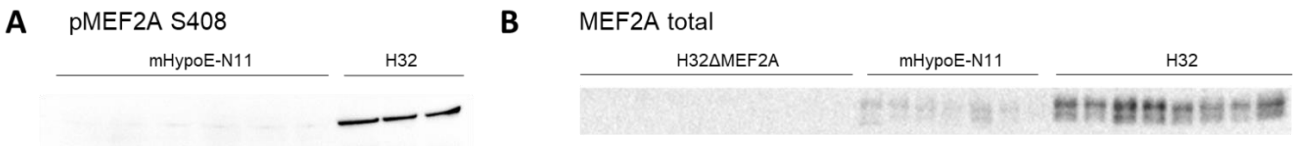

Figure A3. (A) and (B) Characterization of pMEF2A S408 and MEF2A total in mHypoE-N11, H32ΔMEF2A and H32 cells.

4 Functional characterization of the oxytocin receptor variant A218T

4.1 Abstract

The *OTR* gene variant rs4686302, a non-synonymous SNP resulting in the OTR variant A218T, has been associated with core characteristics of ASD, social cognition deficits/attention disorders, and trait empathy in healthy persons. However, the underlying molecular mechanism that causes those traits is unknown. In this study, we provide evidence that the OTR variant A218T as well as an *OTR* gene duplication alters OT-induced intracellular signaling. In a functional *in vitro* study we created two monoclonal HEK293 cell lines, stably expressing either the OTR wildtype or the A218T variant. We performed whole genome and RNA sequencing with a subsequent gene ontology (GO) analysis and assessed several cellular parameters like the OTR protein stability, MAPK pathway activation and Ca^{2+} signaling. Upon stimulation with OT, RNA Sequencing analysis revealed 7823 differentially regulated genes, with 429 genes being associated with ASD. Our study provides new insights into the cellular effects of genetic variations affecting the *OTR* that have been associated with ASD, and their functional consequences on cellular processes as well as gene expression.

4.2 Introduction

The neuropeptide OT is involved in the regulation of diverse behaviors such as anxiety, reciprocal trust, aggression, or affective behavior (Jurek and Neumann, 2018). In addition, it has been suggested as biomarker and target for treatment of ASD since it has been shown to significantly improve the social impairments of autistic children (Parker *et al.*, 2014; Parker *et al.*, 2017). However, the therapeutic efficiency is highly variable between individuals (for meta review see (Bakermans-Kranenburg and van Ijzendoorn, 2014)). Numerous SNPs in the *OTR* have been mapped and associated with a plethora of psychological traits in GWAS, however, most of the SNPs associated with a trait are intronic and/or synonymous mutations (Jurek and Neumann, 2018). Since non-synonymous SNPs can affect the protein structure and thereby its function, they presumably generate the most significant impact on the phenotype. The SNP rs4686302 is located within the coding region of the third exon in the human *OTR* gene and is a non-

synonymous SNP, leading to an amino acid exchange of alanine to threonine at the position 218 (A218T) in the OTR protein. This position is located within the fifth transmembrane domain of the OTR protein, where it is prone to affect the recently described protein structure of the OTR (Waltenspühl Y. *et al.*, 2020). These structural changes could affect the overall protein stability of the OTR, thereby changing the available receptor protein on the cell surface, representing a quantitative effect of the SNP. In addition, a qualitative effect of the SNP would encompass a change in protein structure that affects the positioning within or outside of caveolin-1-enriched lipid raft, and therefore the coupled intracellular signaling cascades (Cassoni *et al.*, 2004). It has previously been shown that receptor positioning is a decisive factor for PKA or Ca^{2+}-dependent signaling and has opposing outcomes for cell proliferation (Cassoni *et al.*, 2004; Reversi *et al.*, 2006). Activation of the OTR and the subsequent coupling to one of its Gα proteins eventuates in Ca^{2+} release from intracellular stores in hypothalamic explants (Tobin *et al.*, 2011) as well as Ca^{2+} influx from the extracellular space through TRPV2 channels in hypothalamic neuronal cell culture (van den Burg *et al.*, 2015). Ca^{2+}-dependent signaling transactivates the MAPK pathway, with ERK1/2 being the core factor for the behavioral anxiolytic and anti-stress effects of OT *in vivo* (Blume *et al.*, 2008; Jurek *et al.*, 2012; Jurek *et al.*, 2015). The MAPK-ERK1/2 pathway signals to the nucleus to regulate gene transcription (Kyriakis and Avruch, 2012), which we monitored by RNA-Sequencing identifying OTR-regulated genes that are affected by the presence of *OTR* gene variants.

On a behavioral level, rs4686302 has been linked to core symptoms of ASD and social cognition deficits (Francis *et al.*, 2016; Kalyoncu *et al.*, 2019). Besides these psychological conditions, rs4686302 has been associated with emotional empathy in non-clinical Chinese samples (Wu *et al.*, 2012). To our knowledge, there is only one functional study showing that patients with the rs4686302 SNP display a higher sensitivity to OT stimulation, causing premature birth as well as a reduced cesarean section prevalence (Fueg *et al.*, 2019). However, the mechanism underlying the increased sensitivity of the receptor in this setting has not been addressed yet.

In order to better understand the underlying mechanisms that could explain the behavioral and physiological phenotypes, we aimed to characterize the functional relevance of the OTR A218T on a cellular level. Therefore, we transduced HEK293 cells with an N-terminal FLAG-tagged *OTR*

that comprises the reference sequence or the rs4686302 SNP. By means of FLAG-tag-directed fluorescence-activated cell sorting (FACS) we isolated single clones of OTR-positive cells to create a monoclonal wildtype and a SNP-containing cell line. To control for genomic effects and map the insertion site of the *OTR* gene we conducted whole genome sequencing. Assessment of OTR stability, Ca^{2+} influx, activation of receptor-coupled signaling cascades, and consequential alterations in gene transcription have been conducted in wildtype and SNP-containing cells. This experimental setup allows us to determine the functional relevance of the rs4686302 SNP, and assemble a comprehensive model of cellular effects that would ultimately affect complex behavioral traits associated with ASD.

4.3 Material and methods

4.3.1 Cell culture

The HEK293 cell line was obtained from Prof. Dr. Eugen Kerkhoff from University Hospital Regensburg. Human HEK293 cells were cultured in DMEM (#D8437, Sigma Aldrich, Darmstadt, Germany), supplemented with 10 % heat-inactivated Gold fetal bovine serum (#FBS-HI-11A, Capricorn, Germany), and Penicillin/Streptomycin (#P4333, Sigma Aldrich, Darmstadt, Germany) at 37 °C and 5 % CO2 until 80 % confluency. Passaging was performed at least once a week by gentle trypsinization.

4.3.2 Transduction of HEK293 cells with *OTR* gene variants

For a stable integration of the *OTR* variants in the genome, moloney murine leukemia virus (MMLV) vectors were designed using VectorBuilder (Neu-Isenburg, Germany) and HEK293 cells were transduced according to the manufacturer's protocol. Wildtype MMLV virus has a plus-strand linear RNA genome. An MMLV retroviral vector is first constructed as a plasmid in *E. coli*. It is then transfected into packaging cells along with several helper plasmids. Inside the packaging cells, vector DNA located between the two long terminal repeats (LTRs) is transcribed into RNA, and viral proteins expressed by the helper plasmids further package the RNA into the virus. When the virus is added to target cells, the RNA cargo is shuttled into cells where it is reversely transcribed into DNA and randomly integrated in the host genome. The *OTR* gene that was placed in-between the two LTRs during vector construction is permanently inserted into host DNA

alongside the rest of the viral genome. Vector construction, amplification and packaging has been executed by VectorBuilder (Neu-Isenburg, Germany).

The constructs contained the respective human *OTR* gene (transcript variant 1, accession number NM_000916.3) or the SNP-containing variant (rs4686302) and an N-terminal 3xFLAG tag conjugated to the gene. To examine the transduction efficiency, and the further inheritance of the transduced genome, a control virus expressing EGFP was used. Genetically unmodified HEK293 cells served as reference for all transductions.

4.3.3 Establishment of monoclonal cell lines expressing the OTR

In order to reduce the variability among the resulting polyclonal cell populations, we aimed to use monoclonal cell lines for our approaches. Single cell sorting was performed by FACS at the Central FACS Facility of the Regensburg Center for Interventional Immunology. Cells were stained with an anti-DDDDK tag antibody conjugated with Phycoerythrin (ab72469, abcam, Cambridge, UK) prior to the flow cytometry. Positively transduced cells were deposited individually in a 96-well plate and re-cultured for several weeks using a mixture of fresh and conditioned medium. Conditioned medium was generated by cultivating HEK293 cells in normal growth medium to near confluency. The medium now containing growth factors released by the cell layer was removed and stored at 4°C until further use.

4.3.4 Whole-genome sequencing

Two cell lines, one expressing the reference and one the SNP-containing *OTR* gene, were chosen based on their expression levels of the OTR protein, validated by FLAG-tag Western Blot. For further analysis, including the genomic integration site of the constructs, cells were sent to the company CeGaT GmbH (Tübingen) for whole-genome sequencing and subsequent bioinformatics analyses.

4.3.5 Cytosolic calcium imaging with Fura-2/AM

The basal cytosolic Ca^{2+} amount and the OT-induced cellular Ca^{2+} response were assessed using the ratiometric Ca^{2+} indicator Fura-2/AM. 7×10^5 cells were seeded on sterile glass coverslips (diameter 25 mm), placed in 6-well plates, and grown overnight in medium, humidified air and 5 % CO_2. On the next day, cells were loaded with 2 µM Fura-2/AM and Pluronic F127 in OptiMEM

(Life Technologies, Carlsbad, USA) for 30 min at 37 °C, humidified air and 5 % CO_2. For imaging, the loading medium was replaced by assay buffer (140 mM NaCl, 5 mM KCl, 1.8 mM $CaCl_2$, 1 mM $MgSO_4$, 10 mM glucose, and 10 mM HEPES) and the coverslip was mounted in a chamber on the inverted microscope (ZEISS Observer Z.1, Jena, Germany) equipped with a Fluar 40/1.3 objective lens (ZEISS). Cells were illuminated with light of 340 and 380 nm (BP 340/30 HE, BP 387/15 HE) using a fast wavelength switching and excitation device (Lambda DG-4, Sutter Instrument, Novato, USA), and fluorescence was detected at 510 nm (BP 510/90 HE and FT 409) using an AxioCam MRm LCD camera (ZEISS). The cytosolic Ca^{2+} level was analyzed as fluorescence ratio at 510 nm after excitation at 340 and 380 nm. Solutions (Ringer +/- Ca^{2+}) and OT (final concentration 100 nM) were applied with a perfusion system. Regions of interest were drawn over selected cells in the visual field using the Zen imaging software (ZEISS) and FIJI/ImageJ. Ca^{2+} traces were plotted with the Origin Software (OriginLab, version 9.7.0.188) evaluating the basal cytosolic Ca^{2+}, area under the curve, amplitude as well as full width half maximum.

4.3.6 Protein isolation and Western blot

The expression or phosphorylation levels of the proteins FLAG and ERK1/2 were detected via Western blot analysis. For the extraction of proteins, cells were scraped in 1 mL ice-cold PBS using a cell scraper (#83.1830, Sarstedt, Nümbrecht, Germany), centrifuged and resuspended in 100 µl RIPA lysis buffer (R0278, Sigma Aldrich, Darmstadt, Germany) supplemented with HALT inhibitor and EDTA (78444, Thermo Fisher, Waltham, MA) to obtain whole cell lysates. Western blotting was performed as previously described in (Meyer *et al.*, 2018). 20 to 30 µg of whole cell extract were loaded and separated in a 12 % Mini PROTEAN or Criterion TGX Stainfree gel (Bio-Rad, Feldkirchen, Germany), respectively. Semi-dry blotting of separated proteins to nitrocellulose membranes was conducted using the FAST Blotter by Bio-Rad. Stainfree total protein method by Bio-Rad served as protein loading control. Specific antibodies for anti-DDDDK (ab1162, abcam, Cambridge, UK) revealed expression levels of the protein of interest, as well as phosphorylation levels of ERK1/2.

4.3.7 RNA Sequencing and gene ontology analysis

Effects of the receptor variant on the cellular transcriptome were analyzed by RNA Sequencing. Three samples of each cell line were stimulated with 100 nM OT for 1 hour and sent to the company CeGaT GmbH (Tübingen) for performance and evaluation of the transcriptome, including a subsequent GO analysis of differentially regulated genes between the two distinct OTR variant containing cell lines. For RNA sequencing, trimmed raw reads were aligned to the human reference genome (hg19) using STAR (version 2.5.2b). Differential expression analysis between groups was performed with DESeq2 (version 1.24.0) in R (version 3.6.1) (R Core Team 2015). DESeq2 uses a negative binomial generalized linear model to test for differential expression based on gene counts. The list of genes associated with ASD was downloaded from the SFARI database (https://gene.sfari.org/autdb/GS_Home.do) and compared to the list of differentially regulated genes obtained from the transcriptome analysis. Additionally, genes were categorized according to the gene scoring module of SFARI. Genes scored as category 1 show high confidence, meaning each of these genes has been clearly implicated in ASD, and meet the most rigorous threshold of genome-wide significance. Category 2 represents strong candidates that are uniquely implicated by WGAS reaching genome-wide significance and that have most likely a functional effect. In category 3, genes with a suggestive evidence with certain proof from significant but unreplicated studies are listed. For GO analysis, significantly down- and up-regulated genes were extracted using a log2 fold change of 0.58. Using the R-package GOfuncR (Grote, 2020) we identified significantly enriched and depleted GO terms for up- and down-regulated genes separately, as well as in the combined dataset. GOfuncR uses a hypergeometric test to identify over- and underrepresented GO terms in a set of genes given the distribution of GO terms in the background (e.g. the human transcriptome).

4.3.8 Cycloheximide protein degradation assay

The turnover of the OTR protein was determined using cycloheximide (CHX)-mediated inhibition of de novo protein synthesis. Cells were seeded, and subsequently treated with 20 µg/ml CHX (Sigma, Taufkirchen, Germany) for 0-24 hours. Proteins were isolated with RIPA and Western Blot analysis was performed. The expression of 3x-FLAG was analyzed in whole protein lysate.

4.3.9 Statistical analysis

Statistical analyses was performed using Sigma Plot (version 13.0, Systat Software). Data was analyzed either by t-test or two-way ANOVA followed by Tukey post hoc test as indicated in the figure legends or text. Statistical significance was accepted at $p < 0.05$. Due to the large number of genes in the RNA sequencing data set, Benjamini-Hochberg multiple-testing correction was used for controlling false discovery rate (p_{adj}, adjusted p-value). In Ca^{2+} imaging experiments, n represents number of cells/traces, in Western Blots, n represents number of cell lysates. Data are presented as mean + standard error of the mean.

4.4 Results

Whole genome sequencing of the two human HEK293 cell lines expressing an *OTR* variant was performed in order to validate the successful transduction and to identify the localization of insertion sites (Table 4). The genomic analysis revealed that the *OTR* WT construct was inserted on chromosome 8 at the indicated position, which is located within the *MYC* gene. The *OTR* SNP construct was inserted twice on chromosome 6 at the two indicated positions, which are located within the *NUDT3* and *USP45* gene.

Table 4. Identified insertion points of the oxytocin receptor (OTR) gene constructs in human HEK293 cells.

Cell line	Chromosome	Position	Gene
OTR WT	8	128799928	MYC
OTR A218T	6	34292480	NUDT3
	6	99962623	USP45

Additionally, for each insertion point, ten genes upstream and downstream of the location were extracted and analyzed for potential dysregulations by the insertion. Comparison with the differentially expressed genes from the transcriptomic analysis revealed several genes close to the insertion points that are significantly differently regulated between the two cell lines (Table 5).

Table 5. Differentially expressed genes and their p-value close to the insertion points.

Insertion point	Gene	Adjusted p-value
MYC	MYC	5.24e-33
	FAM49B	0.025
	LPCAT1	7.66e-23
	FAM84B	0.0005
	ASAP1	0.01
NUDT3	SCUBE3	1.16e-5
	SNRPC	0.006
	GRM4	0.0007
	ITPR3	1.35e-32
	UQCC2	0.004
	HMGA1	6.36e-16
USP45	MMS22L	0.04
	POU3F2	0.04
	FBXL4	5.73e-5
	COQ3	1.73e-5
	PNISR	5.99e-26
	USP45	0.02
	CCNC	1.94e-7
	SIM1	7.04e-5
	ASCC3	0.0001

The double gene insertion in the OTR A218T cell line results in a 1.36-fold upregulation of the *OTR* transcript, which was confirmed by RNA Sequencing, and a 1.78-fold upregulation of the protein compared to the OTR WT expressing cells (Figure 13A-C). Due to a lack of specificity of OTR antibodies (Yoshida *et al.*, 2009), we detected OTR expression via the 3x-FLAG tag, whose specificity could be confirmed in a control experiment (data not shown).

Furthermore, we aimed to analyze the stability of the OTR variants using the CHX chase protein degradation assay. The OTR protein stability was assessed by incubating cells for 0 to 24 hours with 20 µg/ml of CHX, a well-known inhibitor of eukaryotic translation (Figure 13E). The OTR protein expression was quantified at different time points after CHX treatment as percentage of the initial protein level (0 min of CHX treatment) and detected via the 3xFLAG-tag. Results from protein degradation analysis suggest that the OTR A218T protein is significantly more stable than the OTR WT variant (Figure 13D).

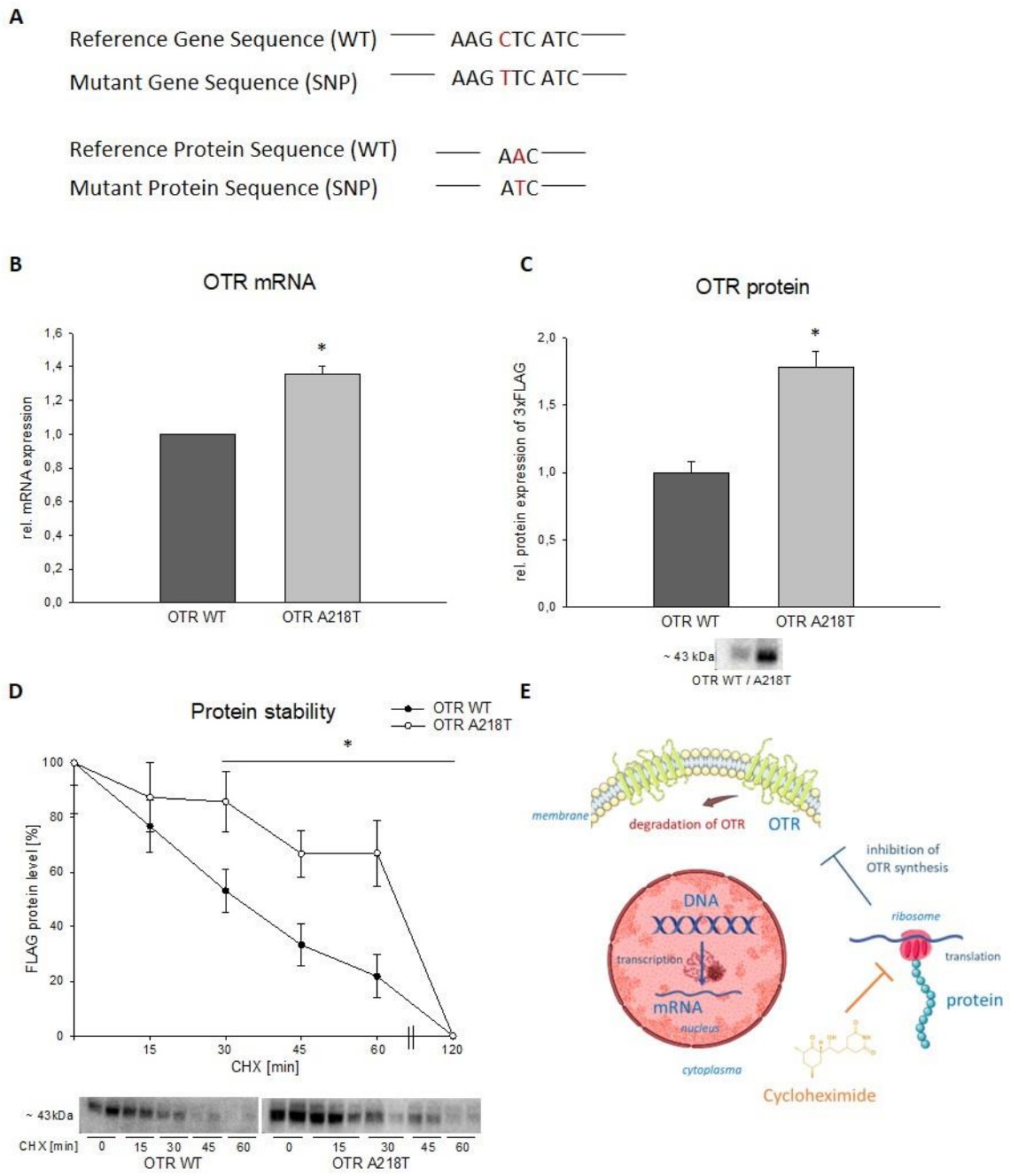

Figure 13. (A) Gene and resulting protein sequence of the wildtype (WT) and mutant OTR variant A218T. The mutation of the base cytosine (WT) to thymine (SNP) in the gene sequences leads to an amino acid exchange of in the protein sequence. The change in the nucleotide triplet codes for a threonine (SNP) instead on an alanine (WT) in the OTR protein. (B) Relative mRNA expression level of the oxytocin receptor (*OTR*) revealed by RNA sequencing in cells expressing the A218T variant compared to OTR WT. The *OTR* mRNA level is significantly higher in the A218T compared to WT cells. * $p_{adj} < 0.001$. (C) Relative protein expression of 3x-FLAG tag reflecting the OTR expression in the WT compared to A218T cell line. T-test revealed a significant increased protein expression of the OTR in the A218T cells. n = 6. * p = 0.005. (D) Protein stability evaluated by cycloheximide (CHX) assay. HEK293 cells expressing either the WT OTR or OTR mutant A218T were treated with CHX (20 µg/ml) for the indicated times (in min), and 3xFLAG-tag was detected in Western Blot. FLAG levels after treatment with CHX were quantified as percentage of the initial FLAG protein level (0 min of CHX treatment). Two-way ANOVA revealed a significant effect between the

cell lines. CHX treatment leads to a significant reduction of the initial protein level beginning after 30 min incubation in both cell lines. There is no significant interaction between cell line and treatment. Data are shown as mean ± SEM. n = 4-6 for each data point. * p (cell line) = 0.002. * p (treatment) < 0.001. (E) Scheme of CHX inhibition effect on protein translation. The schematic art pieces used in this figure were provided by Servier Medical art (http://servier.com/Powerpoint-image-bank). Servier Medical Art by Servier is licensed under a Creative Commons Attribution 3.0 Unported License.

In order to study the impact of the OTR variants on the OT-induced Ca^{2+} influx, we performed Ca^{2+} imaging using Fura-2/AM. We evaluated the Ca^{2+} response of the cells in presence and absence of Ca^{2+} in the Ringer solution to elucidate the source (extra- versus intracellular, representative traces Figure 14A and 14B). Two-way ANOVA revealed a significantly reduced cytosolic Ca^{2+} concentration in the A218T cells compared to OTR WT under physiological conditions as well as in absence of extracellular Ca^{2+} (Figure 14C). The amplitude of the OT-induced Ca^{2+} peak was lower in the OTR WT cells incubated in Ca^{2+}-free Ringer compared to the A218T cells in the same medium and to the WT cells when incubated in Ca^{2+}-containing Ringer solution (Figure 14D). The area under the curve revealed a cell-line specific main effect showing a higher increase in the cytosolic Ca^{2+} concentration upon OT stimulation in the OTR A218T compared to the WT cell line (Figure 14E). The full width at half maximum (FWHM), which reflects the kinetics of the OT-induced Ca^{2+} response, differed significantly between the two cell lines irrespective from the bathing solution, indicating a prolonged OT-induced Ca^{2+} response in the A218T cells (Figure 14F).

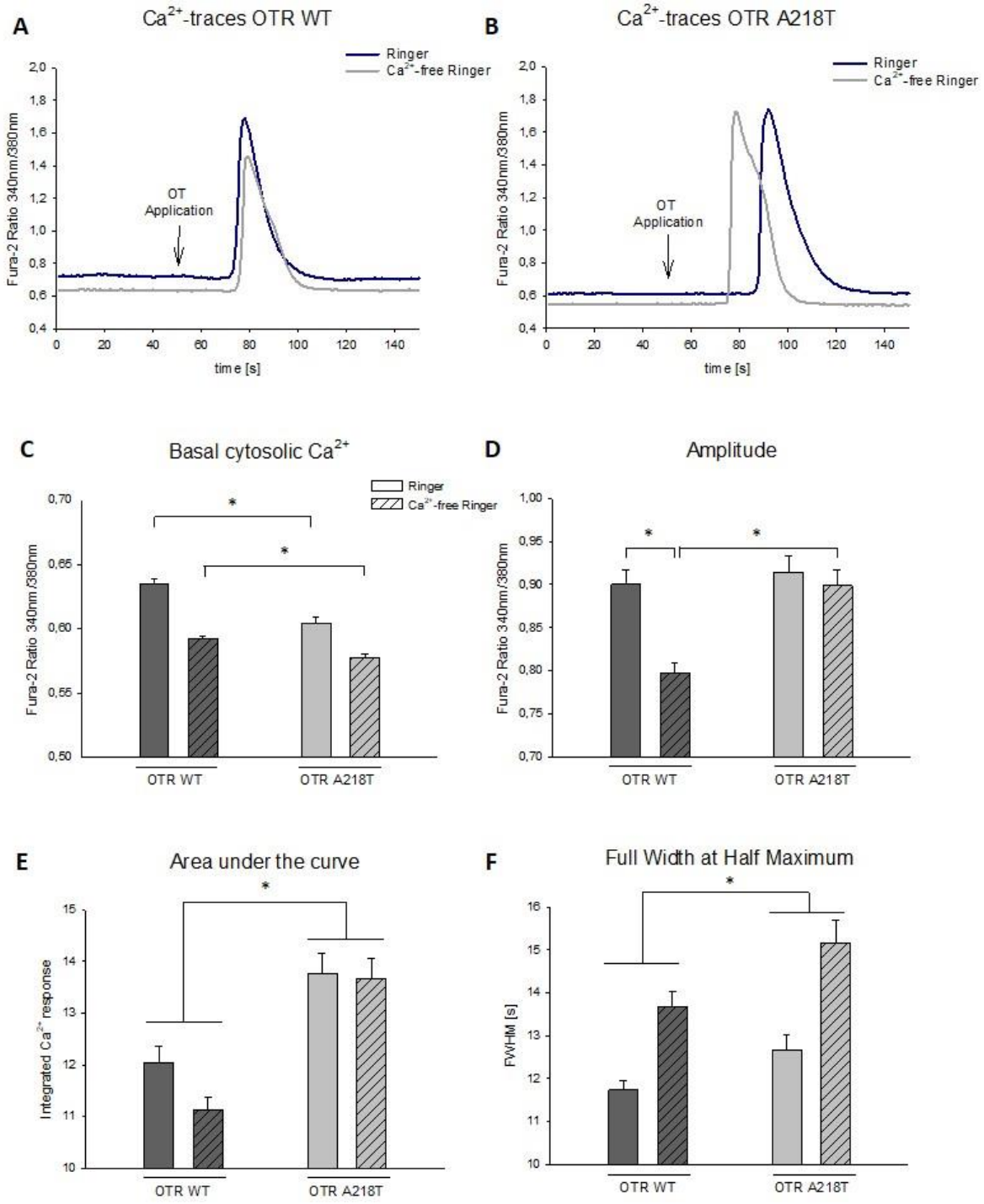

Figure 14. (A) and (B) Representative Ca^{2+}-traces of cells encoding either the OTR wildtype (WT) or A218T variant after stimulation with 100 nM oxytocin (OT) in presence (grey line) or absence (red line) of Ca^{2+} in Ringer. Time shift in (B) is not representative. (C) Basal Fura-2 340 nm/380 nm ratios of the OTR WT and OTR mutant cell line. The cell line encoding the OTR A218T variant has a significantly reduced concentration of basal cytosolic Ca^{2+} compared to OTR WT under both, physiological and Ca^{2+}-free conditions. * $p < 0.001$. (D) Fura-2 340 nm/380 nm ratio amplitudes of the OTR WT and OTR A218T cell line after application of 100 nM OT. The maximal amplitude of OT-induced Ca^{2+}-peaks in OTR WT cells is significantly reduced in absence of extracellular Ca^{2+} in comparison to the generated peak under physiological conditions as well as to the amplitude of the OTR A218T mutant under the Ca^{2+}-free conditions.

* $p < 0.001$. Moreover, there is a statistically significant interaction between cell line and treatment (+/- Ca^{2+} in Ringer), * $p = 0.01$. (E) The area under the curve is significantly increased in OTR A218T compared to OTR WT cells under both conditions. The area under the curve is calculated and shown as an integral over time above the baseline. * $p < 0.001$. (F) Two-way ANOVA revealed a main effect between the cell lines regarding the full width half maximum (FWHM) in the OTR A218T cells reflecting a prolonged Ca^{2+} response. * $p = 0.02$. Sample size for graphs C, D, E and F: n (OTR WT + Ringer) = 91, n (OTR WT + Ca^{2+}-free Ringer) = 96, n (OTR A218T + Ringer) = 63, n (OTR A218T + Ca^{2+}-free Ringer) = 89.

To assess MAPK pathway activation, the basal and OT-induced phosphorylation levels of ERK1/2 were assessed by Western Blot. Incubation of the OTR WT or OTR A218T cells with 100 nM OT over a time course of one hour resulted in a significant increased phosphorylation of ERK2 as it has been already shown by several studies (Blume *et al.*, 2008; Jurek *et al.*, 2012) (Figure 15B). No significant effect of OT-induced phosphorylation of ERK1 could be detected, which might be due to the small sample size (Figure 15A). However, there was a trend towards a main effect between the cell lines, with a significant effect after 60 min. Since 60 min of OT-incubation revealed the overall strongest effects, the stimulation was repeated with greater sample size. A direct comparison of the two cell lines on a basal level or after one hour incubation with 100 nM OT revealed a significant reduced MAPK activation in the OTR A218T cells reflected by both, pERK1 (Figure 15C) and pERK2 (Figure 15D) levels.

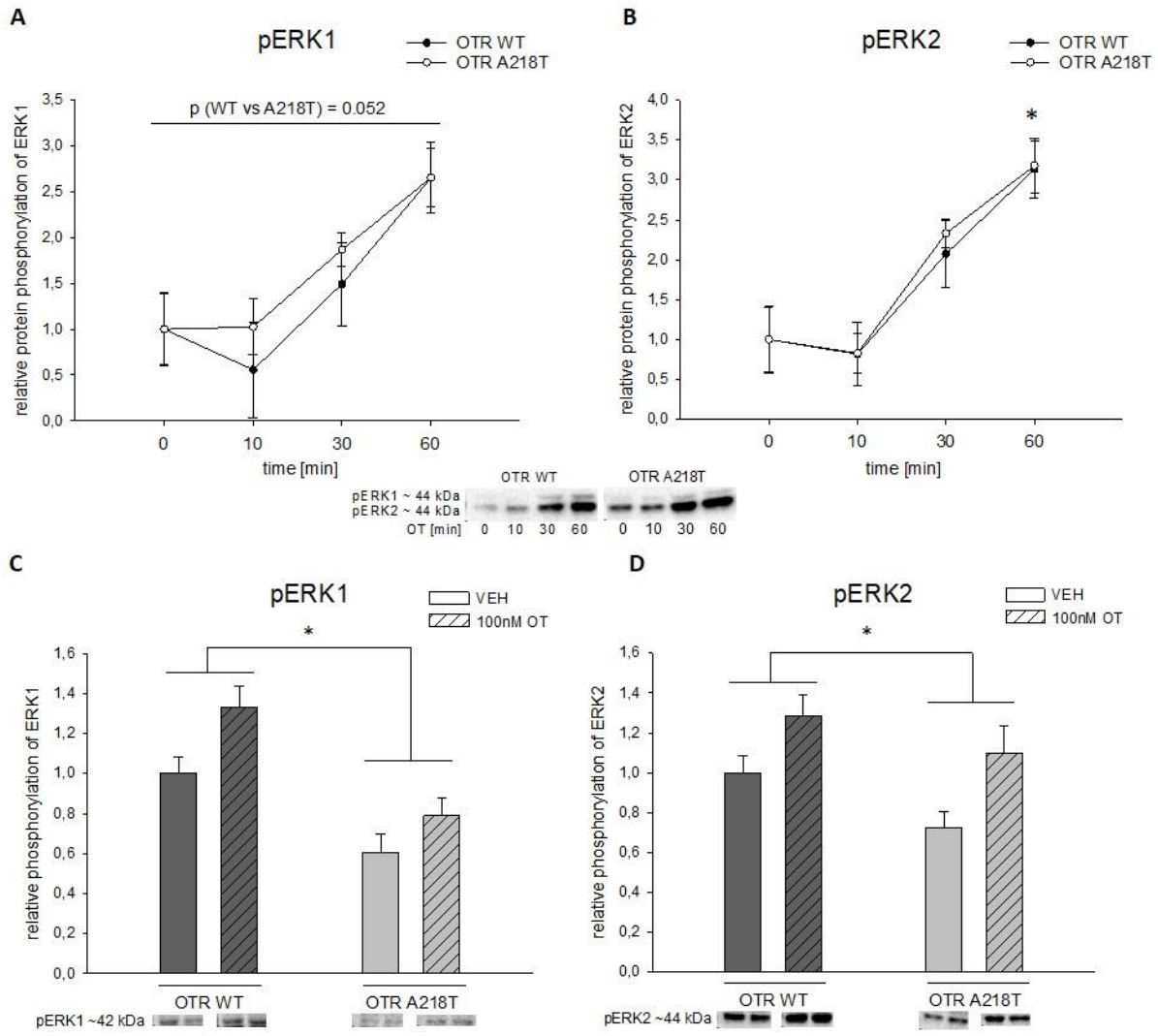

Figure 15. (A) Timeline of ERK1 phosphorylation in OTR WT and OTR A218T cells after stimulation with 100 nM oxytocin (OT) for 10, 30 or 60 min. Two-way ANOVA did not reveal a significant effect between the cell lines in the ERK1 phosphorylation, although there was a trend ($p = 0.052$). n = 5 per group. (B) Timeline of ERK2 phosphorylation in OTR WT and OTR A218T cells after stimulation with 100 nM OT for 10, 30 or 60 min. There was a significant effect in the OT treatment, but no difference in them time pattern of phosphorylation between the cell lines. * p (60 min vs. 0 min) = 0.022. n = 5 per group. (C) and (D) Relative phosphorylation of ERK1 (C) and ERK2 (D) in OTR WT and A218T cells after treatment with 100 nM OT for 1h. Direct comparison of the cell lines revealed that the OTR A218T cells show a lower phosphorylation level than the OTR WT cells independent from the treatment present (VEH/OT). * $p < 0.049$. n = 10 per group.

In order to analyze differences in target gene expression, three samples per cell line that have been stimulated with 100 nM OT for one hour were sent for RNA sequencing, which revealed a large cohort of significantly regulated genes in OT-stimulated OTR A218T cells, when compared to expression levels in stimulated OTR WT cells. One sample in the OTR WT group had to be removed because of a strong deviation in the hierarchical clustering of the samples according to the similarity of their expression data.

When filtered by corrected significance $p_{adj} < 0.05$, a number of 7823 genes were differentially regulated (Table 6). The top 100 differentially expressed genes are listed in a heatmap (Figure 16).

Table 6. Statistically significant differentially expressed genes in comparison group A vs. group B.

Group A	**Group B**	**Number of significant regulated genes (p_{adj}<0.05)**
OTR A218T	OTR WT	7823

429 of those genes have been identified as ASD risk genes after comparison with the database provided by SFARI. Additionally, the filtered genes have been classified according to the gene scoring module in different categories ranging from 1 (high confidence) to 3 (suggestive evidence). 107 differentially expressed genes have fallen in category 1 of the ASD scoring, the 50 most frequently reported are listed Table 7.

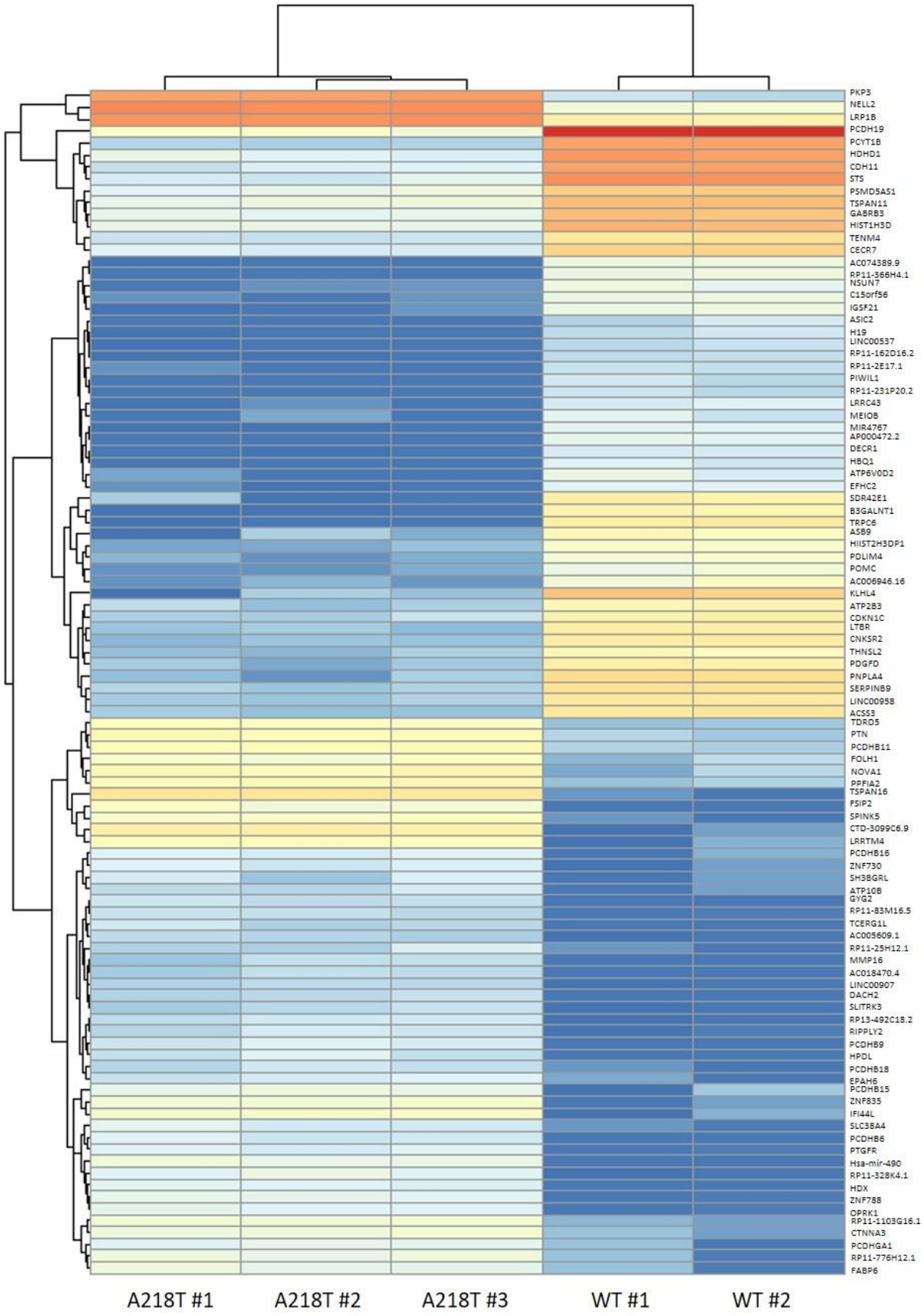
PKP3
NELL2
LRP1B
PCDH19
PCYT1B
HDHD1
CDH11
STS
PSMD5AS1
TSPAN11
GABRB3
HIST1H3D
TENM4
CECR7
AC074389.9
RP11-366H4.1
NSUN7
C15orf56
IGSF21
ASIC2
H19
LINC00537
RP11-162D16.2
RP11-2E17.1
PIWIL1
RP11-231P20.2
LRRC43
MEIOB
MIR4767
AP000472.2
DECR1
HBQ1
ATP6V0D2
EFHC2
SDR42E1
B3GALNT1
TRPC6
ASB9
HIIST2H3DP1
PDLIM4
POMC
AC006946.16
KLHL4
ATP2B3
CDKN1C
LTBR
CNKSR2
THNSL2
PDGFD
PNPLA4
SERPINB9
LINC00958
ACSS3
TDRD5
PTN
PCDHB11
FOLH1
NOVA1
PPFIA2
TSPAN16
FSIP2
SPINK5
CTD-3099C6.9
LRRTM4
PCDHB16
ZNF730
SH3BGRL
ATP10B
GYG2
RP11-83M16.5
TCERG1L
AC005609.1
RP11-25H12.1
MMP16
AC018470.4
LINC00907
DACH2
SLITRK3
RP13-492C18.2
RIPPLY2
PCDHB9
HPDL
PCDHB18
EPAH6
PCDHB15
ZNF835
IFI44L
SLC38A4
PCDHB6
PTGFR
Hsa-mir-490
RP11-328K4.1
HDX
ZNF788
OPRK1
RP11-1103G16.1
CTNNA3
PCDHGA1
RP11-776H12.1
FABP6
A218T #1
A218T #2
A218T #3
WT #1
WT #2

Figure 16. Heatmap of the top 100 differentially expressed genes in the OTR A218T compared to OTR WT cells. Color-coded values represent the log2FoldChange expression after normalization and averaging over the biological replicates in each cell line. Genes (rows) and cell lines (columns) were clustered hierarchically according to similarity between expression levels.

Table 7. The most frequently reported ASD-associated genes, which are differentially expressed in OTR A218T compared to OTR WT cells, with full gene name, the number (#) of reports, and log2FoldChange from transcriptome analysis of the cell lines. Underlined with a color code from red to blue, positive value indicates a higher expression in A218T compared to WT, while a negative value refers to a reduced expression.

Gene	Gene name	# of reports	log2FoldChange
SHANK3	SH3 and multiple ankyrin repeat domains 3	84	-0.52
MECP2	Methyl CpG binding protein 2	82	0.27
PTEN	Phosphatase and tensin homolog	62	0.25
SYNGAP1	Synaptic Ras GTPase activating protein 1	56	0.42
CHD8	Chromodomain helicase DNA binding protein 8	54	0.17
FOXP1	Forkhead box P1	50	0.28
CACNA1C	Calcium channel, voltage-dependent, L type, alpha 1C subunit	47	-2.17
ARID1B	AT-rich interaction domain 1B	47	0.20
ANKRD11	Ankyrin repeat domain 11	45	0.21
DYRK1A	Dual-specificity tyrosine-(Y)-phosphorylation regulated kinase 1A	45	0.33
TCF4	Transcription factor 4	45	0.56
FOXP2	Forkhead box P2	43	0.63
STXBP1	Syntaxin binding protein 1	42	-0.75
ADNP	Activity-dependent neuroprotector homeobox	41	0.28
CHD2	Chromodomain helicase DNA binding protein 2	40	0.43
GABRB3	Gamma-aminobutyric acid (GABA) A receptor, beta 3	38	-4.78
SHANK2	SH3 and multiple ankyrin repeat domains 2	35	-2.41
SCN8A	Sodium channel, voltage gated, type VIII, alpha subunit	35	0.50
MBD5	Methyl-CpG binding domain protein 5	35	0.62
PCDH19	Protocadherin 19	34	-7.10
MED13L	Mediator complex subunit 13-like	33	0.19
POGZ	Pogo transposable element with ZNF domain	33	0.51
TSC2	Tuberous sclerosis 2	32	-0.20
CHD7	Chromodomain helicase DNA binding protein 7	28	0.28
UBE3A	Ubiquitin protein ligase E3A	27	0.15
IQSEC2	IQ motif and Sec7 domain 2	26	-1.62
TRIO	Trio Rho guanine nucleotide exchange factor	26	0.16
ANK3	Ankyrin 3	26	0.20
FOXG1	Forkhead box G1	26	0.40
ASXL3	Additional sex combs like 3	25	0.29
SETD5	SET domain containing 5	25	0.46
NF1	Neurofibromin 1	24	-0.14
ZBTB20	Zinc finger and BTB domain containing 20	23	1.08
RAI1	Retinoic acid induced 1	22	-0.39
TSC1	Tuberous sclerosis 1	21	-0.32

CUL3	Cullin 3	21	0.15
TBL1XR1	Transducin beta like 1 X-linked receptor 1	21	0.21
ATRX	Alpha thalassemia/mental retardation syndrome X-linked	21	0.31
VPS13B	Vacuolar protein sorting 13 homolog B (yeast)	20	0.21
DEAF1	DEAF1 transcription factor	19	-0.15
DDX3X	DEAD (Asp-Glu-Ala-Asp) box helicase 3, X-linked	19	0.20
NBEA	Neurobeachin	19	0.29
WAC	WW domain containing adaptor with coiled-coil	19	0.33
KMT2C	Lysine (K)-specific methyltransferase 2C	18	0.16
BCL11A	B-cell CLL/lymphoma 11A (zinc finger protein)	18	0.42
NRXN3	Neurexin 3	18	0.71
ARX	Aristaless related homeobox	17	-1.24
NSD1	Nuclear receptor binding SET domain protein 1	17	0.14
ANK2	Ankyrin 2, neuronal	17	0.32

GO analysis of the differentially expressed genes between the OTR WT and A218T cell line was conducted using a log2FoldChange cutoff of 1.5. The analysis was done using only the up-regulated genes, only the down-regulated genes and up- and down-regulated genes together (Table 8).

Table 8. Number (#) of analyzed genes and enriched gene ontology (GO) terms. GO terms were identified for genes significantly up- and down-regulated in OTR A218T compared to WT cells separately, as well as in the combined dataset.

Dataset	# of significant genes	Genes with GO annotation (in %)	Biological processes	Cellular components	Molecular functions
Up-regulated	804	61.94	50	14	19
Down-regulated	1803	81.2	306	92	26
Both	2607	75.26	286	90	23

Not all human genes have been annotated yet, therefore only a certain percentage of the differentially expressed genes have a GO annotation. However, most genes with an annotation are assigned to several GO terms. Since the GO has a tree-like structure, there is a redundancy in the data. In line with the results obtained in this study and in previous publications of our group, a few GO terms were selected from the huge dataset and assigned to OTR-coupled and/or ASD-related processes (Table 9).

Table 9. Selection of gene ontology (GO) terms up- and downregulated in OTR A218T vs WT cells with identification number assigned to oxytocin receptor-coupled processes.

	GO term	GO ID
Receptor binding and stability	oxytocin receptor binding	GO:0031855
	cellular response to cycloheximide	GO:0071409
Calcium signaling	calcium-mediated signaling	GO:0019722
	cellular response to calcium ion	GO:0071277
	calcium ion homeostasis	GO:0055074
	calcium ion transport	GO:0006816
	calcium ion transmembrane import into cytosol	GO:0097553
	calcium ion transmembrane transport	GO:0070588
	calcium ion transmembrane transport via high voltage-gated calcium channel	GO:0061577
	calcium ion transmembrane transport via low voltage-gated calcium channel	GO:0090676
MAPK signaling	MAPK cascade	GO:0000165
	p38 MAPK cascade	GO:0038066
	activation of MAPK activity	GO:0000187
	activation of MAPKK activity	GO:0000186
	activation of MAPKKK activity	GO:0000185
Connectivity	cell-cell adhesion	GO:0098609
	cell-cell adhesion mediated by integrin	GO:0033631
	cell-cell signaling	GO:0007267
	integrin-mediated signaling pathway	GO:0007229
Cellular morphology	cytoskeleton organization	GO:0007010
	actin cytoskeleton organization	GO:0030036
	intermediate filament organization	GO:0045109
	microtubule cytoskeleton organization	GO:0000226
	cell morphogenesis	GO:0000902
	dendrite extension	GO:0097484
	axon extension	GO:0048675
Mitochondrial function	mitochondrial calcium ion homeostasis	GO:0051560
	mitochondrial calcium ion transmembrane transport	GO:0006851
	mitochondrial ATP synthesis coupled electron transport	GO:0042775
	mitochondrial ATP synthesis coupled proton transport	GO:0042776
	mitochondrial respiratory chain complex assembly	GO:0033108

4.5 Discussion

In this study, we evaluated the cellular effects caused by genetic variations affecting the *OTR* gene. We aimed to assess the functional relevance of the non-synonymous SNP rs4686302, which has been associated with core symptoms of ASD, cognition deficits, empathy, and preterm birth (Wu *et al.*, 2012; Francis *et al.*, 2016; Kalyoncu *et al.*, 2019; Kim *et al.*, 2013). Our approach of using MMLVs to permanently integrate the *OTR* gene into the HEK293 genome granted us with a stable expression level in the monoclonal cell line, however, it bears the risk of unwanted disruption of host genes. Having analyzed the data generated by the whole genome sequencing, we identified the integration site(s) of the *OTR*, and thereby recognized a few target genes that might have been affected for technical reasons instead of OT treatment. In the OTR WT cell line, the construct was integrated into the host genome on chromosome 8, and in the OTR A218T cells twice on chromosome 6. This affected three different genes, namely *MYC*, *NUDT3*, and *USP45*. Additionally, differentially regulated genes that are located close to the insertion sites were listed and should be carefully interpreted. The double insertion of the SNP construct resulting in a higher expression of OTR mRNA and protein bears clinical relevance. An increased prevalence of CNVs, including duplications or deletions of certain genes, have been found in individuals with ASD. One case study confirming such a variation affecting the *OTR* gene, presents a 9-year old boy with pervasive developmental disorder suffering from obesity and behavioral issues, underscoring the role of an *OTR* gene duplication with consecutive overexpression in ASD (Bittel *et al.*, 2006). This level of precise in-depth genomic information is not addressed in the majority of such studies, and has rarely been discussed.

The SNP rs4686302 is located within the coding sequence of Exon 3 and leads to an alanine/threonine amino acid exchange. Such exchange in the amino acid sequence is prone to induce self-aggregation of the resulting peptide due to the inherent preferences of alanine to form helices and of threonine to support beta-sheet structures (Podoly *et al.*, 2010). Interestingly, we have found stabilizing effects of this SNP on receptor protein stability. Using CHX as a potent translational inhibitor, we could provide evidence that the OTR A218T variant shows significantly longer half-life kinetics suggesting an increased protein stability. Because of this conformational change leading to an enhanced stability, receptor properties like ligand binding might be

affected, as it has been recently described for rs4686302 (Fueg *et al.*, 2019). In line with the already reported increased sensitivity to OT, we found that the OT-induced increase in intracellular Ca^{2+} levels is higher in OTR A218T cells compared to the OTR WT cells. Moreover, the kinetic profile of the Ca^{2+} response indicates a prolonged signal duration in the OTR A218T cells. This suggests that the neuroprotective strategy to prevent Ca^{2+} cytotoxicity, i.e. a cell's mechanism of shutting down Ca^{2+} channels in order to stop Ca^{2+} entry (Duncan *et al.*, 2010), might be compromised when the OTR A218T variant is expressed. Additionally, WT and A218T cells show differences with respect to the Ca^{2+} source they mainly rely on. While the OT-evoked Ca^{2+} increase in the cytoplasm of OTR WT cells is highly dependent on influx from the extracellular space, the signal in OTR A218T cells is maintained by the release from intracellular Ca^{2+} stores. Since several Ca^{2+}-gated channels in the plasma membrane of the cell line expressing the mutant OTR A218T are downregulated, the use of intracellular sources might have compensatory reasons. Particularly noteworthy in this context is the *TRPC6*, being strongest downregulated by a factor of 9.35. This was accompanied by a similar, but less pronounced downregulation of *TRPC3*. TRPC3 is known to form a complex with TRPC6 (Tang *et al.*, 2018). Disruption of TRPC6 expression has been associated with ASD (Griesi-Oliveira *et al.*, 2015). In addition to that, the alpha 1C subunit of the voltage-gated L-type calcium channel (*CACNA1C*), which is among the most prominent ASD-associated genes, was downregulated by a factor of 2.17 in the OTR A218T cells. In line with the consequently reduced permeability for Ca^{2+}, lower basal levels of cytosolic Ca^{2+} have been detected in the OTR A218T cells. The observed differences in Ca^{2+} dynamics might play an important role in maintaining downstream signal specificity, such as the MAPK cascade, and thereby, influence the regulation of ERK-dependent cellular processes.

Stimulation with 100 nM OT for 60 min revealed a significantly reduced MAPK pathway activation in the OTR A218T compared to the OTR WT cells. Since the anxiolytic effect of OT is mediated via the phosphorylation of ERK1/2 (Blume *et al.*, 2008; Jurek *et al.*, 2012), we hypothesize that the attenuated phosphorylation level in the OTR A218T cells could, to some extent, account for comorbid anxiety disorders occurring in some cases of ASD. Furthermore, the diminished activity of the ERK1/2 pathway impacts transcriptional regulation by downstream transcription factors. Whether gene transcription is up- or downregulated depends on the transcription factor and its

phosphorylation site, e.g. MEF2A is pERK1/2-dependent and inhibits gene transcription upon S408 phosphorylation, but activates gene transcription upon Thr312/319 phosphorylation (Meyer *et al.*, 2018; Potthoff and Olson, 2007). We have mapped changes in the transcriptome of OTR WT versus OTR A218T by means of RNA-Sequencing. As both cell line derive from the same mother-cell line, changes in the transcriptome can be traced back to the induced genomic alterations. The transcriptome analysis revealed a large cohort of significantly regulated genes in OT-stimulated OTR A218T cells, when compared to expression levels in stimulated OTR WT cells. When filtered by corrected significance $p_{adj} < 0.05$, a number of 7823 genes were differentially regulated. Comparison with ASD risk genes revealed that 429 genes among them have been associated with ASD, providing a potential molecular link between the A218T variant and a psychopathological phenotype.

In summary, we have investigated the molecular and cellular effects of OTR variants, and were able to unravel the chain of intracellular events that are ultimately causative for associated behavioral phenotypes. The genetic OTR variant A218T causes enhanced receptor stability, altered Ca^{2+} dynamics, reduced MAPK signaling, and up- and downregulations of several ASD-related target genes. The changes in the transcriptome affect several ASD-associated cellular processes as confirmed by GO analysis. These dysregulations are suggested to underlie the behavioral abnormalities of ASD, so understanding the chain of intracellular events caused by the *OTR* SNP and gene duplication might provide us with a “master-regulator” in the ASD-pathway that could be exploited for clinical treatment options.

5 General discussion

This section aims to put the publications (section 2, 3 and 4) into context with focus on the implications, relevance, and perspectives related to the findings described.

The studies performed during the course of my thesis yielded new insights in the cellular processes and their molecular underpinnings following OTR activation. The results acquire greater importance by referring to the cellular adaptations under pathological conditions like ASD. In patients suffering from the severe neurodevelopmental disorder ASD, a number of alterations in the brain at different levels have been observed that encompass neurite outgrowth, the formation and maintenance of synapses, neuronal connectivity, plasticity, and mitochondrial dysfunction (Gilbert and Man, 2017; Nguyen *et al.*, 2018a; Supekar *et al.*, 2013; Siddiqui *et al.*, 2016). In the following part, I will discuss my main findings referring to the molecular adaptations underlying the neurodevelopmental disorder ASD.

5.1 MEF2A as major regulator of OT-induced effects

In this thesis, I provide evidence that OT leads to morphological alterations in hypothalamic neurons. We could show that OT stimulation leads to a neurite retraction via the MAPK pathway and a subsequent activation of the transcription factor isoform MEF2A by a dephosphorylation at S408.

In another hypothalamic cell line that does not express MEF2A endogenously, OT exhibited opposing effects by inducing neurite outgrowth. Based on my first publication, I could extend the mechanistic insight underlying OT-induced morphological alterations in neurons. The basal expression and activation status of MEF2A turned out to be the decisive factors determining the morphological response to OT, i.e. neurite elongation or retraction. While a knockout of MEF2A induced neurite elongation, a knockin resulted in a reduced neurite length after OT stimulation.

This implies a major role for MEF2A as regulator of OT-induced effects as well as basic cellular events. The family of MEF2 transcription factors regulate a number of genes important for the brain development and synaptogenesis. It has been shown that a MEF2 overexpression reduces the number of synapses, while a knockout induces synaptogenesis, which results in an autistic-like phenotype in mice (Lipton *et al.*, 2009; Tu *et al.*, 2017).

In addition to that, I could identify the phosphatase CaN as novel upstream regulator of MEF2A in neurons, being responsible for its activation and by that, enabling the shift in the morphological response. In this regard, MEF2A S408 could be confirmed as the critical phosphorylation site, being validated by a control experiment, where the serine was exchanged with the phosphomimetic amino acid aspartate (S408D), leading to a loss of function of MEF2A. Since neuronal morphology builds up the base for cellular connectivity and plasticity, these were the processes addressed next.

The integrin family of cell adhesion receptors and their ligands play essential roles in the control of several processes regulating neuronal connectivity (Lilja and Ivaska, 2018). The transmembrane receptors are responsible for cell–ECM interactions and regulating cell–cell interactions. Although their role in the CNS is not well understood so far, one receptor variant of the integrin family, integrin ß3, has been associated with ASD risk (Dohn *et al.*, 2017; Napolioni *et al.*, 2011). Moreover, a plethora of so-called ASD risk genes has been linked to alterations in integrin signaling (Lilja and Ivaska, 2018; Schuch *et al.*, 2014). I identified one member of the integrins, integrin ß1, to be significantly downregulated in MEF2A knockout cells, pointing toward an increased neuronal connectivity in those cells given the reduced cell adhesion and neurite elongation. With ASD being a developmental disorder, the decrease of neonatal neuronal hyperconnectivity is dysregulated at a certain point, causing a state of persistent hyperconnectivity into adulthood (Supekar *et al.*, 2013; Zaslavsky *et al.*, 2019; Tang *et al.*, 2014; Zhang *et al.*, 2016). The state of hyperconnectivity affects various projections on the whole-brain and subsystems level. In line with that, the grade of hyperconnectivity has been positively correlated with symptom severity in ASD, in detail, children with a higher functional connectivity exhibited more severe social deficits (Supekar *et al.*, 2013).

Neurons have a high energy demand and adaptations in their morphology, connectivity, and plasticity are highly sensitive to energy limitations (Vergara *et al.*, 2019). By analyzing mitochondrial function, I could provide evidence that MEF2A is a major regulator of respiratory function of mitochondria, and therefore energy supply, in neurons. The respiratory function and spare respiratory capacity was significantly increased in MEF2A knockout cells. As a result, the amount of supplied energy reflected by the cellular ATP content was elevated in the cells lacking

the transcription factor MEF2A compared to those expressing it. In line with my data, a large proportion of ASD patients suffer from mitochondrial dysfunction and abnormalities in energy generation (Giulivi *et al.*, 2010; Siddiqui *et al.*, 2016). Already in 1985, Coleman and Blass proposed the first hypothesis of ASD coinciding with an underlying comorbidity of mitochondrial dysfunction (Coleman and Blass, 1985).

Taken together, the results from my first two publications (Chapter 2 and 3) imply a central role for MEF2 in ASD and its concomitant adaptations. In the minireview "Anxiolytic and Anxiogenic? How the Transcription Factor MEF2 Might Explain the Manifold Behavioral Effects of Oxytocin." we suggest that the MEF2-mediated effects on morphology and connectivity in OTR-positive neurons might consequently lead to a shift in the connectivity between brain regions of the so-called salience network. This brain network plays a central role in the regulation of complex functions like communication, social behavior, and self-awareness. We hypothesize that MEF2 activity upon OTR activation induces changes on a cellular and subsequently on a network level. As a result of those changes in the salience network, OT can cause alleviating or adverse behavioral responses depending on the emotional context of external stimuli (Figure 17) (Jurek and Meyer, 2020).

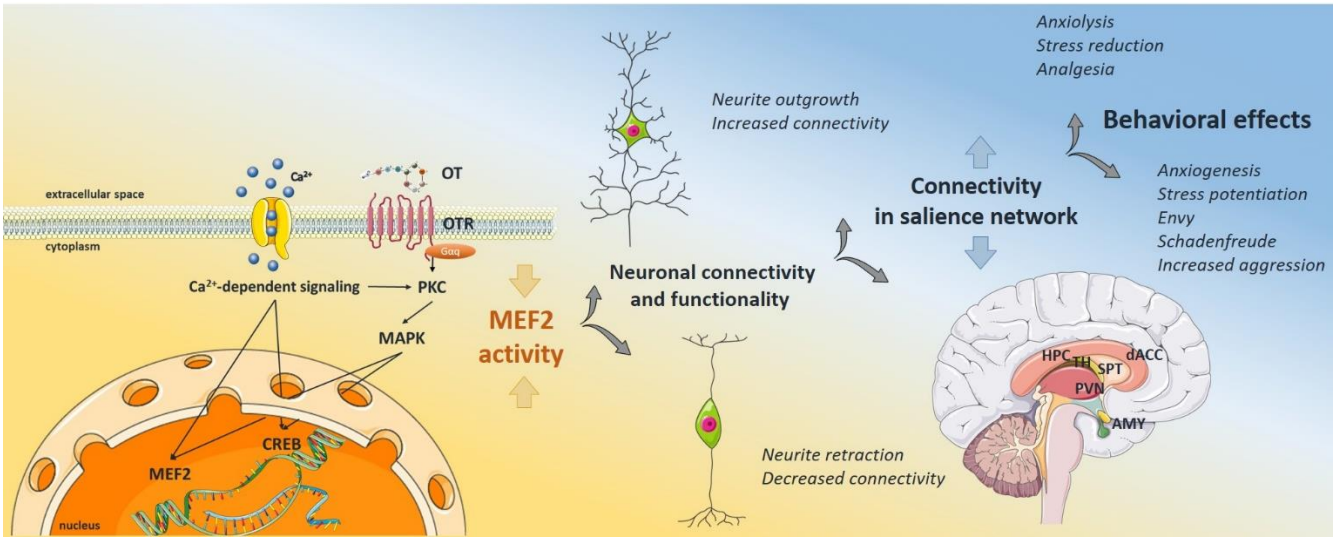

Figure 17. Graphical Abstract adapted from the review "Anxiolytic and Anxiogenic? How the Transcription Factor MEF2 Might Explain the Manifold Behavioral Effects of Oxytocin." (Jurek and Meyer, 2020).

Dysfunctions affecting the salience network have been detected in a variety of psychiatric disorders, including anxiety disorders, post-traumatic stress disorder, schizophrenia, or ASD (Palaniyappan *et al.*, 2012; Green *et al.*, 2016; Akiki *et al.*, 2017; Geng *et al.*, 2015).

Proceeding on the assumption that MEF2 constitutes a central node point in the regulation of several cellular processes important for the mental health, and given the inconsistencies in the clinical studies testing OT as potential treatment for ASD, yields the need to investigate the origin of those irregularities. One major factor determining the predisposition to diseases or the response to a drug treatment, are genetic variations.

5.2 The role of genetic variations affecting the *OTR* gene

Many psychiatric diseases have a strong genetic component reflected by the heritability measures ranging from 30 % to 80 % for the majority of them (Zuchner *et al.*, 2007). The cellular maladaptation found in ASD patients are mostly based on the genetic background of the individuals, as suggested by twin studies that reveal the heritability estimations to be over 80 % (Sandin *et al.*, 2017). The risk for a newborn child is more than 10-fold higher if a previous sibling suffers from ASD (Sandin *et al.*, 2014). The variations in the human genome can appear on multiple scales, ranging from variances in the total chromosome number over duplications or deletions of genes to exchanges of single bases.

Among those genetic factors that have been associated with ASD are SNPs in the *OTR* gene. The proportion of ASD cases explained by common genotyped SNPs is estimated to be around 17 %–60 % (Gratten *et al.*, 2014). The linkage between *OTR* SNPs and mental illness stems mainly from GWAS, and there are just very few molecular studies elucidating the underlying cellular effects (Fueg *et al.*, 2019; Furman *et al.*, 2011).

Therefore, my aim was to assess the molecular effects of SNPs in the *OTR* gene. In the third part of my thesis, I investigated one common OTR variant and could provide evidence for the dependence of OT-induced cellular effects on the genetic background. I focused on the specific *OTR* SNP rs4686302, a non-synonymous SNP located in the third exon of the human *OTR* gene that results in an amino acid exchange of alanine to threonine at the position 218 in the OTR protein. In previous publications, this SNP has been associated with core characteristics of ASD,

social cognition deficits/attention disorders, and trait empathy in healthy persons (Francis *et al.*, 2016; Wu *et al.*, 2012; Kalyoncu *et al.*, 2019).

For that purpose, human HEK293 cells, which do not express the *OTR* endogenously, were virally transduced with a construct either containing the reference or the SNP-containing variant of the *OTR*. For a comprehensive comparison including the identification of the genomic insertion sites of the transduced *OTR* gene in the two cell lines, a WGS was performed. The genomic analysis revealed the insertion of the reference gene on chromosome 8 and a double insertion of the *OTR* gene on chromosome 6 in the cell line transduced with the SNP variant. This gene duplication resulted in an increased mRNA and protein expression of the OTR A218T compared to the OTR WT. Admittedly, we cannot clearly determine if the differences found between the cell lines are due the SNP or to the gene duplication. However, both convey clinical relevance, as many neurodevelopmental disorders are associated with structural anomalies, such as duplications or deletions of certain sections on a chromosome and consequently thereon located genes. Those changes called genomic copy number variants (CNVs) account for a proportion of more than 10 % of ASD cases (Sebat *et al.*, 2007). Although technologies for their detection developed fast and became far more powerful, the interpretation of data is marked by inconsistencies and failing correlations between genotype and phenotype. The same CNV can cause different mental diseases within the same family (Sebat *et al.*, 2009). Besides environmental and sex-specific factors as well as epigenetic modifications that contribute to those variations, a complex interaction of potentially pathogenic CNVs with SNPs might be causative (Velinov, 2019). To our knowledge, just two studies about CNVs affecting the *OTR* have been published so far. In the study from Gregory et al. 119 probands from multiplex autism families were analyzed. The genomic deletion of the *OTR*, previously suggested by the authors, could be confirmed only in one study participant and his mother (Gregory *et al.*, 2009). In a larger proportion of the participants, the authors detected a hypermethylation of the *OTR* gene promoter, with a consequently reduced mRNA expression in ASD patients. In contrast, the case study from Bittel *et al.* presents a 9-year old boy with pervasive developmental disorder, delayed speech, and sudden onset of obesity. Genetic analysis revealed duplications of the 3p25-3p26 genomic region, which results in an overexpression of the *OTR* gene (Bittel *et al.*, 2006). This suggests that

an *OTR* gene duplication with a consecutive OTR overexpression can be causative for a behavioral phenotype falling within the symptomatic classification of ASD. However, both studies highlight the involvement of the *OTR* gene variations in ASD.

Taken together, our findings obtained by the WGS approach provide a detailed genomic information that is rarely addressed in the majority of such studies. In most studies, only the overall protein expression profile of a cell is analyzed, even though the location of inserted genes and possible off-target effects play a crucial role in determining the function of a cell.

For this purpose, we isolated several genes up- and downstream of the insertion sites and checked if they were affected by the construct insertion in order to detect potential off-target effects by disrupted genes. Those genes close to the genomic insertion sites with a differential expression were listed and should be carefully interpreted. The SNP rs4686302 is located within the coding sequence of Exon 3, and leads to an alanine/threonine amino acid exchange. Substitutions of alanine with threonine caused by SNPs, what occurs in various proteins, can induce self-aggregation into amyloid fibrils or other amyloidogenic proteins (Podoly *et al.*, 2010). This is mainly due to the preferences of alanine to form helices and of threonine to support less stable beta-sheet structures. Surprisingly, by analyzing the receptor protein stability by CHX degradation assay, we could provide evidence that the OTR A218T variant shows an increased receptor stability. The consequently enhanced receptor availability in the plasma membrane would lead to an increased ligand binding, which has been recently described for rs4686302 (Fueg *et al.*, 2019).

In line with that, we found that upon OTR activation the rise in intracellular Ca^{2+} levels is higher in OTR A218T compared to OTR WT cells. Additionally, we were able to detect a difference in the Ca^{2+} source. In contrast to the OTR A218T, the OTR WT cells rely more on OT-induced influx of Ca^{2+} from the extracellular space than on the release from intracellular stores. The spatio-temporal properties and dynamics of the intracellular Ca^{2+} signals play an important role in transmitter release in classical synapses (Meinrenken *et al.*, 2003). Furthermore, the OT-induced Ca^{2+} release from intracellular stores suffices for dendritic release of OT (Ludwig *et al.*, 2002). As a consequence, dysregulations in Ca^{2+} signaling can have severe consequences and lead to a disruption of neurological function including signal transmission, excitatory-inhibitory balance

and synaptic plasticity, consequently contributing to the pathophysiology of ASD (Nanou *et al.*, 2018; Nguyen *et al.*, 2018b).

Furthermore, the basal cytosolic Ca^{2+} concentration was lower in the cells encoding the OTR A218T compared to the WT variant. At any given moment, the concentration in cytosolic Ca^{2+} is determined by the balance between Ca^{2+} influx and efflux as well as a permanent exchange with internal stores. In order to keep this balance, a vast array of cellular checkpoints are controlling Ca^{2+} homeostasis, like Ca^{2+} binding proteins, transcriptional networks, ion channels, and ion exchangers in both, the plasma membrane and the membranes of mitochondria and the endoplasmic reticulum. Therefore, dysfunctions in Ca^{2+} signaling are often accompanied by disruptions in the Ca^{2+} regulating organelles. In this context, RNA sequencing revealed a plethora of transcripts involved in this process. Referring to Ca^{2+}-permeable channels in the plasma membrane, the *trpc6* was the overall most prominently downregulated transcript with a change by a factor of 9.35. Intriguingly, the disruption of TRPC6 has been previously associated with ASD (Griesi-Oliveira et al., 2015). Another variant strongly associated with ASD, is the voltage-gated Ca^{2+} channel *CACNA1C*, which was downregulated by a factor of 2.17 in the OTR A218T cells, thereby regulating cellular Ca^{2+} entry, neurotransmitter release and gene expression (Andrade *et al.*, 2019).

Furthermore, various genes of the endoplasmic reticulum and the mitochondria were differentially regulated between the two cell lines. These two organelles communicate with each other by generation of Ca^{2+} signals, forming a link between energy metabolism and signal transmission via changes in the cytosolic free Ca^{2+} concentration (Hayashi and Su, 2007; Patterson *et al.*, 2004). Interestingly, the transcription factor MEF2A was identified as a transcript that was slightly upregulated in the cell line expressing the OTR A218T variant. Since MEF2A regulates mitochondrial function, as described in my second publication (see Chapter 3), we hypothesize that the mitochondrial function is damped in those cells, thereby affecting the cellular Ca^{2+} homeostasis. As an outlook, analysis of the mitochondrial function in those two cell lines would yield further insights in the main key players determining the cellular Ca^{2+} response. Ultimately, the changes in Ca^{2+} concentrations can determine the signaling specificity of downstream cascades and their functional outcomes. In more detail, they can activate or inhibit

the MAPK cascade by regulating protein-protein interactions and the subcellular localization of ERKs (Chuderland and Seger, 2008). In this regard, I could detect a main effect between the two cell lines in the MAPK pathway activation following the stimulation with OT. Compared to the OTR WT cells, the OTR A218T show lower phosphorylation levels of ERK1/2 both, on a basal level and in response to OT. The MAPK signaling cascade is a common pathway that is affected by many genetic variants and its dysregulations have been implicated in ASD (Vithayathil *et al.*, 2018). In addition, it has been shown that the anxiolytic effect of OT is mediated via ERK1/2 activation (Blume *et al.*, 2008; Jurek *et al.*, 2012). A reduction in the basal as well as the OT-induced phosphorylation of ERK1/2 might therefore modulate this behavior. Even though anxiety does not count as core symptom of ASD, there is comorbidity, especially among children. Around 80 % of children with ASD have been diagnosed with clinically significant anxiety (Leyfer *et al.*, 2006). Moreover, anxiety comorbidity is linked to a higher severity of ASD symptoms with impaired psychosocial functioning (Gillott *et al.*, 2001; Klin *et al.*, 2007). An increase in social abilities of ASD patients upon OT treatment might therefore, at least to some extent, be due to its anxiolytic effect.

Besides other crosstalk signaling cascades, the diminished activation of the MAPK pathway affects several downstream transcription factors, which is reflected by the huge amount of altered transcripts found in the transcriptome analysis. 7823 significantly differentially expressed genes have been uncovered in the RNA sequencing. Many of those genes are implicated in the cellular processes that I extensively studied and mentioned above like neuronal morphology, mitochondrial functioning, activation of the MAPK pathway, and Ca^{2+} signaling, as revealed by the GO analysis. In line with this data, 429 genes relevant for ASD have been identified underscoring the important role of the *OTR* for the etiology of ASD.

Since one has to consider that the observed variation in mRNA transcript levels might be compensated by regulatory networks (El-Brolosy and Stainier, 2017), future experiments should focus on a proteomic characterization. Looking at both, the transcriptome and proteome, will give a fundamental insight in the cellular dynamics compared to the rather static genome.

In addition to that, other methodological approaches encompassing the correction of an already existing SNP using the technique of base editing or the use of human tissue biopsies like in the

functional study from Füeg *et al.* could be addressed (Fueg *et al.*, 2019). Given the prevalent phenotypic variation and possible opposing mechanisms or combinatory effects of other existing SNPs, those strategies cannot completely replace a functional characterizations of single SNPs, but extend them in a meaningful way.

Further experiments targeting the receptor function itself including its regional expression and availability at the plasma membrane remain to be assessed. A crystallization of the receptor variant for detection of structural differences would yield further information on the receptor stability and function. Other interesting parameters are the effects on the interaction of the receptor variant with its G proteins as well as how ß-arrestin binding and its subsequent internalization are affected by the amino acid exchange.

Finally yet importantly, all experiments in my studies were performed *in vitro.* Future experiments have to address the validity *in vivo.* Studying conserved signaling pathways in cell lines provides important basic knowledge about cellular mechanisms and reduces the number of experimental animals enormously. However, changes in the properties of the cells keeping them dividing and growing over time under laboratory conditions have to be considered. Moreover, regulations within networks and the synergy between different cell types are neglected and have to be addressed separately. Therefore, the transformation into three-dimensional cell culture, which mimics tissue- and organ specific architecture and thereby allowing better cell-to-cell contact and intercellular signaling networks, would approach this demand. Three-dimensional culture models behave more similar to the cells *in vivo*, and are therefore useful tool in the early stage of research (Edmondson *et al.*, 2014).

In the end, I would like to give some general remarks on SNP-based studies. Indeed, SNPs in the *OTR* gene depict an important factor involved in various psychiatric conditions. However, several limitations in SNP studies have to be considered.

First, there is a strong interaction between polymorphisms and cultural background (Ahsan *et al.*, 2020). Under these conditions, one has to consider possible varieties in studies depending on the ethnicity of the cohort. Besides that, too few studies consult a heterogeneity, such as age, sex or intelligence quotient. In line with that, apart from pure genetics, non-genetic mechanisms affecting mental illness risk should not be underestimated and carefully assessed as well. This

involves intracellular mechanisms like epigenetics but also something impossible to assess by looking into a single cell: the personal environment (Edwards and Myers, 2007).

Finally, empathy is a complex socio-emotional behavior influenced by multiple genes. This single-gene approach focusing on the *OTR* gene neglects interactions with other genes involved in the social and emotional processing. In addition, most of the psychiatric disorders are likely not single-gene disorders that are inherited in a clear recessive or dominant manner. In fact, less than one percent of all ASD cases are attributable to a mutation in a single gene (Lewis *et al.*, 2019). Actually, more than 800 loci with variants have been identified that increase susceptibility to ASD (Sanders *et al.*, 2015). Taken together, although it will not fully explain the heterogeneity and multifactorial nature of ASD, the OTR and its coupled pathways are highly related to the pathogenesis and therefore a promising treatment option for ASD.

5.3 Conclusion

In my thesis, I could extend the network of OTR-coupled signaling cascades involving Ca^{2+}-dependent signaling, the MAPK pathway and their connection with the transcription factor MEF2A. In addition to that, I elucidated the effects following OTR activation on various cellular processes, such as neuronal morphology, connectivity, mitochondrial function, and expression of target genes. In this context, I could confirm a central role for genetic variations affecting the *OTR* gene. In order to understand the complex role of the OTR in psychosocial disorders and make OT a safe treatment option as well as a source of potential biomarkers for an early diagnosis, especially in the case of ASD, we need more functional studies addressing genetic variants. Understanding the nature of gene variations and their effects on the transcriptome and proteome will provide an essential profile contributing to the understanding of phenotypic variation.

6 Abbreviations

µM	Micromolar
µm	Micrometer
µs	Microsecond
ANOVA	Analysis of variance
ASD	Autism spectrum disorder
ATP	Adenosine triphosphate
BSA	Bovine serum albumin
Ca^{2+}	Calcium
cAMP	Cyclic adenosine monophosphate
CaN	Calcineurin
cacna1c	Voltage-gated L-type calcium channel alpha 1C subunit gene
CHX	Cycloheximide
CNV	Copy number variant
CO_2	Carbon dioxide
D	Aspartate
DNA	Deoxyribonucleic acid
ECM	Extracellular matrix
E.g.	For example (exempli gratia)
ERK	Extracellular signal regulated kinase
FCCP	Carbonyl cyanide-4 (trifluoromethoxy) phenylhydrazone
FWHM	Full width half maximum
GWAS	Genome-wide association studies
HEK	Human embryonic kidney

I.e.	That is (id est)
IHC	Immunohistochemistry
INH	Inhibitor
LTR	Long terminal repeat
MAPK	Mitogen-activated protein kinase
MEF	Myocyte enhancer factor
MEK	Mitogen-activated protein kinase kinase
mM	Millimolar
ms	Millisecond
mV	Millivolt
nM	Nanomolar
Na^+	Sodium
OCR	Oxygen consumption rate
OT	Oxytocin
OTA	Oxytocin receptor antagonist
OTR	Oxytocin receptor gene
OTR	Oxytocin receptor
p	Phosphorylated
PBS	Phosphate buffered saline
PKC	Protein kinase c
rel	Relative
RNA	Ribonucleic acid
S	Serine
scrRNA	Scrambled RNA
SD	Standard Deviation

SEM	Standard error of the mean
siRNA	Small interfering RNA
SNP	Single nucleotide polymorphism
TBS	Tris buffered saline
TBS-T	Tris buffered saline with tween
TGOT	[Thr^4,Gly^7]-Oxytocin
trpc	Transient receptor potential channel gene
TRPC	Transient receptor potential channel
VEH	Vehicle
VP	Vasopressin
WB	Western Blot
WT	Wildtype

7 References

Acevedo, B. P., Aron, A., Fisher, H. E. and Brown, L. L. (2012) Neural correlates of long-term intense romantic love. Soc Cogn Affect Neurosci, 7, 145-159.

Ahsan, T., Urmi, N. J. and Sajib, A. A. (2020) Heterogeneity in the distribution of 159 drug-response related SNPs in world populations and their genetic relatedness. PLoS One, 15, e0228000.

Akhtar, M. W., Kim, M. S., Adachi, M., Morris, M. J., Qi, X., Richardson, J. A., Bassel-Duby, R., Olson, E. N., Kavalali, E. T. and Monteggia, L. M. (2012) In vivo analysis of MEF2 transcription factors in synapse regulation and neuronal survival. PLoS One, 7, e34863.

Akiki, T. J., Averill, C. L. and Abdallah, C. G. (2017) A Network-Based Neurobiological Model of PTSD: Evidence From Structural and Functional Neuroimaging Studies. Curr Psychiatry Rep, 19, 81.

Alaerts, K., Bernaerts, S., Vanaudenaerde, B., Daniels, N. and Wenderoth, N. (2019) Amygdala-Hippocampal Connectivity Is Associated With Endogenous Levels of Oxytocin and Can Be Altered by Exogenously Administered Oxytocin in Adults With Autism. Biol Psychiatry Cogn Neurosci Neuroimaging, 4, 655-663.

Andrade, A., Brennecke, A., Mallat, S., Brown, J., Gomez-Rivadeneira, J., Czepiel, N. and Londrigan, L. (2019) Genetic Associations between Voltage-Gated Calcium Channels and Psychiatric Disorders. Int J Mol Sci, 20.

Aoki, Y., Yahata, N., Watanabe, T., Takano, Y., Kawakubo, Y., Kuwabara, H., Iwashiro, N., Natsubori, T., Inoue, H., Suga, M., Takao, H., Sasaki, H., Gonoi, W., Kunimatsu, A., Kasai, K. and Yamasue, H. (2014) Oxytocin improves behavioural and neural deficits in inferring others' social emotions in autism. Brain, 137, 3073-3086.

Bakermans-Kranenburg, M. J. and van Ijzendoorn, M. H. (2014) A sociability gene? Meta-analysis of oxytocin receptor genotype effects in humans. Psychiatr Genet, 24, 45-51.

Bakos, J., Srancikova, A., Havranek, T. and Bacova, Z. (2018) Molecular Mechanisms of Oxytocin Signaling at the Synaptic Connection. Neural Plast, 2018, 4864107.

Bakos, J., Strbak, V., Ratulovska, N. and Bacova, Z. (2012) Effect of oxytocin on neuroblastoma cell viability and growth. Cellular and molecular neurobiology, 32, 891-896.

Bales, K. L., Perkeybile, A. M., Conley, O. G., Lee, M. H., Guoynes, C. D., Downing, G. M., Yun, C. R., Solomon, M., Jacob, S. and Mendoza, S. P. (2013) Chronic intranasal oxytocin causes long-term impairments in partner preference formation in male prairie voles. Biological psychiatry, 74, 180-188.

Barbosa, A. C., Kim, M. S., Ertunc, M., Adachi, M., Nelson, E. D., McAnally, J., Richardson, J. A., Kavalali, E. T., Monteggia, L. M., Bassel-Duby, R. and Olson, E. N. (2008) MEF2C, a transcription factor that facilitates learning and memory by negative regulation of synapse numbers and function. Proceedings of the National Academy of Sciences of the United States of America, 105, 9391-9396.

Bartolak-Suki, E., Imsirovic, J., Nishibori, Y., Krishnan, R. and Suki, B. (2017) Regulation of Mitochondrial Structure and Dynamics by the Cytoskeleton and Mechanical Factors. Int J Mol Sci, 18.

Bikbaev, A., Frischknecht, R. and Heine, M. (2015) Brain extracellular matrix retains connectivity in neuronal networks. Sci Rep, 5, 14527.

Bittel, D. C., Kibiryeva, N., Dasouki, M., Knoll, J. H. and Butler, M. G. (2006) A 9-year-old male with a duplication of chromosome 3p25.3p26.2: clinical report and gene expression analysis. Am J Med Genet A, 140, 573-579.

Blume, A., Bosch, O. J., Miklos, S., Torner, L., Wales, L., Waldherr, M. and Neumann, I. D. (2008) Oxytocin reduces anxiety via ERK1/2 activation: local effect within the rat hypothalamic paraventricular nucleus. Eur J Neurosci, 27, 1947-1956.

References

Borges, G. P., Mico, J. A., Neto, F. L. and Berrocoso, E. (2015) Corticotropin-Releasing Factor Mediates Pain-Induced Anxiety through the ERK1/2 Signaling Cascade in Locus Coeruleus Neurons. The international journal of neuropsychopharmacology / official scientific journal of the Collegium Internationale Neuropsychopharmacologicum (CINP), 18.

Brighton, P. J., Rana, S., Challiss, R. J., Konje, J. C. and Willets, J. M. (2011) Arrestins differentially regulate histamine- and oxytocin-evoked phospholipase C and mitogen-activated protein kinase signalling in myometrial cells. Br J Pharmacol, 162, 1603-1617.

Bringas, M. E., Carvajal-Flores, F. N., Lopez-Ramirez, T. A., Atzori, M. and Flores, G. (2013) Rearrangement of the dendritic morphology in limbic regions and altered exploratory behavior in a rat model of autism spectrum disorder. Neuroscience, 241, 170-187.

Brusco, J. and Haas, K. (2015) Interactions between mitochondria and the transcription factor myocyte enhancer factor 2 (MEF2) regulate neuronal structural and functional plasticity and metaplasticity. The Journal of physiology, 593, 3471-3481.

Busnelli, M. and Chini, B. (2018) Molecular Basis of Oxytocin Receptor Signalling in the Brain: What We Know and What We Need to Know. Curr Top Behav Neurosci, 35, 3-29.

Busnelli, M., Kleinau, G., Muttenthaler, M., Stoev, S., Manning, M., Bibic, L., Howell, L. A., McCormick, P. J., Di Lascio, S., Braida, D., Sala, M., Rovati, G. E., Bellini, T. and Chini, B. (2016) Design and Characterization of Superpotent Bivalent Ligands Targeting Oxytocin Receptor Dimers via a Channel-Like Structure. J Med Chem, 59, 7152-7166.

Campbell, D. B., Datta, D., Jones, S. T., Batey Lee, E., Sutcliffe, J. S., Hammock, E. A. and Levitt, P. (2011) Association of oxytocin receptor (OXTR) gene variants with multiple phenotype domains of autism spectrum disorder. J Neurodev Disord, 3, 101-112.

Carson, D. S., Berquist, S. W., Trujillo, T. H., Garner, J. P., Hannah, S. L., Hyde, S. A., Sumiyoshi, R. D., Jackson, L. P., Moss, J. K., Strehlow, M. C., Cheshier, S. H., Partap, S., Hardan, A. Y. and Parker, K. J. (2015) Cerebrospinal fluid and plasma oxytocin concentrations are positively correlated and negatively predict anxiety in children. Molecular psychiatry, 20, 1085-1090.

Cassoni, P., Sapino, A., Marrocco, T., Chini, B. and Bussolati, G. (2004) Oxytocin and oxytocin receptors in cancer cells and proliferation. J Neuroendocrinol, 16, 362-364.

Chen, F. S., Barth, M. E., Johnson, S. L., Gotlib, I. H. and Johnson, S. C. (2011a) Oxytocin Receptor (OXTR) Polymorphisms and Attachment in Human Infants. Frontiers in psychology, 2, 200.

Chen, F. S., Kumsta, R., von Dawans, B., Monakhov, M., Ebstein, R. P. and Heinrichs, M. (2011b) Common oxytocin receptor gene (OXTR) polymorphism and social support interact to reduce stress in humans. Proceedings of the National Academy of Sciences of the United States of America, 108, 19937-19942.

Chen, S. X., Cherry, A., Tari, P. K., Podgorski, K., Kwong, Y. K. and Haas, K. (2012) The transcription factor MEF2 directs developmental visually driven functional and structural metaplasticity. Cell, 151, 41-55.

Chini, B. and Manning, M. (2007) Agonist selectivity in the oxytocin/vasopressin receptor family: new insights and challenges. Biochem Soc Trans, 35, 737-741.

Chini, B., Manning, M. and Guillon, G. (2008) Affinity and efficacy of selective agonists and antagonists for vasopressin and oxytocin receptors: an "easy guide" to receptor pharmacology. Progress in brain research, 170, 513-517.

Chklovskii, D. B. (2004) Synaptic connectivity and neuronal morphology: two sides of the same coin. Neuron, 43, 609-617.

Choe, H. K., Reed, M. D., Benavidez, N., Montgomery, D., Soares, N., Yim, Y. S. and Choi, G. B. (2015) Oxytocin Mediates Entrainment of Sensory Stimuli to Social Cues of Opposing Valence. Neuron, 87, 152-163.

Chuderland, D. and Seger, R. (2008) Calcium regulates ERK signaling by modulating its protein-protein interactions. Commun Integr Biol, 1, 4-5.

Clapham, D. E. (2007) Calcium signaling. Cell, 131, 1047-1058.

Clipperton-Allen, A. E., Lee, A. W., Reyes, A., Devidze, N., Phan, A., Pfaff, D. W. and Choleris, E. (2012) Oxytocin, vasopressin and estrogen receptor gene expression in relation to social recognition in female mice. Physiology & behavior, 105, 915-924.

Coleman, M. and Blass, J. P. (1985) Autism and lactic acidosis. J Autism Dev Disord, 15, 1-8.

Conti, F., Sertic, S., Reversi, A. and Chini, B. (2009) Intracellular trafficking of the human oxytocin receptor: evidence of receptor recycling via a Rab4/Rab5 "short cycle". Am J Physiol Endocrinol Metab, 296, E532-542.

Dabrowska, J., Hazra, R., Ahern, T. H., Guo, J. D., McDonald, A. J., Mascagni, F., Muller, J. F., Young, L. J. and Rainnie, D. G. (2011) Neuroanatomical evidence for reciprocal regulation of the corticotrophin-releasing factor and oxytocin systems in the hypothalamus and the bed nucleus of the stria terminalis of the rat: Implications for balancing stress and affect. Psychoneuroendocrinology, 36, 1312-1326.

Dadds, M. R., MacDonald, E., Cauchi, A., Williams, K., Levy, F. and Brennan, J. (2014) Nasal oxytocin for social deficits in childhood autism: a randomized controlled trial. J Autism Dev Disord, 44, 521-531.

de Cavanagh, E. M., Ferder, M., Inserra, F. and Ferder, L. (2009) Angiotensin II, mitochondria, cytoskeletal, and extracellular matrix connections: an integrating viewpoint. American journal of physiology. Heart and circulatory physiology, 296, H550-558.

Descazeaud, V., Mestre, E., Marquet, P. and Essig, M. (2012) Calcineurin regulation of cytoskeleton organization: a new paradigm to analyse the effects of calcineurin inhibitors on the kidney. Journal of cellular and molecular medicine, 16, 218-227.

Devost, D., Wrzal, P. and Zingg, H. H. (2008) Oxytocin receptor signalling. Prog Brain Res, 170, 167-176.

Dietrich, J. B. (2013) The MEF2 family and the brain: from molecules to memory. Cell and tissue research, 352, 179-190.

Dohn, M. R., Kooker, C. G., Bastarache, L., Jessen, T., Rinaldi, C., Varney, S., Mazalouskas, M. D., Pan, H., Oliver, K. H., Velez Edwards, D. R., Sutcliffe, J. S., Denny, J. C. and Carneiro, A. M. D. (2017) The Gain-of-Function Integrin beta3 Pro33 Variant Alters the Serotonin System in the Mouse Brain. J Neurosci, 37, 11271-11284.

Duncan, R. S., Goad, D. L., Grillo, M. A., Kaja, S., Payne, A. J. and Koulen, P. (2010) Control of intracellular calcium signaling as a neuroprotective strategy. Molecules, 15, 1168-1195.

Edmondson, R., Broglie, J. J., Adcock, A. F. and Yang, L. (2014) Three-dimensional cell culture systems and their applications in drug discovery and cell-based biosensors. Assay Drug Dev Technol, 12, 207-218.

Edwards, S. L., Beesley, J., French, J. D. and Dunning, A. M. (2013) Beyond GWASs: illuminating the dark road from association to function. Am J Hum Genet, 93, 779-797.

Edwards, T. M. and Myers, J. P. (2007) Environmental exposures and gene regulation in disease etiology. Environ Health Perspect, 115, 1264-1270.

El-Brolosy, M. A. and Stainier, D. Y. R. (2017) Genetic compensation: A phenomenon in search of mechanisms. PLoS Genet, 13, e1006780.

Estrella, N. L., Desjardins, C. A., Nocco, S. E., Clark, A. L., Maksimenko, Y. and Naya, F. J. (2015) MEF2 transcription factors regulate distinct gene programs in mammalian skeletal muscle differentiation. The Journal of biological chemistry, 290, 1256-1268.

Falougy, H. E., Filova, B., Ostatnikova, D., Bacova, Z. and Bakos, J. (2019) Neuronal morphology alterations in autism and possible role of oxytocin. Endocr Regul, 53, 46-54.

Fiore, R., Khudayberdiev, S., Christensen, M., Siegel, G., Flavell, S. W., Kim, T. K., Greenberg, M. E. and Schratt, G. (2009) Mef2-mediated transcription of the miR379-410 cluster regulates activity-dependent dendritogenesis by fine-tuning Pumilio2 protein levels. The EMBO journal, 28, 697-710.

Flavell, S. W., Cowan, C. W., Kim, T. K., Greer, P. L., Lin, Y., Paradis, S., Griffith, E. C., Hu, L. S., Chen, C. and Greenberg, M. E. (2006) Activity-dependent regulation of MEF2 transcription factors suppresses excitatory synapse number. Science (New York, N.Y, 311, 1008-1012.

Flavell, S. W., Kim, T. K., Gray, J. M., Harmin, D. A., Hemberg, M., Hong, E. J., Markenscoff-Papadimitriou, E., Bear, D. M. and Greenberg, M. E. (2008) Genome-wide analysis of MEF2 transcriptional program reveals synaptic target genes and neuronal activity-dependent polyadenylation site selection. Neuron, 60, 1022-1038.

Francis, S. M., Kim, S. J., Kistner-Griffin, E., Guter, S., Cook, E. H. and Jacob, S. (2016) ASD and Genetic Associations with Receptors for Oxytocin and Vasopressin-AVPR1A, AVPR1B, and OXTR. Front Neurosci, 10, 516.

Freedman, M. L., Monteiro, A. N., Gayther, S. A., Coetzee, G. A., Risch, A., Plass, C., Casey, G., De Biasi, M., Carlson, C., Duggan, D., James, M., Liu, P., Tichelaar, J. W., Vikis, H. G., You, M. and Mills, I. G. (2011) Principles for the post-GWAS functional characterization of cancer risk loci. Nat Genet, 43, 513-518.

Freitag, C. M. and Konrad, K. (2014) Autism spectrum disorder: underlying neurobiology. J Neural Transm (Vienna), 121, 1077-1079.

Freund-Mercier, M. J., Stoeckel, M. E. and Klein, M. J. (1994) Oxytocin receptors on oxytocin neurones: histoautoradiographic detection in the lactating rat. J Physiol, 480 (Pt 1), 155-161.

Fueg, F., Santos, S., Haslinger, C., Stoiber, B., Schaffer, L., Grunblatt, E., Zimmermann, R. and Simoes-Wust, A. P. (2019) Influence of oxytocin receptor single nucleotide sequence variants on contractility of human myometrium: an in vitro functional study. BMC Med Genet, 20, 178.

Furman, D. J., Chen, M. C. and Gotlib, I. H. (2011) Variant in oxytocin receptor gene is associated with amygdala volume. Psychoneuroendocrinology, 36, 891-897.

Garcia-Cabezas, M. A., Barbas, H. and Zikopoulos, B. (2018) Parallel Development of Chromatin Patterns, Neuron Morphology, and Connections: Potential for Disruption in Autism. Frontiers in neuroanatomy, 12, 70.

Geng, H., Li, X., Chen, J., Li, X. and Gu, R. (2015) Decreased Intra- and Inter-Salience Network Functional Connectivity is Related to Trait Anxiety in Adolescents. Front Behav Neurosci, 9, 350.

Gilbert, J. and Man, H. Y. (2017) Fundamental Elements in Autism: From Neurogenesis and Neurite Growth to Synaptic Plasticity. Front Cell Neurosci, 11, 359.

Gillott, A., Furniss, F. and Walter, A. (2001) Anxiety in high-functioning children with autism. Autism, 5, 277-286.

Gimpl, G. and Fahrenholz, F. (2001) The oxytocin receptor system: structure, function, and regulation. Physiol Rev, 81, 629-683.

Giulivi, C., Zhang, Y. F., Omanska-Klusek, A., Ross-Inta, C., Wong, S., Hertz-Picciotto, I., Tassone, F. and Pessah, I. N. (2010) Mitochondrial dysfunction in autism. JAMA, 304, 2389-2396.

Gossett, L. A., Kelvin, D. J., Sternberg, E. A. and Olson, E. N. (1989) A new myocyte-specific enhancer-binding factor that recognizes a conserved element associated with multiple muscle-specific genes. Molecular and cellular biology, 9, 5022-5033.

Gratten, J., Wray, N. R., Keller, M. C. and Visscher, P. M. (2014) Large-scale genomics unveils the genetic architecture of psychiatric disorders. Nat Neurosci, 17, 782-790.

Green, S. A., Hernandez, L., Bookheimer, S. Y. and Dapretto, M. (2016) Salience Network Connectivity in Autism Is Related to Brain and Behavioral Markers of Sensory Overresponsivity. J Am Acad Child Adolesc Psychiatry, 55, 618-626 e611.

Gregory, S. G., Connelly, J. J., Towers, A. J., Johnson, J., Biscocho, D., Markunas, C. A., Lintas, C., Abramson, R. K., Wright, H. H., Ellis, P., Langford, C. F., Worley, G., Delong, G. R., Murphy, S. K., Cuccaro, M. L., Persico, A. and Pericak-Vance, M. A. (2009) Genomic and epigenetic evidence for oxytocin receptor deficiency in autism. BMC Med, 7, 62.

Griesi-Oliveira, K., Acab, A., Gupta, A. R., Sunaga, D. Y., Chailangkarn, T., Nicol, X., Nunez, Y., Walker, M. F., Murdoch, J. D., Sanders, S. J., Fernandez, T. V., Ji, W., Lifton, R. P., Vadasz, E., Dietrich, A., Pradhan, D., Song, H., Ming, G. L., Gu, X., Haddad, G., Marchetto, M. C., Spitzer, N., Passos-Bueno, M. R., State, M. W. and Muotri, A. R. (2015) Modeling non-syndromic autism and the impact of TRPC6 disruption in human neurons. Mol Psychiatry, 20, 1350-1365.

Griffiths, E. J. and Rutter, G. A. (2009) Mitochondrial calcium as a key regulator of mitochondrial ATP production in mammalian cells. Biochim Biophys Acta, 1787, 1324-1333.

Grinevich, V., Knobloch-Bollmann, H. S., Eliava, M., Busnelli, M. and Chini, B. (2016) Assembling the Puzzle: Pathways of Oxytocin Signaling in the Brain. Biological psychiatry.

Grote, S. (2020) GOfuncR: Gene ontology enrichment using FUNC. R package version 1.8.0.

Guastella, A. J., Gray, K. M., Rinehart, N. J., Alvares, G. A., Tonge, B. J., Hickie, I. B., Keating, C. M., Cacciotti-Saija, C. and Einfeld, S. L. (2015) The effects of a course of intranasal oxytocin on social behaviors in youth diagnosed with autism spectrum disorders: a randomized controlled trial. J Child Psychol Psychiatry, 56, 444-452.

Hayashi, T. and Su, T. P. (2007) Sigma-1 receptor chaperones at the ER-mitochondrion interface regulate Ca(2+) signaling and cell survival. Cell, 131, 596-610.

Hurlemann, R. (2017) Oxytocin-Augmented Psychotherapy: Beware of Context. Neuropsychopharmacology, 42, 377.

Ichida, M. and Finkel, T. (2001) Ras regulates NFAT3 activity in cardiac myocytes. The Journal of biological chemistry, 276, 3524-3530.

International HapMap, C., Frazer, K. A., Ballinger, D. G., Cox, D. R., Hinds, D. A., Stuve, L. L., Gibbs, R. A., Belmont, J. W., Boudreau, A., Hardenbol, P., Leal, S. M., Pasternak, S., Wheeler, D. A., Willis, T. D., Yu, F., Yang, H., Zeng, C., Gao, Y., Hu, H., Hu, W., Li, C., Lin, W., Liu, S., Pan, H., Tang, X., Wang, J., Wang, W., Yu, J., Zhang, B., Zhang, Q., Zhao, H., Zhao, H., Zhou, J., Gabriel, S. B., Barry, R., Blumenstiel, B., Camargo, A., Defelice, M., Faggart, M., Goyette, M., Gupta, S., Moore, J., Nguyen, H., Onofrio, R. C., Parkin, M., Roy, J., Stahl, E., Winchester, E., Ziaugra, L., Altshuler, D., Shen, Y., Yao, Z., Huang, W., Chu, X., He, Y., Jin, L., Liu, Y., Shen, Y., Sun, W., Wang, H., Wang, Y., Wang, Y., Xiong, X., Xu, L., Waye, M. M., Tsui, S. K., Xue, H., Wong, J. T., Galver, L. M., Fan, J. B., Gunderson, K., Murray, S. S., Oliphant, A. R., Chee, M. S., Montpetit, A., Chagnon, F., Ferretti, V., Leboeuf, M., Olivier, J. F., Phillips, M. S., Roumy, S., Sallee, C., Verner, A., Hudson, T. J., Kwok, P. Y., Cai, D., Koboldt, D. C., Miller, R. D., Pawlikowska, L., Taillon-Miller, P., Xiao, M., Tsui, L. C., Mak, W., Song, Y. Q., Tam, P. K., Nakamura, Y., Kawaguchi, T., Kitamoto, T., Morizono, T., Nagashima, A., et al. (2007) A second generation human haplotype map of over 3.1 million SNPs. Nature, 449, 851-861.

Jafarzadeh, N., Javeri, A., Khaleghi, M. and Taha, M. F. (2014) Oxytocin improves proliferation and neural differentiation of adipose tissue-derived stem cells. Neuroscience letters, 564, 105-110.

Jurek, B. and Meyer, M. (2020) Anxiolytic and Anxiogenic? How the Transcription Factor MEF2 Might Explain the Manifold Behavioral Effects of Oxytocin. Front Endocrinol (Lausanne), 11, 186.

Jurek, B. and Neumann, I. D. (2018) The Oxytocin Receptor: From Intracellular Signaling to Behavior. Physiol Rev, 98, 1805-1908.

Jurek, B., Slattery, D. A., Hiraoka, Y., Liu, Y., Nishimori, K., Aguilera, G., Neumann, I. D. and van den Burg, E. H. (2015) Oxytocin Regulates Stress-Induced Crf Gene Transcription through CREB-Regulated Transcription Coactivator 3. J Neurosci, 35, 12248-12260.

Jurek, B., Slattery, D. A., Maloumby, R., Hillerer, K., Koszinowski, S., Neumann, I. D. and van den Burg, E. H. (2012) Differential contribution of hypothalamic MAPK activity to anxiety-like behaviour in virgin and lactating rats. PloS one, 7, e37060.

Kalyoncu, T., Ozbaran, B., Kose, S. and Onay, H. (2019) Variation in the Oxytocin Receptor Gene Is Associated With Social Cognition and ADHD. J Atten Disord, 23, 702-711.

Kang, Y. S., Bae, M. K., Kim, J. Y., Jeong, J. W., Yun, I., Jang, H. O. and Bae, S. K. (2011) Visfatin induces neurite outgrowth in PC12 cells via ERK1/2 signaling pathway. Neuroscience letters, 504, 121-126.

Kim, J., Stirling, K. J., Cooper, M. E., Ascoli, M., Momany, A. M., McDonald, E. L., Ryckman, K. K., Rhea, L., Schaa, K. L., Cosentino, V., Gadow, E., Saleme, C., Shi, M., Hallman, M., Plunkett, J., Teramo, K. A., Muglia, L. J., Feenstra, B., Geller, F., Boyd, H. A., Melbye, M., Marazita, M. L., Dagle, J. M. and Murray, J. C. (2013) Sequence variants in oxytocin pathway genes and preterm birth: a candidate gene association study. BMC Med Genet, 14, 77.

Klahr, A. M., Klump, K. and Burt, S. A. (2015) A constructive replication of the association between the oxytocin receptor genotype and parenting. J Fam Psychol, 29, 91-99.

Klin, A., Saulnier, C. A., Sparrow, S. S., Cicchetti, D. V., Volkmar, F. R. and Lord, C. (2007) Social and communication abilities and disabilities in higher functioning individuals with autism spectrum disorders: the Vineland and the ADOS. J Autism Dev Disord, 37, 748-759.

Kosfeld, M., Heinrichs, M., Zak, P. J., Fischbacher, U. and Fehr, E. (2005) Oxytocin increases trust in humans. Nature, 435, 673-676.

Kulkarni, V. A. and Firestein, B. L. (2012) The dendritic tree and brain disorders. Molecular and cellular neurosciences, 50, 10-20.

Kumsta, R. and Heinrichs, M. (2013) Oxytocin, stress and social behavior: neurogenetics of the human oxytocin system. Curr Opin Neurobiol, 23, 11-16.

Kyriakis, J. M. and Avruch, J. (2012) Mammalian MAPK signal transduction pathways activated by stress and inflammation: a 10-year update. Physiol Rev, 92, 689-737.

Langle, S. L., Poulain, D. A. and Theodosis, D. T. (2002) Neuronal-glial remodeling: a structural basis for neuronal-glial interactions in the adult hypothalamus. Journal of physiology, Paris, 96, 169-175.

Latchney, S. E., Jiang, Y., Petrik, D. P., Eisch, A. J. and Hsieh, J. (2015) Inducible knockout of Mef2a, -c, and -d from nestin-expressing stem/progenitor cells and their progeny unexpectedly uncouples neurogenesis and dendritogenesis in vivo. FASEB J, 29, 5059-5071.

Lautermilch, N. J. and Spitzer, N. C. (2000) Regulation of calcineurin by growth cone calcium waves controls neurite extension. J Neurosci, 20, 315-325.

Lestanova, Z., Bacova, Z., Kiss, A., Havranek, T., Strbak, V. and Bakos, J. (2016) Oxytocin Increases Neurite Length and Expression of Cytoskeletal Proteins Associated with Neuronal Growth. J Mol Neurosci, 59, 184-192.

Lestanova, Z., Puerta, F., Alanazi, M., Bacova, Z., Kiss, A., Castejon, A. M. and Bakos, J. (2017) Downregulation of Oxytocin Receptor Decreases the Length of Projections Stimulated by Retinoic Acid in the U-87MG Cells. Neurochemical research, 42, 1006-1014.

Lewis, E. M. A., Meganathan, K., Baldridge, D., Gontarz, P., Zhang, B., Bonni, A., Constantino, J. N. and Kroll, K. L. (2019) Cellular and molecular characterization of multiplex autism in human induced pluripotent stem cell-derived neurons. Mol Autism, 10, 51.

Leyfer, O. T., Folstein, S. E., Bacalman, S., Davis, N. O., Dinh, E., Morgan, J., Tager-Flusberg, H. and Lainhart, J. E. (2006) Comorbid psychiatric disorders in children with autism: interview development and rates of disorders. J Autism Dev Disord, 36, 849-861.

Li, K., Nakajima, M., Ibanez-Tallon, I. and Heintz, N. (2016) A Cortical Circuit for Sexually Dimorphic Oxytocin-Dependent Anxiety Behaviors. Cell.

Lilja, J. and Ivaska, J. (2018) Integrin activity in neuronal connectivity. J Cell Sci, 131.

Lipton, S. A., Li, H., Zaremba, J. D., McKercher, S. R., Cui, J., Kang, Y. J., Nie, Z., Soussou, W., Talantova, M., Okamoto, S. and Nakanishi, N. (2009) Autistic phenotype from MEF2C knockout cells. Science, 323, 208.

Liu, L., Cavanaugh, J. E., Wang, Y., Sakagami, H., Mao, Z. and Xia, Z. (2003) ERK5 activation of MEF2-mediated gene expression plays a critical role in BDNF-promoted survival of developing but not mature cortical neurons. Proceedings of the National Academy of Sciences of the United States of America, 100, 8532-8537.

Ludwig, M., Sabatier, N., Bull, P. M., Landgraf, R., Dayanithi, G. and Leng, G. (2002) Intracellular calcium stores regulate activity-dependent neuropeptide release from dendrites. Nature, 418, 85-89.

Lukas, M., Toth, I., Reber, S. O., Slattery, D. A., Veenema, A. H. and Neumann, I. D. (2011) The neuropeptide oxytocin facilitates pro-social behavior and prevents social avoidance in rats and mice. Neuropsychopharmacology, 36, 2159-2168.

Maes, M., Anderson, G., Betancort Medina, S. R., Seo, M. and Ojala, J. O. (2019) Integrating Autism Spectrum Disorder Pathophysiology: Mitochondria, Vitamin A, CD38, Oxytocin, Serotonin and Melatonergic Alterations in the Placenta and Gut. Curr Pharm Des, 25, 4405-4420.

Manning, M., Stoev, S., Chini, B., Durroux, T., Mouillac, B. and Guillon, G. (2008) Peptide and non-peptide agonists and antagonists for the vasopressin and oxytocin V1a, V1b, V2 and OT receptors: research tools and potential therapeutic agents. Progress in brain research, 170, 473-512.

Marir, R., Virsolvy, A., Wisniewski, K., Mion, J., Haddou, D., Galibert, E., Meraihi, Z., Desarmenien, M. G. and Guillon, G. (2013) Pharmacological characterization of FE 201874, the first selective high affinity rat V1A vasopressin receptor agonist. British journal of pharmacology, 170, 278-292.

Martinetz, S., Meinung, C. P., Jurek, B., von Schack, D., van den Burg, E. H., Slattery, D. A. and Neumann, I. D. (2019) De Novo Protein Synthesis Mediated by the Eukaryotic Elongation Factor 2 Is Required for the Anxiolytic Effect of Oxytocin. Biological psychiatry, 85, 802-811.

Mattson, M. P., Gleichmann, M. and Cheng, A. (2008) Mitochondria in neuroplasticity and neurological disorders. Neuron, 60, 748-766.

Meinrenken, C. J., Borst, J. G. and Sakmann, B. (2003) Local routes revisited: the space and time dependence of the Ca2+ signal for phasic transmitter release at the rat calyx of Held. J Physiol, 547, 665-689.

Meyer-Lindenberg, A., Domes, G., Kirsch, P. and Heinrichs, M. (2011) Oxytocin and vasopressin in the human brain: social neuropeptides for translational medicine. Nature reviews. Neuroscience, 12, 524-538.

Meyer, M., Berger, I., Winter, J. and Jurek, B. (2018) Oxytocin alters the morphology of hypothalamic neurons via the transcription factor myocyte enhancer factor 2A (MEF-2A). Molecular and cellular endocrinology, 477, 156-162.

Meyer, M., Kuffner, K., Winter, J., Neumann, I. D., Wetzel, C. H. and Jurek, B. (2020) Myocyte Enhancer Factor 2A (MEF2A) Defines Oxytocin-Induced Morphological Effects and Regulates Mitochondrial Function in Neurons. Int J Mol Sci, 21.

Molkentin, J. D. (2004) Calcineurin-NFAT signaling regulates the cardiac hypertrophic response in coordination with the MAPKs. Cardiovasc Res, 63, 467-475.

Morrow, E. M., Yoo, S. Y., Flavell, S. W., Kim, T. K., Lin, Y., Hill, R. S., Mukaddes, N. M., Balkhy, S., Gascon, G., Hashmi, A., Al-Saad, S., Ware, J., Joseph, R. M., Greenblatt, R., Gleason, D., Ertelt, J. A., Apse, K. A., Bodell, A., Partlow, J. N., Barry, B., Yao, H., Markianos, K., Ferland, R. J., Greenberg, M. E. and Walsh, C. A. (2008) Identifying autism loci and genes by tracing recent shared ancestry. Science, 321, 218-223.

Mugele, K., Kugler, H. and Spiess, J. (1993) Immortalization of a fetal rat brain cell line that expresses corticotropin-releasing factor mRNA. DNA and cell biology, 12, 119-126.

Murtazina, D. A., Chung, D., Ulloa, A., Bryan, E., Galan, H. L. and Sanborn, B. M. (2011) TRPC1, STIM1, and ORAI influence signal-regulated intracellular and endoplasmic reticulum calcium dynamics in human myometrial cells. Biol Reprod, 85, 315-326.

Nanou, E., Lee, A. and Catterall, W. A. (2018) Control of Excitation/Inhibition Balance in a Hippocampal Circuit by Calcium Sensor Protein Regulation of Presynaptic Calcium Channels. J Neurosci, 38, 4430-4440.

Napolioni, V., Lombardi, F., Sacco, R., Curatolo, P., Manzi, B., Alessandrelli, R., Militerni, R., Bravaccio, C., Lenti, C., Saccani, M., Schneider, C., Melmed, R., Pascucci, T., Puglisi-Allegra, S., Reichelt, K. L., Rousseau, F., Lewin, P. and Persico, A. M. (2011) Family-based association study of ITGB3 in autism spectrum disorder and its endophenotypes. Eur J Hum Genet, 19, 353-359.

Naya, F. J., Black, B. L., Wu, H., Bassel-Duby, R., Richardson, J. A., Hill, J. A. and Olson, E. N. (2002) Mitochondrial deficiency and cardiac sudden death in mice lacking the MEF2A transcription factor. Nature medicine, 8, 1303-1309.

Neumann, I. D. and Landgraf, R. (2012) Balance of brain oxytocin and vasopressin: implications for anxiety, depression, and social behaviors. Trends Neurosci, 35, 649-659.

Nguyen, H. T. N., Kato, H., Masuda, K., Yamaza, H., Hirofuji, Y., Sato, H., Pham, T. T. M., Takayama, F., Sakai, Y., Ohga, S., Taguchi, T. and Nonaka, K. (2018a) Impaired neurite development associated with mitochondrial dysfunction in dopaminergic neurons differentiated from exfoliated deciduous tooth-derived pulp stem cells of children with autism spectrum disorder. Biochem Biophys Rep, 16, 24-31.

Nguyen, R. L., Medvedeva, Y. V., Ayyagari, T. E., Schmunk, G. and Gargus, J. J. (2018b) Intracellular calcium dysregulation in autism spectrum disorder: An analysis of converging organelle signaling pathways. Biochim Biophys Acta Mol Cell Res, 1865, 1718-1732.

Palaniyappan, L., White, T. P. and Liddle, P. F. (2012) The concept of salience network dysfunction in schizophrenia: from neuroimaging observations to therapeutic opportunities. Curr Top Med Chem, 12, 2324-2338.

Parker, K. J., Garner, J. P., Libove, R. A., Hyde, S. A., Hornbeak, K. B., Carson, D. S., Liao, C. P., Phillips, J. M., Hallmayer, J. F. and Hardan, A. Y. (2014) Plasma oxytocin concentrations and OXTR polymorphisms predict social impairments in children with and without autism spectrum disorder. Proc Natl Acad Sci U S A, 111, 12258-12263.

Parker, K. J., Oztan, O., Libove, R. A., Sumiyoshi, R. D., Jackson, L. P., Karhson, D. S., Summers, J. E., Hinman, K. E., Motonaga, K. S., Phillips, J. M., Carson, D. S., Garner, J. P. and Hardan, A. Y. (2017) Intranasal oxytocin treatment for social deficits and biomarkers of response in children with autism. Proceedings of the National Academy of Sciences of the United States of America, 114, 8119-8124.

Passoni, I., Leonzino, M., Gigliucci, V., Chini, B. and Busnelli, M. (2016) Carbetocin is a Functional Selective Gq Agonist That Does Not Promote Oxytocin Receptor Recycling After Inducing beta-Arrestin-Independent Internalisation. J Neuroendocrinol, 28.

Patterson, R. L., Boehning, D. and Snyder, S. H. (2004) Inositol 1,4,5-trisphosphate receptors as signal integrators. Annu Rev Biochem, 73, 437-465.

Perrino, B. A., Ng, L. Y. and Soderling, T. R. (1995) Calcium regulation of calcineurin phosphatase activity by its B subunit and calmodulin. Role of the autoinhibitory domain. The Journal of biological chemistry, 270, 340-346.

Peter, J., Burbach, H., Adan, R. A., Lolait, S. J., van Leeuwen, F. W., Mezey, E., Palkovits, M. and Barberis, C. (1995) Molecular neurobiology and pharmacology of the vasopressin/oxytocin receptor family. Cell Mol Neurobiol, 15, 573-595.

Peters, S., Slattery, D. A., Uschold-Schmidt, N., Reber, S. O. and Neumann, I. D. (2014) Dose-dependent effects of chronic central infusion of oxytocin on anxiety, oxytocin receptor binding and stress-related parameters in mice. Psychoneuroendocrinology, 42, 225-236.

Pfeiffer, B. E., Zang, T., Wilkerson, J. R., Taniguchi, M., Maksimova, M. A., Smith, L. N., Cowan, C. W. and Huber, K. M. (2010) Fragile X mental retardation protein is required for synapse elimination by the activity-dependent transcription factor MEF2. Neuron, 66, 191-197.

Podoly, E., Hanin, G. and Soreq, H. (2010) Alanine-to-threonine substitutions and amyloid diseases: butyrylcholinesterase as a case study. Chem Biol Interact, 187, 64-71.

Pon, J. R. and Marra, M. A. (2016) MEF2 transcription factors: developmental regulators and emerging cancer genes. Oncotarget, 7, 2297-2312.

Pont, J. N., McArdle, C. A. and Lopez Bernal, A. (2012) Oxytocin-stimulated NFAT transcriptional activation in human myometrial cells. Molecular endocrinology (Baltimore, Md, 26, 1743-1756.

Potthoff, M. J. and Olson, E. N. (2007) MEF2: a central regulator of diverse developmental programs. Development, 134, 4131-4140.

Pulipparacharuvil, S., Renthal, W., Hale, C. F., Taniguchi, M., Xiao, G., Kumar, A., Russo, S. J., Sikder, D., Dewey, C. M., Davis, M. M., Greengard, P., Nairn, A. C., Nestler, E. J. and Cowan, C. W. (2008) Cocaine regulates MEF2 to control synaptic and behavioral plasticity. Neuron, 59, 621-633.

Reversi, A., Rimoldi, V., Brambillasca, S. and Chini, B. (2006) Effects of cholesterol manipulation on the signaling of the human oxytocin receptor. Am J Physiol Regul Integr Comp Physiol, 291, R861-869.

Ripamonti, S., Ambrozkiewicz, M. C., Guzzi, F., Gravati, M., Biella, G., Bormuth, I., Hammer, M., Tuffy, L. P., Sigler, A., Kawabe, H., Nishimori, K., Toselli, M., Brose, N., Parenti, M. and Rhee, J. (2017) Transient oxytocin signaling primes the development and function of excitatory hippocampal neurons. eLife, 6.

Robert, F. and Pelletier, J. (2018) Exploring the Impact of Single-Nucleotide Polymorphisms on Translation. Front Genet, 9, 507.

Rossignol, D. A. and Frye, R. E. (2014) Evidence linking oxidative stress, mitochondrial dysfunction, and inflammation in the brain of individuals with autism. Frontiers in physiology, 5, 150.

Sanborn, B. M. (2007) Hormonal signaling and signal pathway crosstalk in the control of myometrial calcium dynamics. Seminars in cell & developmental biology, 18, 305-314.

Sanborn, B. M., Dodge, K., Monga, M., Qian, A., Wang, W. and Yue, C. (1998) Molecular mechanisms regulating the effects of oxytocin on myometrial intracellular calcium. Adv Exp Med Biol, 449, 277-286.

Sanders, S. J., He, X., Willsey, A. J., Ercan-Sencicek, A. G., Samocha, K. E., Cicek, A. E., Murtha, M. T., Bal, V. H., Bishop, S. L., Dong, S., Goldberg, A. P., Jinlu, C., Keaney, J. F., 3rd, Klei, L., Mandell, J. D., Moreno-De-Luca, D., Poultney, C. S., Robinson, E. B., Smith, L., Solli-Nowlan, T., Su, M. Y., Teran, N. A., Walker, M. F., Werling, D. M., Beaudet, A. L., Cantor, R. M., Fombonne, E., Geschwind, D. H., Grice, D. E., Lord, C., Lowe, J. K., Mane, S. M., Martin, D. M., Morrow, E. M., Talkowski, M. E., Sutcliffe, J. S., Walsh, C. A., Yu, T. W., Autism Sequencing, C., Ledbetter, D. H., Martin, C. L., Cook, E. H., Buxbaum, J. D., Daly, M. J., Devlin, B., Roeder, K. and State, M. W. (2015) Insights into Autism Spectrum Disorder Genomic Architecture and Biology from 71 Risk Loci. Neuron, 87, 1215-1233.

Sandin, S., Lichtenstein, P., Kuja-Halkola, R., Hultman, C., Larsson, H. and Reichenberg, A. (2017) The Heritability of Autism Spectrum Disorder. JAMA, 318, 1182-1184.

Sandin, S., Lichtenstein, P., Kuja-Halkola, R., Larsson, H., Hultman, C. M. and Reichenberg, A. (2014) The familial risk of autism. JAMA, 311, 1770-1777.

Schneiderman, I., Zagoory-Sharon, O., Leckman, J. F. and Feldman, R. (2012) Oxytocin during the initial stages of romantic attachment: relations to couples' interactive reciprocity. Psychoneuroendocrinology, 37, 1277-1285.

Schuch, J. B., Muller, D., Endres, R. G., Bosa, C. A., Longo, D., Schuler-Faccini, L., Ranzan, J., Becker, M. M., dos Santos Riesgo, R. and Roman, T. (2014) The role of beta3 integrin gene variants in Autism Spectrum Disorders--diagnosis and symptomatology. Gene, 553, 24-30.

Sebat, J., Lakshmi, B., Malhotra, D., Troge, J., Lese-Martin, C., Walsh, T., Yamrom, B., Yoon, S., Krasnitz, A., Kendall, J., Leotta, A., Pai, D., Zhang, R., Lee, Y. H., Hicks, J., Spence, S. J., Lee, A. T., Puura, K., Lehtimaki, T., Ledbetter, D., Gregersen, P. K., Bregman, J., Sutcliffe, J. S., Jobanputra, V., Chung, W., Warburton, D., King, M. C., Skuse, D., Geschwind, D. H., Gilliam, T. C., Ye, K. and Wigler, M. (2007) Strong association of de novo copy number mutations with autism. Science, 316, 445-449.

Sebat, J., Levy, D. L. and McCarthy, S. E. (2009) Rare structural variants in schizophrenia: one disorder, multiple mutations; one mutation, multiple disorders. Trends Genet, 25, 528-535.

Shalizi, A., Bilimoria, P. M., Stegmuller, J., Gaudilliere, B., Yang, Y., Shuai, K. and Bonni, A. (2007) PIASx is a MEF2 SUMO E3 ligase that promotes postsynaptic dendritic morphogenesis. J Neurosci, 27, 10037-10046.

Shalizi, A., Gaudilliere, B., Yuan, Z., Stegmuller, J., Shirogane, T., Ge, Q., Tan, Y., Schulman, B., Harper, J. W. and Bonni, A. (2006) A calcium-regulated MEF2 sumoylation switch controls postsynaptic differentiation. Science (New York, N.Y, 311, 1012-1017.

She, H., Yang, Q., Shepherd, K., Smith, Y., Miller, G., Testa, C. and Mao, Z. (2011) Direct regulation of complex I by mitochondrial MEF2D is disrupted in a mouse model of Parkinson disease and in human patients. J Clin Invest, 121, 930-940.

Shlykov, S. G., Yang, M., Alcorn, J. L. and Sanborn, B. M. (2003) Capacitative cation entry in human myometrial cells and augmentation by hTrpC3 overexpression. Biol Reprod, 69, 647-655.

Siddiqui, M. F., Elwell, C. and Johnson, M. H. (2016) Mitochondrial Dysfunction in Autism Spectrum Disorders. Autism Open Access, 6.

Skuse, D. H., Lori, A., Cubells, J. F., Lee, I., Conneely, K. N., Puura, K., Lehtimaki, T., Binder, E. B. and Young, L. J. (2014) Common polymorphism in the oxytocin receptor gene (OXTR) is associated with human social recognition skills. Proc Natl Acad Sci U S A, 111, 1987-1992.

Supekar, K., Uddin, L. Q., Khouzam, A., Phillips, J., Gaillard, W. D., Kenworthy, L. E., Yerys, B. E., Vaidya, C. J. and Menon, V. (2013) Brain hyperconnectivity in children with autism and its links to social deficits. Cell Rep, 5, 738-747.

Tachibana, M., Kagitani-Shimono, K., Mohri, I., Yamamoto, T., Sanefuji, W., Nakamura, A., Oishi, M., Kimura, T., Onaka, T., Ozono, K. and Taniike, M. (2013) Long-term administration of intranasal oxytocin is a safe and promising therapy for early adolescent boys with autism spectrum disorders. J Child Adolesc Psychopharmacol, 23, 123-127.

Tang, G., Gudsnuk, K., Kuo, S. H., Cotrina, M. L., Rosoklija, G., Sosunov, A., Sonders, M. S., Kanter, E., Castagna, C., Yamamoto, A., Yue, Z., Arancio, O., Peterson, B. S., Champagne, F., Dwork, A. J., Goldman, J. and Sulzer, D. (2014) Loss of mTOR-dependent macroautophagy causes autistic-like synaptic pruning deficits. Neuron, 83, 1131-1143.

Tang, Q., Guo, W., Zheng, L., Wu, J. X., Liu, M., Zhou, X., Zhang, X. and Chen, L. (2018) Structure of the receptor-activated human TRPC6 and TRPC3 ion channels. Cell Res, 28, 746-755.

Tansey, K. E., Brookes, K. J., Hill, M. J., Cochrane, L. E., Gill, M., Skuse, D., Correia, C., Vicente, A., Kent, L., Gallagher, L. and Anney, R. J. L. (2010) Oxytocin receptor (OXTR) does not play a major role in the aetiology of autism: genetic and molecular studies. Neurosci Lett, 474, 163-167.

Theodosis, D. T. (2002) Oxytocin-secreting neurons: A physiological model of morphological neuronal and glial plasticity in the adult hypothalamus. Frontiers in neuroendocrinology, 23, 101-135.

Tobin, V. A., Douglas, A. J., Leng, G. and Ludwig, M. (2011) The involvement of voltage-operated calcium channels in somato-dendritic oxytocin release. PloS one, 6, e25366.

Tomaselli, K., Doherty, P., Emmett, C., Damsky, C., Walsh, F. and Reichardt, L. (1993) Expression of beta 1 integrins in sensory neurons of the dorsal root ganglion and their functions in neurite outgrowth on two laminin isoforms. The Journal of Neuroscience, 13, 4880-4888.

Tomizawa, K., Iga, N., Lu, Y. F., Moriwaki, A., Matsushita, M., Li, S. T., Miyamoto, O., Itano, T. and Matsui, H. (2003) Oxytocin improves long-lasting spatial memory during motherhood through MAP kinase cascade. Nat Neurosci, 6, 384-390.

Tost, H., Kolachana, B., Hakimi, S., Lemaitre, H., Verchinski, B. A., Mattay, V. S., Weinberger, D. R. and Meyer-Lindenberg, A. (2010) A common allele in the oxytocin receptor gene (OXTR) impacts prosocial temperament and human hypothalamic-limbic structure and function. Proceedings of the National Academy of Sciences of the United States of America, 107, 13936-13941.

Tu, S., Akhtar, M. W., Escorihuela, R. M., Amador-Arjona, A., Swarup, V., Parker, J., Zaremba, J. D., Holland, T., Bansal, N., Holohan, D. R., Lopez, K., Ryan, S. D., Chan, S. F., Yan, L., Zhang, X., Huang, X., Sultan, A., McKercher, S. R., Ambasudhan, R., Xu, H., Wang, Y., Geschwind, D. H., Roberts, A. J., Terskikh, A. V., Rissman, R. A., Masliah, E., Lipton, S. A. and Nakanishi, N. (2017) NitroSynapsin therapy for a mouse MEF2C haploinsufficiency model of human autism. Nat Commun, 8, 1488.

Ulloa, A., Gonzales, A. L., Zhong, M., Kim, Y. S., Cantlon, J., Clay, C., Ku, C. Y., Earley, S. and Sanborn, B. M. (2009) Reduction in TRPC4 expression specifically attenuates G-protein coupled receptor-stimulated increases in intracellular calcium in human myometrial cells. Cell Calcium, 46, 73-84.

van den Burg, E. H., Stindl, J., Grund, T., Neumann, I. D. and Strauss, O. (2015) Oxytocin Stimulates Extracellular Ca Influx Through TRPV2 Channels in Hypothalamic Neurons to Exert Its Anxiolytic Effects. Neuropsychopharmacology.

Velinov, M. (2019) Genomic Copy Number Variations in the Autism Clinic-Work in Progress. Front Cell Neurosci, 13, 57.

Vergara, R. C., Jaramillo-Riveri, S., Luarte, A., Moenne-Loccoz, C., Fuentes, R., Couve, A. and Maldonado, P. E. (2019) The Energy Homeostasis Principle: Neuronal Energy Regulation Drives Local Network Dynamics Generating Behavior. Front Comput Neurosci, 13, 49.

Verhallen, R. J., Bosten, J. M., Goodbourn, P. T., Lawrance-Owen, A. J., Bargary, G. and Mollon, J. D. (2017) The Oxytocin Receptor Gene (OXTR) and Face Recognition. Psychol Sci, 28, 47-55.

Vithayathil, J., Pucilowska, J. and Landreth, G. E. (2018) ERK/MAPK signaling and autism spectrum disorders. Prog Brain Res, 241, 63-112.

Waltenspühl Y., Schöppe J., Ehrenmann J., Kummer L. and Pückthun A. (2020) Crystal structure of the human oxytocin receptor. preprint.

Walum, H., Lichtenstein, P., Neiderhiser, J. M., Reiss, D., Ganiban, J. M., Spotts, E. L., Pedersen, N. L., Anckarsater, H., Larsson, H. and Westberg, L. (2012) Variation in the oxytocin receptor gene is associated with pair-bonding and social behavior. Biol Psychiatry, 71, 419-426.

Watanabe, T., Abe, O., Kuwabara, H., Yahata, N., Takano, Y., Iwashiro, N., Natsubori, T., Aoki, Y., Takao, H., Kawakubo, Y., Kamio, Y., Kato, N., Miyashita, Y., Kasai, K. and Yamasue, H. (2014) Mitigation of sociocommunicational deficits of autism through oxytocin-induced recovery of medial prefrontal activity: a randomized trial. JAMA Psychiatry, 71, 166-175.

Weisman, O., Pelphrey, K. A., Leckman, J. F., Feldman, R., Lu, Y., Chong, A., Chen, Y., Monakhov, M., Chew, S. H. and Ebstein, R. P. (2015) The association between 2D:4D ratio and cognitive empathy is contingent on a common polymorphism in the oxytocin receptor gene (OXTR rs53576). Psychoneuroendocrinology, 58, 23-32.

Wermter, A. K., Kamp-Becker, I., Hesse, P., Schulte-Korne, G., Strauch, K. and Remschmidt, H. (2010) Evidence for the involvement of genetic variation in the oxytocin receptor gene (OXTR) in the etiology of autistic disorders on high-functioning level. Am J Med Genet B Neuropsychiatr Genet, 153B, 629-639.

Werner, E. and Werb, Z. (2002) Integrins engage mitochondrial function for signal transduction by a mechanism dependent on Rho GTPases. The Journal of cell biology, 158, 357-368.

Wiegand, V. and Gimpl, G. (2012) Specification of the cholesterol interaction with the oxytocin receptor using a chimeric receptor approach. Eur J Pharmacol, 676, 12-19.

Winter, J., Meyer, M., Berger, I., Peters, S., Royer, M., Langgartner, D., Reber, S. O., Kuffner, K., Schmidtner, A. K., Hübner, K., Hartmann, F., Bludau, A., Bianchi, M., Stang, S., Bosch, O. J., Slattery, D. A., van den Burg, E., Neumann, I. D. and Jurek, B. (2020) Chronic oxytocin-driven alternative splicing of CRFR2α induces anxiety.

Won, J. H., Ahn, K. H., Back, M. J., Ha, H. C., Jang, J. M., Kim, H. H., Choi, S. Z., Son, M. and Kim, D. K. (2015) DA-9801 promotes neurite outgrowth via ERK1/2-CREB pathway in PC12 cells. Biological & pharmaceutical bulletin, 38, 169-178.

Wu, N., Li, Z. and Su, Y. (2012) The association between oxytocin receptor gene polymorphism (OXTR) and trait empathy. J Affect Disord, 138, 468-472.

Xiong, T. Q., Chen, L. M., Tan, B. H., Guo, C. Y., Li, Y. N., Zhang, Y. F., Li, S. L., Zhao, H. and Li, Y. C. (2018) The effects of calcineurin inhibitor FK506 on actin cytoskeleton, neuronal survival and glial reactions after pilocarpine-induced status epilepticus in mice. Epilepsy Res, 140, 138-147.

Xu, C., You, X., Liu, W., Sun, Q., Ding, X., Huang, Y. and Ni, X. (2015) Prostaglandin F2alpha regulates the expression of uterine activation proteins via multiple signalling pathways. Reproduction, 149, 139-146.

Yatawara, C. J., Einfeld, S. L., Hickie, I. B., Davenport, T. A. and Guastella, A. J. (2016) The effect of oxytocin nasal spray on social interaction deficits observed in young children with autism: a randomized clinical crossover trial. Molecular psychiatry, 21, 1225-1231.

Ying, L., Becard, M., Lyell, D., Han, X., Shortliffe, L., Husted, C. I., Alvira, C. M. and Cornfield, D. N. (2015) The transient receptor potential vanilloid 4 channel modulates uterine tone during pregnancy. Sci Transl Med, 7, 319ra204.

Yoshida, M., Takayanagi, Y., Inoue, K., Kimura, T., Young, L. J., Onaka, T. and Nishimori, K. (2009) Evidence that oxytocin exerts anxiolytic effects via oxytocin receptor expressed in serotonergic neurons in mice. J Neurosci, 29, 2259-2271.

Young, A. M., Chakrabarti, B., Roberts, D., Lai, M. C., Suckling, J. and Baron-Cohen, S. (2016) From molecules to neural morphology: understanding neuroinflammation in autism spectrum condition. Molecular autism, 7, 9.

Yuen, K. W., Garner, J. P., Carson, D. S., Keller, J., Lembke, A., Hyde, S. A., Kenna, H. A., Tennakoon, L., Schatzberg, A. F. and Parker, K. J. (2014) Plasma oxytocin concentrations are lower in depressed vs. healthy control women and are independent of cortisol. J Psychiatr Res, 51, 30-36.

Zaslavsky, K., Zhang, W. B., McCready, F. P., Rodrigues, D. C., Deneault, E., Loo, C., Zhao, M., Ross, P. J., El Hajjar, J., Romm, A., Thompson, T., Piekna, A., Wei, W., Wang, Z., Khattak, S., Mufteev, M., Pasceri, P., Scherer, S. W., Salter, M. W. and Ellis, J. (2019) SHANK2 mutations associated with autism spectrum disorder cause hyperconnectivity of human neurons. Nat Neurosci, 22, 556-564.

Zatkova, M., Bacova, Z., Puerta, F., Lestanova, Z., Alanazi, M., Kiss, A., Reichova, A., Castejon, A. M., Ostatnikova, D. and Bakos, J. (2018) Projection length stimulated by oxytocin is modulated by the inhibition of calcium signaling in U-87MG cells. J Neural Transm (Vienna), 125, 1847-1856.

Zatkova, M., Reichova, A., Bacova, Z. and Bakos, J. (2019) Activation of the Oxytocin Receptor Modulates the Expression of Synaptic Adhesion Molecules in a Cell-Specific Manner. J Mol Neurosci, 68, 171-180.

Zhang, S. J., Zou, M., Lu, L., Lau, D., Ditzel, D. A., Delucinge-Vivier, C., Aso, Y., Descombes, P. and Bading, H. (2009) Nuclear calcium signaling controls expression of a large gene pool: identification of a gene program for acquired neuroprotection induced by synaptic activity. PLoS Genet, 5, e1000604.

Zhang, Z., Cao, M., Chang, C. W., Wang, C., Shi, X., Zhan, X., Birnbaum, S. G., Bezprozvanny, I., Huber, K. M. and Wu, J. I. (2016) Autism-Associated Chromatin Regulator Brg1/SmarcA4 Is Required for Synapse Development and Myocyte Enhancer Factor 2-Mediated Synapse Remodeling. Molecular and cellular biology, 36, 70-83.

Zhou, C. J., Yada, T., Kohno, D., Kikuyama, S., Suzuki, R., Mizushima, H. and Shioda, S. (2001) PACAP activates PKA, PKC and Ca(2+) signaling cascades in rat neuroepithelial cells. Peptides, 22, 1111-1117.

Zuchner, S., Roberts, S. T., Speer, M. C. and Beckham, J. C. (2007) Update on psychiatric genetics. Genet Med, 9, 332-340.

8 Acknowledgements

Zuallererst möchte ich mich bei meinem Betreuer Dr. Benjamin Jurek bedanken. Vielen Dank lieber Ben für deine Unterstützung, Kritik, Geduld und Motivation, die du mir stets hast zukommen lassen. Selbst in den stürmischsten Zeiten konnte ich dich immer um Rat fragen. Danke für alles!

Vielen Dank auch an Prof. Dr. Inga Neumann für die Möglichkeit und Mittel an diesem Lehrstuhl zu promovieren und Teil dieses wissenschaftlichen Netzwerks zu sein. Danke für die konstruktive Kritik und stets anregenden wissenschaftlichen Diskussionen.

I would like to thank the GRK 2174 neuroscience graduate program “Neurobiology of emotion dysfunctions”. I profited a lot from being part of such a scientific network. Thanks to the other nine PhD students for all the scientific and non-scientific meetings.
Ich möchte mich ganz herzlich bei Prof. Christian Wetzel, Dr. Vladimir Milenkovic und Dr. Kerstin Kuffner für die erfolgreiche Kollaboration bedanken.

Thanks to my bachelor, master and internship students Lisa Steffens, Piret Kleis, Laura Stangl, Carina Mayer and Carolin Molthof.
Ein Dankeschön geht auch an unsere technischen Assistenten und Sekretärinnen für die technische als auch die administrative Unterstützung.

I would like to thank all my colleagues, office mates and friends in the lab for their friendship, support, help, discussion and valuable contributions to this work. I sincerely thank the whole AG Harn Solo, AG Neumann, AG Flor and AG Egger for the warm atmosphere and the PH group for many unforgettable memories.

Vielen lieben Dank an Max Müller für das Korrekturlesen und die Unterstützung.

Zu guter Letzt ein großes Dankeschön an meine Familie für den Rückhalt und die Erdung.